NASA CR-72180

CPRL 8-67

FINAL REPORT

ANALYTICAL AND EXPERIMENTAL STUDY OF POROUS METAL IONIZERS

by

A. Y. Cho and C. D. Hendricks

Prepared for

NATIONAL AERONAUTICS AND SPACE ADMINISTRATION

April 10, 1967

Contract NAS-3-8904

Technical Management
NASA Lewis Research Center
Cleveland, Ohio
Electric Propulsion Office
Mr. Tom Riley

CHARGED PARTICLE RESEARCH LABORATORY
DEPARTMENT OF ELECTRICAL ENGINEERING
ENGINEERING EXPERIMENT STATION
UNIVERSITY OF ILLINOIS
URBANA, ILLINOIS, 61801

ACKNOWLEDGMENT

This Final Report has been made possible by the enthusiastic and substantial contributions of Mr. William Keenan and our technician Jack Jacobsen. We also wish to thank Miss Helen Thornburgh who typed the manuscript.

This work was supported by NASA Lewis Research Center, Cleveland, Ohio, under contract NAS-3-8904.

PRECEDING PAGE BLANK NOT FILMED.

TABLE OF CONTENTS

	Page
SUMMARY	xi
INTRODUCTION	1
EXPERIMENTAL METHOD	2
Transmission Coefficient	2
Neutral Fraction as a Function of Current Density	4
Critical Temperature as a Function of Current Density	4
EXPERIMENTAL APPARATUS	6
Source Assembly	6
Accelerating Electrode	6
Neutral Detector	10
Transmissivity Measurement	10
EXPERIMENTAL RESULTS	16
Test No. 1 - NASA electron-beam weld EOS W-10 per cent-Ta (NASA 3-6269, slab No. 10 polished surface)	16
Test No. 2 - HRL 3.9 micron (machined and rhodium brazed by University of Illinois)	16
Test No. 3 - HRL 3.9 micron (Electron-beam weld by NASA No. 1)	20
Test No. 4 - HRL 3.9 micron (NASA electron-beam welded No. 2)	27
Test No. 5 - LeRC 4.2 micron (NASA electron-beam welded)	34
Test No. 6 - EOS 1B-N20 (EOS electron-beam welded)	34
Test No. 7 - LeRC 3.5 micron	42
Test No. 8 - EOS ORNL 4.2 micron	46
Test No. 9 - EOS ORNL 3.5 micron	46
Test No. 10 - EOS 1B-N20 (EOS electron-beam welded)	58
REFERENCES	71
APPENDIX	72

LIST OF ILLUSTRATIONS

Figure		Page
1	Experimental apparatus	7
2	Schematic diagram of the cesium ion source assembly	8
3	Accelerating electrode structure	9
4	Neutral detector with shutter mechanism	11
5	Transmissivity measurement of the porous pellet	13
6	Photograph of complete experimental assembly	14
7	Schematic diagram of complete experimental configuration in cross section	15
8	The change in neutral fraction versus cesium ion current density as the source was cleaned by long time operation at high temperature and finally sputtered by cesium ions	17
9	Cesium neutral fraction as a function of emitter temperature	18
10	Neutral fraction as a function of cesium ion current density	19
11	Photomicrograph of HRL 3.9 micron after machining	21
12	Photomicrograph of HRL 3.9 micron after de-infiltration of copper	22
13	Photomicrograph of HRL 3.9 micron after slight electrolytic etching	23
14	Neutral fraction as a function of current density	24
15	Neutral fraction as a function of emitter temperature	25
16	Neutral fraction as a function of cesium ion current density	26
17	Neutral fraction as a function of emitter temperature	28
18	Neutral fraction as a function of cesium ion current density	29
19	Improvement of critical temperatures after each sputter cleaning by cesium ions	30
20	Neutral fraction as a function of emitter temperature	31

Figure		Page
21	Neutral fraction as a function of cesium ion current for clean and oxygenated surface	32
22	Sputter cleaning of an absorbed oxygen layer on a clean tungsten surface	33
23	Neutral fraction as a function of cesium ion current density	35
24	Neutral fraction as a function of emitter temperature	36
25	Photomicrograph at 500x of EOS 1B-N20	37
26	Photomicrograph at 1000x of EOS 1B-N20	38
27	Neutral fraction as a function of cesium ion current density	40
28	Neutral fraction as a function of emitter temperature	41
29	Neutral fraction as a function of current density	43
30	Neutral fraction as a function of emitter temperature	44
31	Neutral fraction as a function of emitter temperature	45
32	Neutral fraction as a function of current density	47
33	Neutral fraction as a function of emitter temperature	48
34	Neutral fraction as a function of emitter temperature	49
35	Neutral fraction as a function of emitter temperature	50
36	Neutral fraction as a function of emitter temperature	51
37	Neutral fraction as a function of emitter temperature	52
38	Neutral fraction as a function of current density	53
39	Neutral fraction as a function of emitter temperature	54
40	Neutral fraction as a function of emitter temperature	55
41	Neutral fraction as a function of emitter temperature	56
42	Neutral fraction as a function of emitter temperature	57

LIST OF ILLUSTRATIONS (cont.)

Figure		Page
43	Neutral fraction as a function of current density	59
44	Neutral fraction as a function of emitter temperature	60
45	Neutral fraction as a function of emitter temperature	61
46	Neutral fraction as a function of emitter temperature	62
47	Neutral fraction as a function of emitter temperature	63
48	Photomicrograph at 1000x of EOS W-10% ta	64
49	Photomicrograph at 1000x of HRL 3.9 micron	65
50	Photomicrograph at 1000x of LeRC 4.2 micron	66
51	Photomicrograph at 1000x of LeRC 3.5 micron	67
52	Photomicrograph at 1000x of ORNL 4.2 micron	68
53	Photomicrograph at 1000x of ORNL 3.5 micron	69
54	Photomicrograph at 1000x of EOS 1B-N 13	70

SUMMARY

This experimental work was conducted to determine the performance of porus tungsten ionizers. The purpose was to determine the type of plug which had the highest efficiency of ionization.

In addition to the outgassing treatment, all the sources were heated in a pressure of 1×10^{-5} torr of oxygen in order to reduce their carbon contents.[1,2,3] Since the oxygen adsorbed layer is extremely stable up to temperatures as high as 1800° K,[4] the source was sputtered by cesium ions before a clean surface data was taken. To test the reproducibility of our testing system, HRL 3.9 micron (rhodium brazed) source was re-examined for the second time (other sources were tested in between). The second set of data coincided exactly with the previous results after one sputter cleaning to remove the adsorbed oxygen layer.

A comparison of the performance of a rhodium brazed and an electron-beam welded source of the same porous material (HRL 3.9 micron) was conducted. The first electron-beam welded source showed a much higher neutral fraction than the rhodium brazed one. The high neutral fraction was believed due to contamination during the welding process. Care was taken during the welding for a second electron-beam welded source. After extensive cleaning the second electron-beam welded source showed a lower neutral than the rhodium brazed source and less degradation in performance as the current density increases. This along with the fact that both electron-beam welded sources had a transmissivity twice as high as that of the rhodium brazed, one may conclude that there was further sintering during the rhodium brazing ($\sim$ 2240° K).

EOS 1B-N20 low equivalent density (51.55%) special etched structure (see Figures 25 and 26) has the lowest neutral fraction for a given current density.

When one compares the performance of the LeRC 3.5 micron to LeRC 4.2 micron and ORNL 3.5 micron to ORNL 4.2 micron, one finds that the neutral fraction of 3.5 micron increases slower than that of 4.2 micron with increasing cesium ion density. The performance at 20 ma/cm^2 definitely shows the superiority of the 3.5 micron over that of the 4.2 micron. The explanation of this is that the current density per pore for a given ion current is lower for the 3.5 micron than the 4.2 micron.

The influence of molecular current density in each pore can be traced to the relative collision probability between cesium molecules and between cesium and the tungsten walls of the pore; if cesium with cesium collision dominates, the resulting cesium beam will be un-ionized.

In a recent paper[5] it was indicated that tungsten-tantalum alloy has a low work function (3.8 ev) for W-3 per cent Ta to W-20 per cent Ta. However, our results do not agree. The work function for W-10 per cent Ta was measured to be 4.7 ev by the surface ionization method.

TABLE I

HISTORY OF TEST SPECIMENS
PRIOR TO TESTING BY U OF I

TEST NO.	MATERIAL SOURCE & CONTRACT	COMPOSITION & QUANTITY	FABRICATION HISTORY
1	EOS[a] NAS3-6269 Slab 10	90W + 10T2	Electron beam welded by NASA[b]
2	HRL[c] NAS3-7105 Slab 337	3.9 micron W, 100%	Brazed by U of I
3	"	"	First electron beam weld by NASA
4	"	"	Second electron beam weld by NASA
5	NASA	4.2 micron W, 100%	Electron beam welded by NASA
6	EOS NAS3-7103 Mod 6	1% B (as BN) + 99% W	Electron beam welded by EOS
7	NASA	3.5 micron W, 100%	Electron beam welded by NASA
8	NASA	4.2 micron W, 100%	Electron beam welded by EOS
9	NASA	3.5 micron W, 100%	Electron beam welded by EOS
10	EOS NAS3-7103 Mod 6	1% B (as BN) + 99% W	Electron beam welded by EOS Electron beam welded by EOS

a Electro Optical Systems, Pasadena, California

b Lewis Research Center of NASA, Cleveland, Ohio

c Hughes Research Laboratory, Malibu, California

TABLE II

Tabulated Test Parameters and Evaluation

Test No.	Material Source	Trans Coef. Before / After	Surface Work Function at Low Current Density	Neutral Fraction at 10 ma/cm^2 (1600° K)	Critical Temp. at 10 ma/cm^2	Neutral Fraction at 20 ma/cm^2 (1600° K)	Detail Result	Comments
1	EOS 10% Ta NAS 3-6269 Slab 10	1.53×10^{-5} (after)	4.75 ev	0.68%	1430° K	1.5%	Figure 8 through Figure 10	10% Tantalum does not seem to lower the work function (Ref. 5)
2	HRL 3.9μ NAS 3-7105 Slab 337	6.85×10^{-5} (after)	4.7 ev	0.46%	1490° K	1.5%	Figure 14 and Figure 15	Rhodium brazed showed a factor of two lower in transmissivity than the electron beam welded
3	HRL 3.9μ NAS 3-7105 Slab 337 Electron beam welded No. 1	1.15×10^{-4} 1.27×10^{-4}	4.9 ev	14%	1400° K	18%	Figure 16 and Figure 17	Good performance below 1 ma/cm^2 degrades very rapidly, above 1 ma/cm^2 possible Cs leakage at high feed rate or contamination in great depth.
4	HRL 3.9μ NAS 3-7105 Slab 337 Electron beam welded No. 2	1.30×10^{-4} 1.31×10^{-4}	4.7 ev	0.6%	1400° K	0.8%	Figure 18 through Figure 22	Showed contamination when first put in operation--the neutral fract decreased from 20% to 1%

TABLE II (cont.)
Tabulated Test Parameters and Evaluation

Test No.	Material Source	Trans Coef. Before After	Surface Work Function at Low Current Density	Neutral Fraction at 10 ma/cm^2 (1600° K)	Critical Temp. at 10 ma/cm^2	Neutral Fraction at 20 ma/cm^2 (1600° K)	Detail Result	Comments
								at 10 ma/cm^2 after first sputter cleani It is one of the bes sources after the co taminants are remove
5	NASA LeRC 4.2μ	1.18×10^{-4} 1.13×10^{-4}	4.7 ev	20%	1600° K	40%	Figure 23 and Figure 24	Very Poor
6	EOS NAS 3-7103 Mod 6	2.26×10^{-4}	4.9 ev	0.44%	1360° K	0.7%	Figure 27 and Figure 28	Excellent results starting from the initial operation
7	NASA LeRC 3.5μ	7.5×10^{-5} 7.5×10^{-5}	4.7 ev	0.7%	1410° K	1.2%	Figure 29 through Figure 31	Initially showed contamination
8	NASA ORNL 4.2μ	1.08×10^{-4} 1.63×10^{-4}	4.8 ev	2.2%	1400° K	15%	Figure 32 through Figure 37	Badly contaminated when first placed in operation--rapid degradation in performance with increasing current density
9	NASA ORNL 3.5μ	1.36×10^{-4} 1.31×10^{-4}	4.7 ev	3.2%	1500° K	5%	Figure 38 through Figure 42	Poor

TABLE II(cont.)

Tabulated Test Parameters and Evaluation

Test No.	Material Source	Trans Coef. Before After	Surface Work Function at Low Current Density	Neutral Fraction at 10 ma/cm^2 (1600° K)	Critical Temp. at 10 ma/cm^2	Neutral Fraction at 20 ma/cm^2 (1600° K)	Detail Result	Comments
10	EOS NAS 3-7103 Mod 6 No. 2	1.79×10^{-4} 3.4×10^{-4}	4.8 ev	0.8%	1400° K	5%	Figure 43 through Figure 47	Excellent Performance at low current density. Fast increase of neutral fraction with current density indicates poor pore distribution.

INTRODUCTION

This is a final report which covers the period from March 1966 to February 1967. The work was performed at the Department of Electrical Engineering, University of Illinois, under the contract NAS-3-8904 from Lewis Research Center of the National Aeronautics and Space Administration. The goal of this program is to conduct an experimental study toward gaining a better understanding of the behavior of cesium surface ionization on porous tungsten. Nine porous pellets were supplied by the Lewis Laboratories. The object of the investigation was to determine the transmission coefficient, the neutral efflux as a function of current density up to 20 ma/cm^2 and the critical temperature as a function of current density at intervals of 1 ma/cm^2, 5 ma/cm^2, 10 ma/cm^2 and 20 ma/cm^2.

The neutral efflux and the critical temperature may vary widely depending on the porous structure, the pore size, the transmission coefficient, the "alloying" material and finally, the unknown contaminants introduced in the pellet during fabrication. The unknown contaminants are probably the most influential factor in determining the neutral efflux and the critical temperature.

Among the nine pellets tested in this reporting period were porous structures of compressed spherical powders (Hughes 3.9 micron) and specially prepared structures (EOS 1B-X120). Grain sizes of 3 microns to 4 microns led to transmission coefficients which varied from 10^{-4} to 10^{-5} (the transmission coefficients were measured on samples of 20 mil thickness). In addition, some tungsten pellets were "alloyed" with a small percentage of tantalum and boron metals.

EXPERIMENTAL METHOD

The porous tungsten ionizers were compared on the basis of transmission coefficient, neutral fraction and critical temperature as a function of current density.

Transmission Coefficient

The main flow mechanism of cesium through the porous pellet is molecular flow rather than viscous flow, since the mean free path is much longer than the dimension of the pore. Therefore, the measurement of transmissivity should be conducted under a pressure less than a few mm Hg.

The transmissivity is defined as the ratio of the number of molecules coming out of the front surface to the number of molecules hitting the back surface of the emitter. The transmissivity of a hole to vacuum is unity. Another way of defining it is the ratio of pumping speed with and without the porous plug in place. The pumping speed of a hole to vacuum is

$$S = \frac{\Gamma A}{n} \tag{1}$$

where Γ is the diffusion rate in number of molecules/cm^2sec

A is the area of the hole in cm^2

n is the density in number of molecules/cc

From the kinetic theory of gases we know that

$$\Gamma = \frac{n\bar{v}}{4} \tag{2}$$

and

$$\bar{v} = \sqrt{\frac{8kT}{\pi m}} \tag{3}$$

where $\bar{v}$ is the mean velocity of the molecules,

k is the Boltzmann constant,

T is the temperature and

m is the mass of the molecule.

Substituting Equation (2) and Equation (3) into Equation (1) will give the pumping speed of a hole

$$S = A \sqrt{\frac{kT}{2\pi m}} = A \times 11{,}600 \text{ cc/sec} \tag{4}$$

for air at room temperature. The pressure variation of a fixed volume can be expressed as

$$p = p_o \exp\left(-\frac{St}{V}\right) \tag{5}$$

where p_o is the pressure at time, t, equal to zero,

S is the pumping speed and

V is the volume of the container.

Equation (5) can be rewritten as

$$t = -\frac{V}{S} \ln \frac{p}{p_o} \tag{6}$$

When the porous plug is in place, one can measure the time Δt required to pump the pressure from p_1 to p_2. The transmissivity, T, can be calculated from Equation (4) and Equation (6)

$$T = \frac{-\frac{V}{S} \ln \frac{p_2}{p_1}}{\Delta t} = \frac{-\frac{V}{A\sqrt{\frac{2\pi m}{kT}}} \ln \frac{p_2}{p_1}}{\Delta t} \tag{7}$$

Neutral Fraction as a Function of Current Density

An omega-field accelerating system was chosen over the grid structure for this experiment. The "open" structure eliminates the scattering of cesium molecules which would give ambiguous neutral efflux readings. Other advantages are no cesium accumulation on the accelerating structure to produce a low work function surface which causes high drain currents and no back sputtering of the accelerating structure material to contaminate the ion emission surface.

The neutral efflux was measured by a hot filament neutral detector with a shutter mechanism to separate the true neutral cesium reading from the background current. Measurements were made as a function of cesium ion current density from 1 ma/cm^2 to 25 ma/cm^2. The ion beam was collected by a baffled current collector which was biased to recollect its secondary electrons. The baffled collector was also liquid nitrogen cooled to prevent any backstreaming of cesium which could result in charge exchange and false neutral readings from the detector.

The drain current from the accelerating electrode and the source current from the ionizer were monitored to cross check the baffled collector reading.

Critical Temperature as a Function of Current Density

The critical temperature was taken at intervals of 1 ma/cm^2, 5 ma/cm^2, 10 ma/cm^2 and 20 ma/cm^2. Prior to each reading, the emission surface was sputtered by cesium ions to remove any contaminants which might have come from the vacuum system or the interior of the porous plug. A clean surface thus prepared is believed to give a true critical temperature.

The surface sputtering was accomplished by lowering a hot tungsten ribbon close to the emission surface. When the emitter has a potential

negative with respect to the ribbon, the neutral cesium coming from the emitter will be surface ionized on the ribbon and accelerated back to sputter the emitter surface.

The critical temperature was measured by an optical pyrometer and a thermocouple to provide a cross check. Tungsten - 5 per cent rhenium versus tungsten - 26 per cent rhenium was used as the thermocouple.

The experimental arrangement is similar to that of the previous work.[6,7] The experiment was conducted in a demountable glass T with stainless steel end-plates and teflon O-rings as shown in Figure 1. The vacuum station consists of a 150 liter/sec ion pump and two sorption pumps to eliminate any possible back diffusion of oil vapor which would carbonize the hot tungsten surface. The total pressure in the vacuum system was of the order of 10^{-8} torr and contained mostly untrapped cesium.

Source Assembly

The pellet was machined to 0.156 inches in diameter and 0.020 inches thick. One of the pellets was rhodium brazed to the molybdenum plenum while the other eight were electron beam welded. Figure 2 shows a cross-section of the source assembly with a tantalum heater in place. The 0.060 inch O.D. molybdenum feed tube slid for about 1.5 inches into a thick wall molybdenum tube which was connected to the cesium reservoir. The precision fitting of these two tubes and the cascade differential pumping along the overlapping portion assured that there was no leakage of cesium at the junction. The cesium reservoir was formed by 0.5 inch O.D. OFHC copper tubing with one end pinch-sealed. A glass ampoule of cesium was placed in the reservoir. The ampoule was crushed from the outside of the vacuum system after the chamber was evacuated.

Accelerating Electrode

The accelerating electrode was made of 5 mil tungsten sheet so that it was possible to pass current through the sheet to keep it hot and thus to prevent the accumulation of cesium that Figure 3 shows. The edge of the electrode has been spot welded with a polished 50 mil ring to avoid

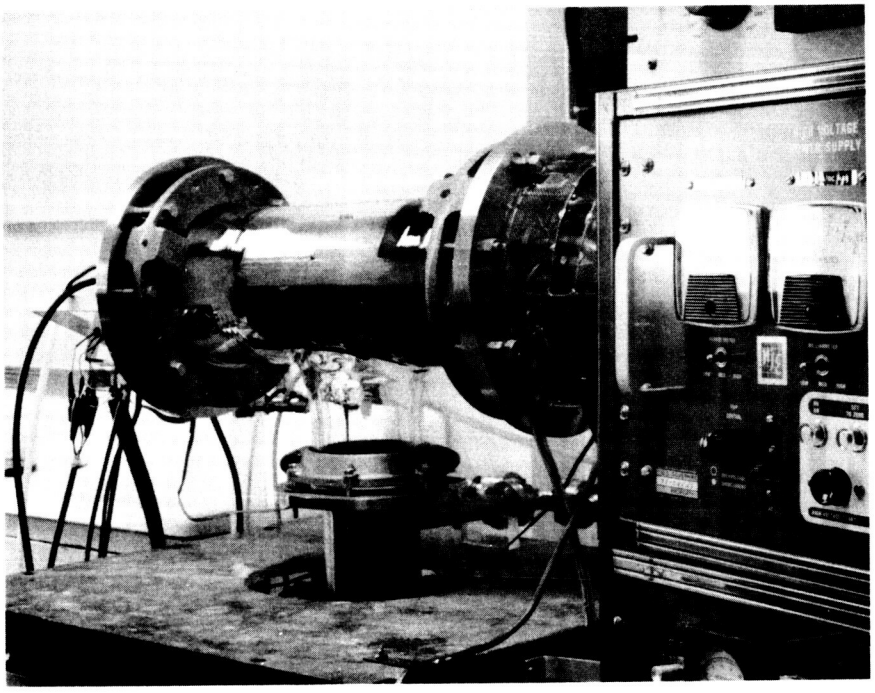

Figure 1. Experimental apparatus

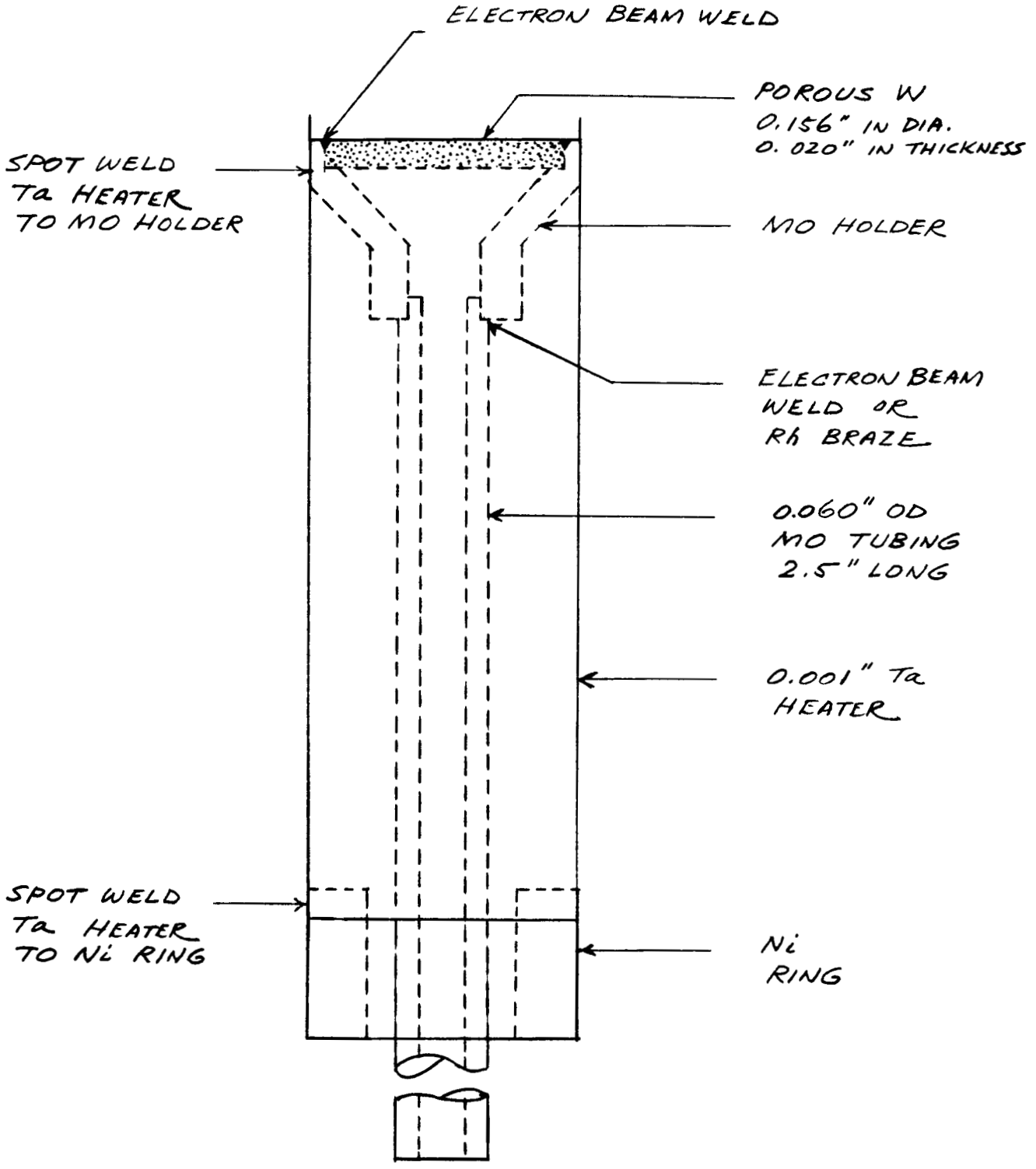

Figure 2. Schematic diagram of the cesium ion source assembly

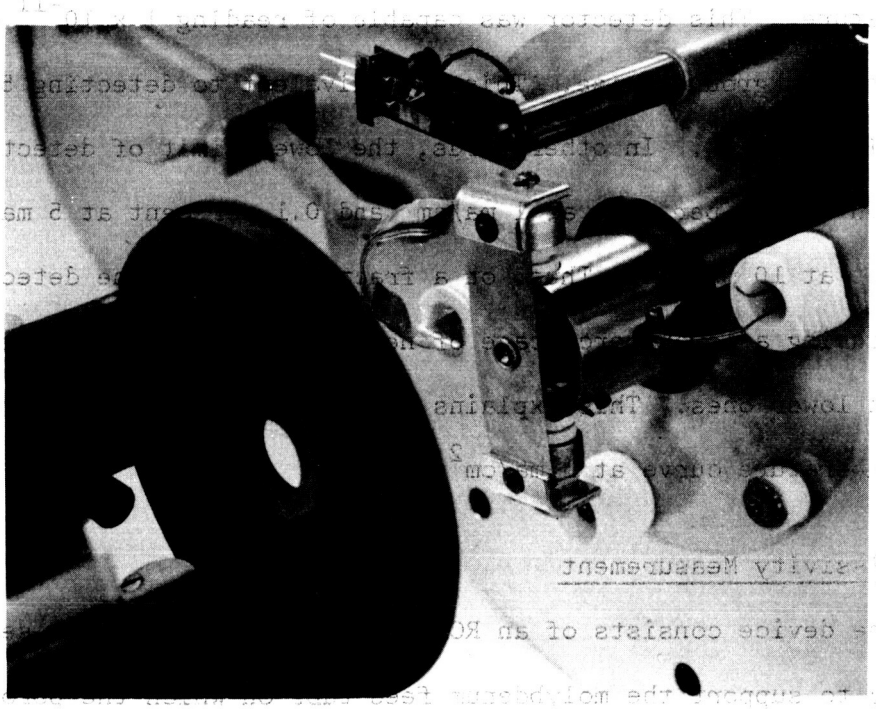

Figure 3. Accelerating electrode structure

a localized high electric field. This electrode reduced the drain current to a negligible amount.

Neutral Detector

The neutral detector was stationary and liquid nitrogen cooled as shown in Figure 4. The calibration used was based on 100 per cent neutral emission either during a no voltage condition or when the pellet was beyond critical temperature. The neutral reading was not sensitive to the detector ribbon temperature as long as the ribbon was above the critical temperature. This detector was capable of reading 1×10^{-11} amp with the existing background noise. This is equivalent to detecting 5×10^{-6} amp of cesium per cm^2. In other words, the lower limit of detection of neutral fraction is 0.5 per cent at 1 ma/cm^2 and 0.1 per cent at 5 ma/cm^2 and 0.05 per cent at 10 ma/cm^2. Thus, on a fractional basis the detector is capable of measuring a lower percentage of neutrals at higher current densities than at lower ones. This explains some of the flat portions of the critical temperature curve at 1 ma/cm^2.

Transmissivity Measurement

The device consists of an RCA-1946 thermocouple gauge sealed into a fitting to support the molybdenum feed tube on which the porous pellet and plenum are mounted. The entire assembly fits a 3/4 inch diameter Veeco quick-connect fitting on the forepump side of a 6 inch pumping system. The quick-connect fitting is isolated by a bellows valve from the pump which produces a pressure of 10^{-3} torr at the fitting when the valve is open. It was necessary to place the sample in a vacuum for several hours to remove all the adsorbed water vapor before each transmissivity test in order that the data would be reproducible. The output of the RCA-1946

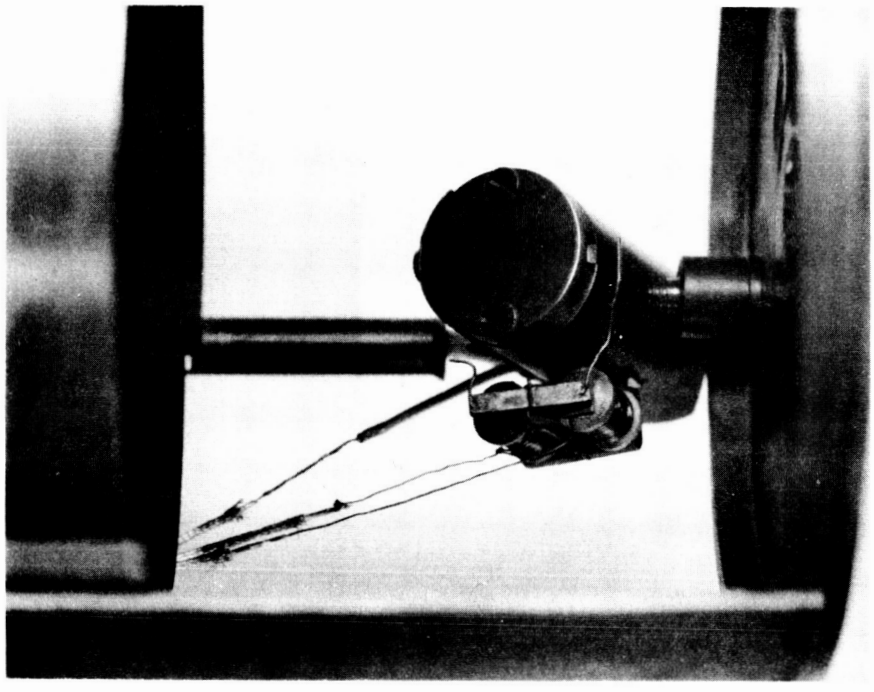

Figure 4. Neutral detector with shutter mechanism

was recorded on a recorder. A typical recorded curve is shown in Figure 5.

The complete experimental assembly is shown in Figures 6 and 7.

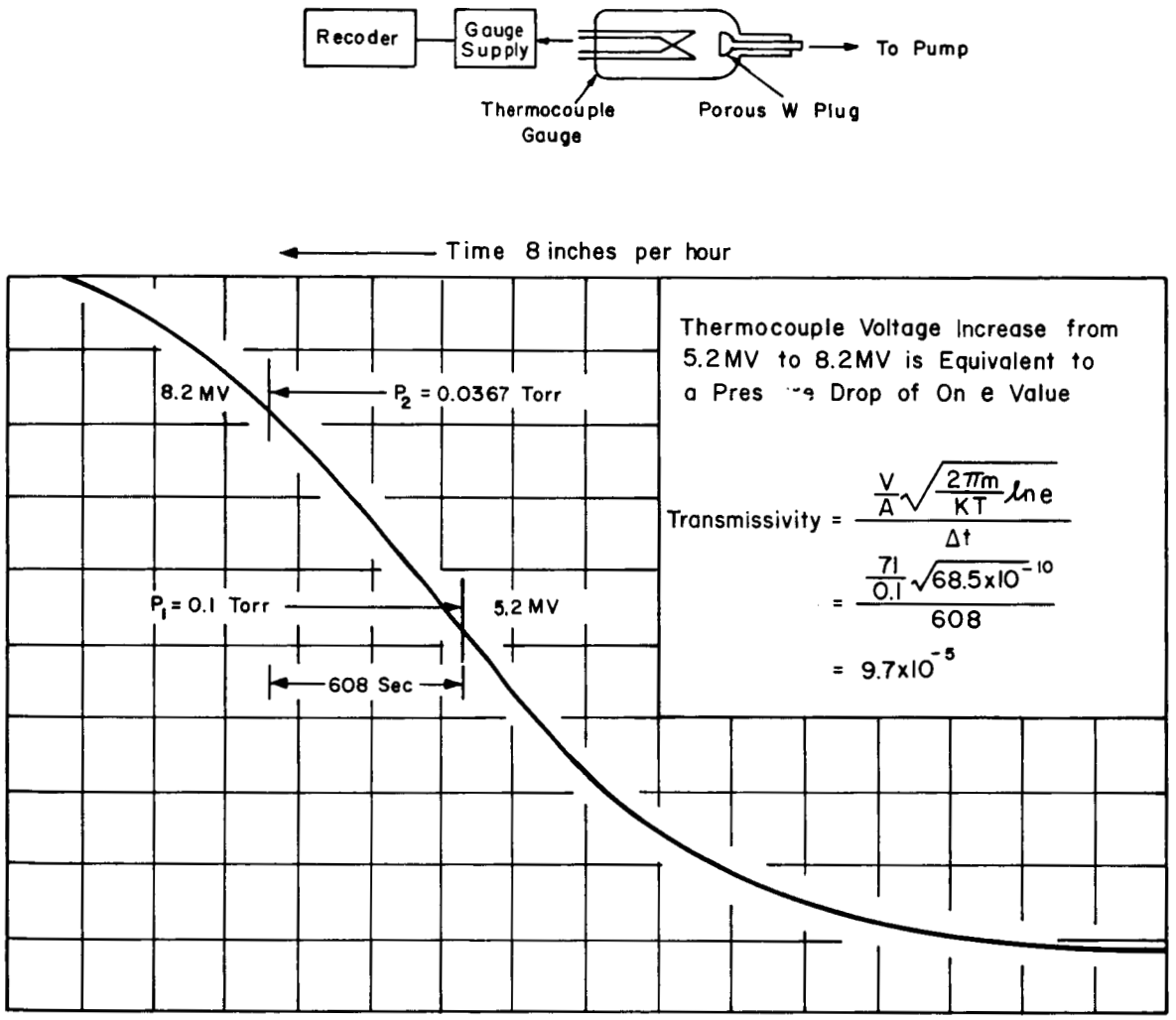

Figure 5. Transmissivity measurement of the porous pellet

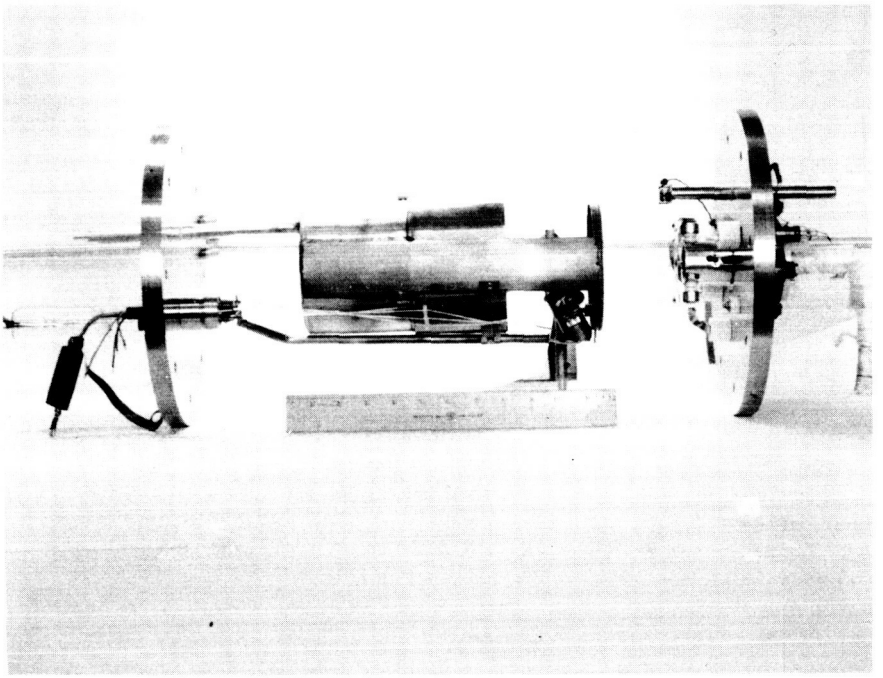

Figure 6. Photograph of complete experimental assembly

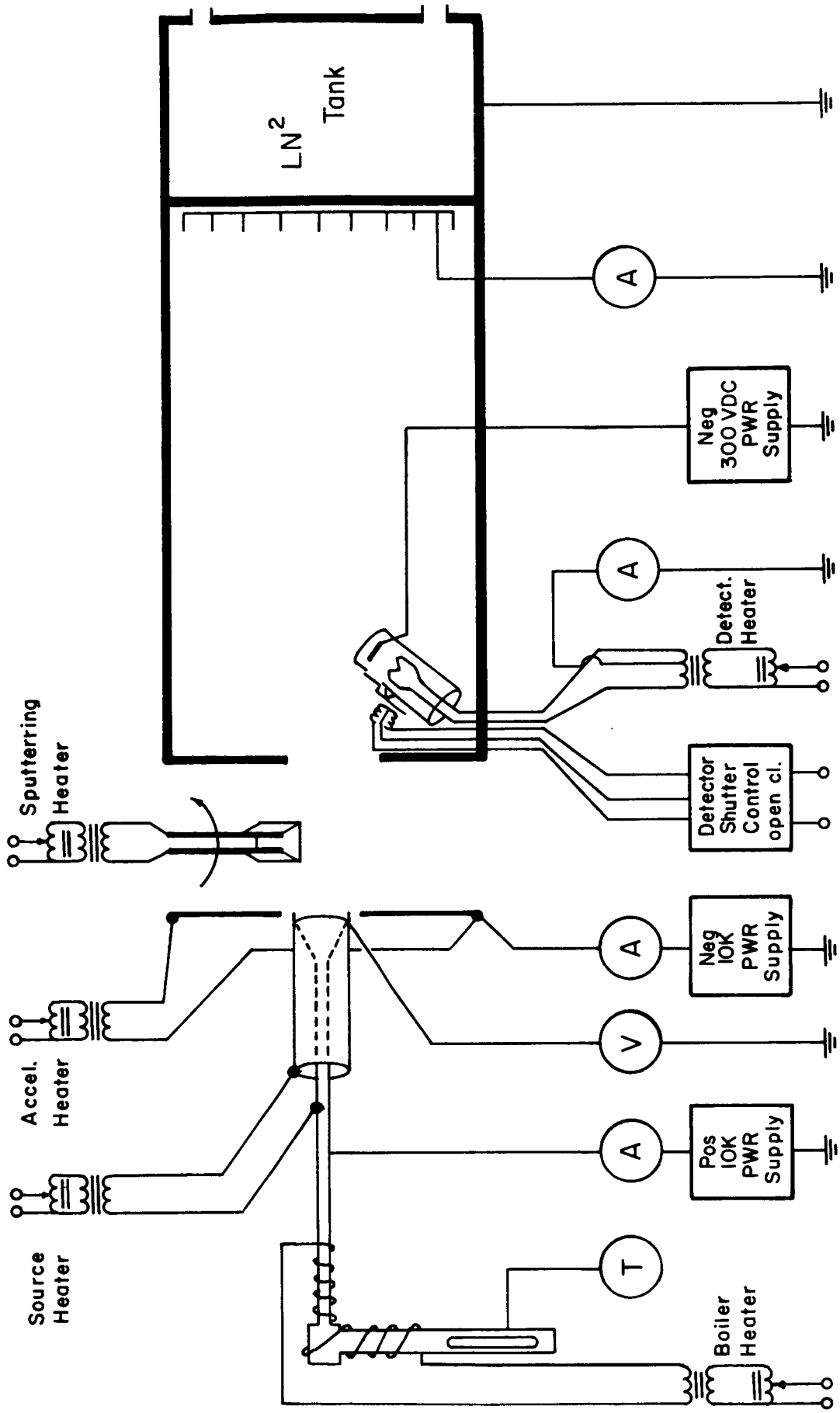

Figure 7. Schematic diagram of complete experimental configuration in cross section

Test No.1 - NASA electron-beam weld EOS W-10 per cent-Ta (NASA 3-6269, slab No. 10 polished surface)

Figure 8 illustrates the gradual improvement of the neutral fraction as the surface of the newly assembled source is cleaned. Prior to taking curve (1), the source was heated at 1600° K for over four hours. Then the source was operated up and down in current density as shown in curves (1), (2), (3) and (4) in Figure 1. The source was then sputtered and curve (5) was taken. The critical temperatures for various current densities were also taken at this time. They were about 50° K higher than the clean data presented in Figure 9. Further sputtering and cleaning was continued until the surface was clean and the data was reproducible. The data for critical temperature at various current densities is shown in Figure 9. Figure 10 shows the current density vs. neutral fraction for the clean EOS W-10 per cent-Ta source. The transmissivity of this pellet has been measured to be 1.53×10^{-5}.

The neutral detector was capable of reading a lower limit of 1×10^{-11} amp (equivalent to 0.5 per cent at 1 ma/cm^2) with the existing background noise as mentioned previously in the text. This explains the flat portion of the critical temperature curve at 1 ma/cm^2 in Figure 9 and the gradual increase in neutral fraction as the current density decreased below 2 ma/cm^2 in Figure 10.

Test No. 2 - HRL 3.9 micron (machined and rhodium brazed by University of Illinois)

This sample was intended as a control sample for the comparison of a rhodium brazed to an electron-beam weld sample of the same porous material.

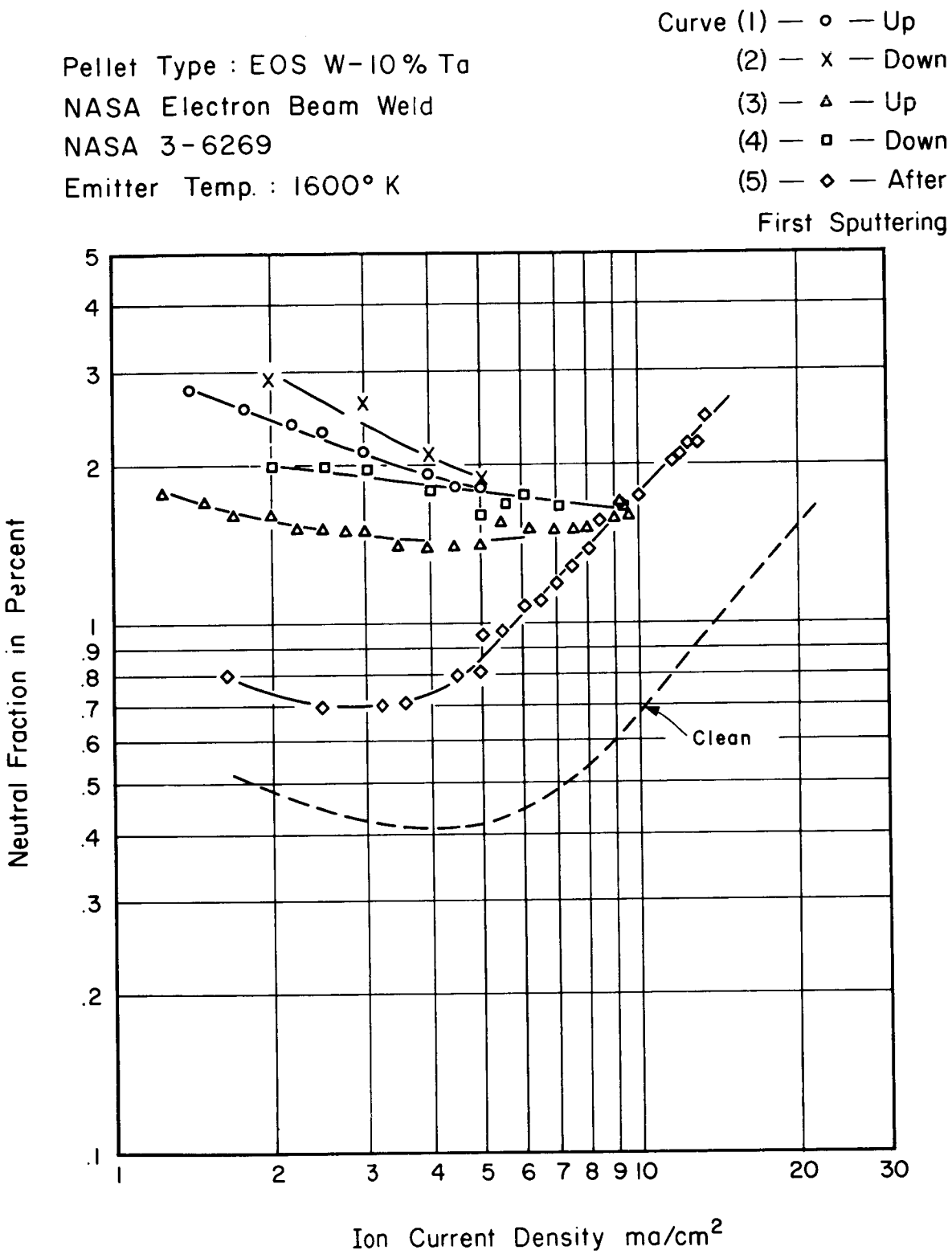

Figure 8. The change in neutral fraction versus cesium ion current density as the source was cleaned by long time operation at high temperature and finally sputtered by cesium ions

Pellet Type : EOS W-10% Ta
NASA Electron Beam Weld
NASA 3-6269

— x — 1.5 ma/cm^2
— □ — 5.0 ma/cm^2
— △ — 10 ma/cm^2
— o — 20 ma/cm^2

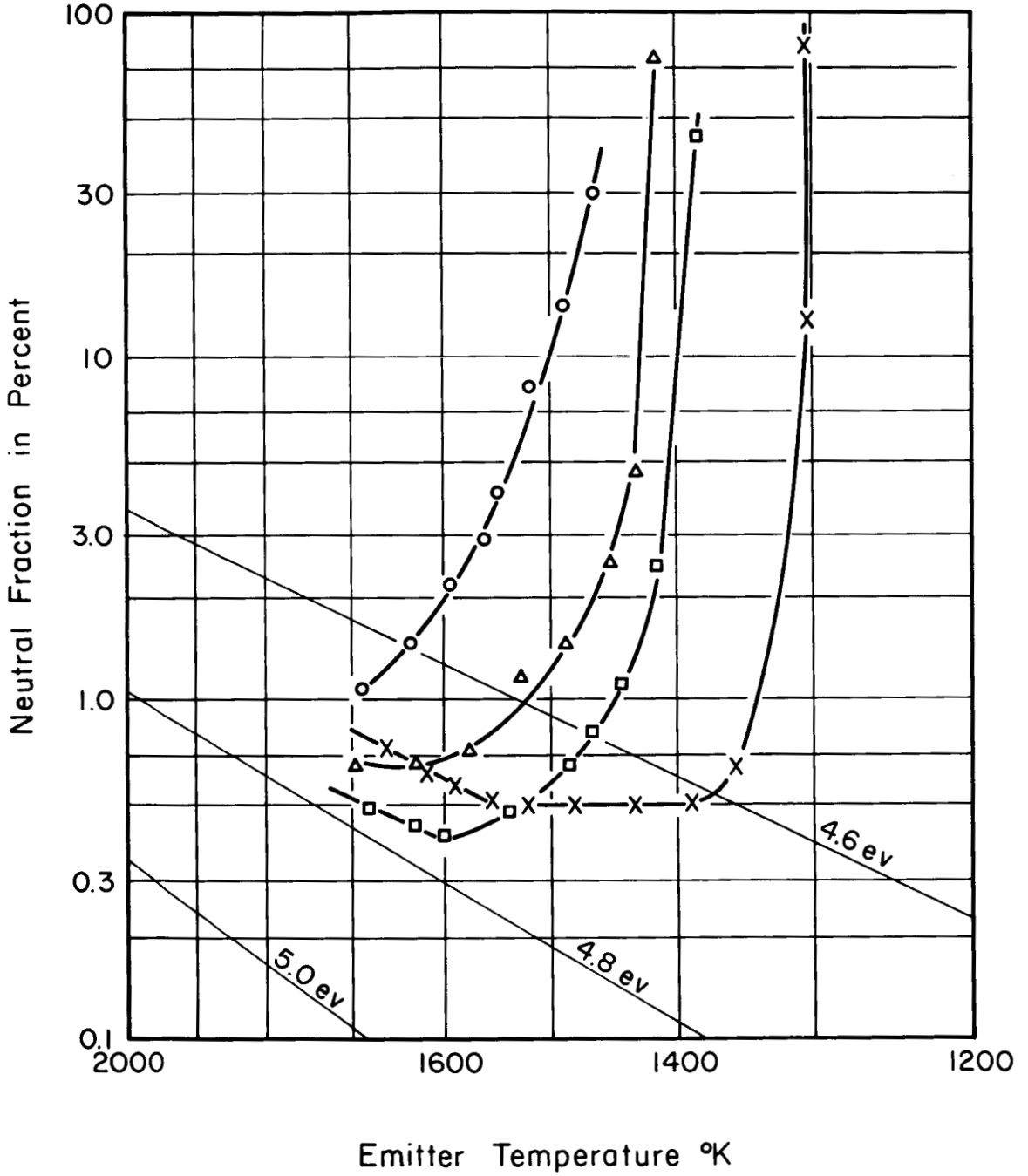

Figure 9. Cesium neutral fraction as a function of emitter temperature

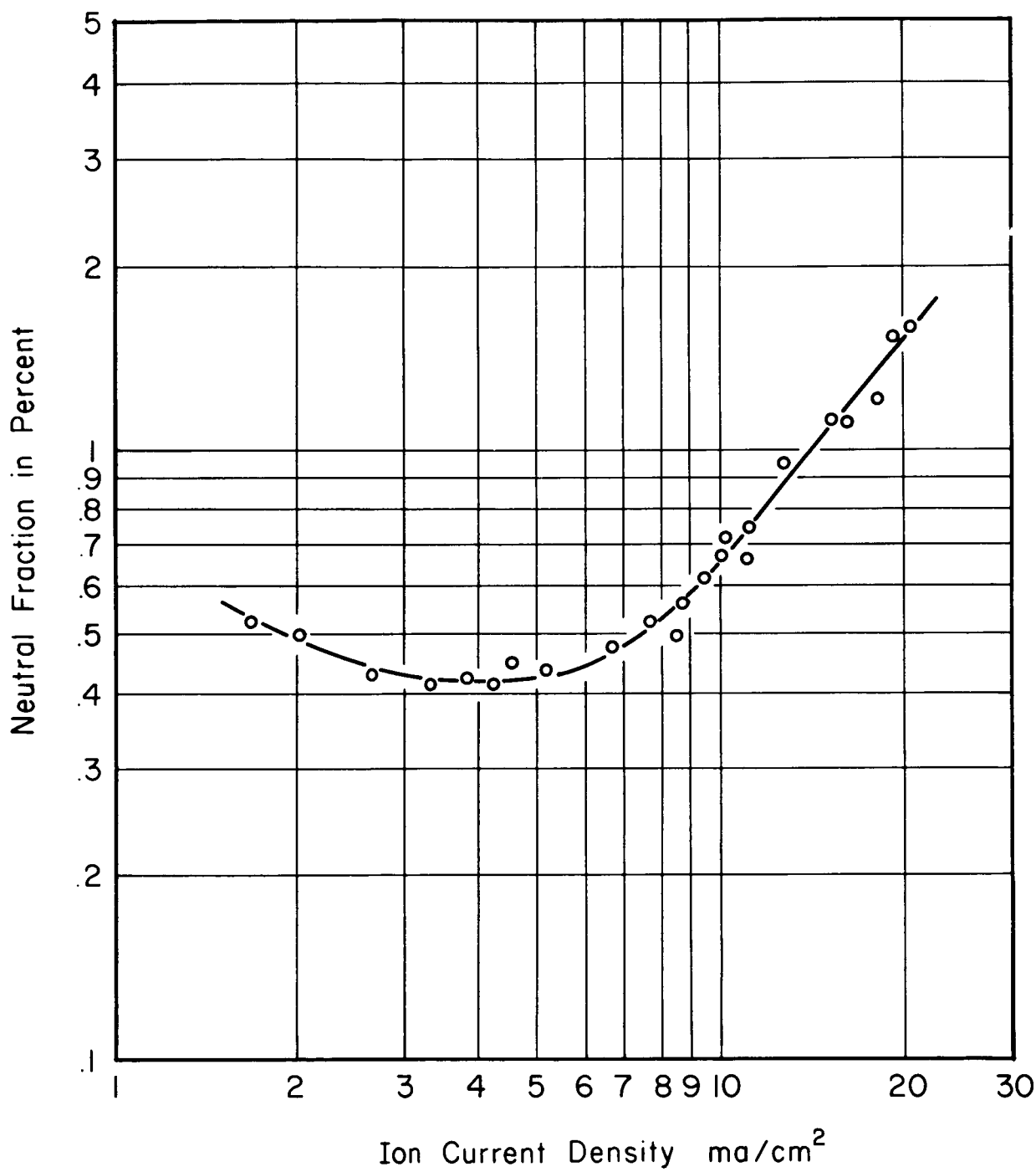

Figure 10. Neutral fraction as a function of cesium ion current density

Figure 11 is a x500 micrograph of the HRL 3.9 micron porous tungsten-copper button as received from the machinist. Figure 12 is a x500 micrograph after the copper has been de-infiltrated. After brazing in a molybdenum plenum the button was electrolytically etched and the result is shown in Figure 13.

Figure 14 shows the neutral fraction as a function of current density before and after the source was cleaned. Also shown in this figure is a curve of a slightly oxygenated surface. This curve was taken after the source was cleaned and then exposed to atmosphere for a short period of time. The effect of a slightly oxygenated surface is supported by its lower neutral fraction and higher critical temperature.[6] With one sputter cleaning the adsorbed oxygen can be removed, and the neutral fraction curve coincides with its clean curve.

Figure 15 shows the neutral fraction as a function of emitter temperature after the surface is cleaned. The transmissivity of this source is 6.85×10^{-5}.

Test No. 3 - HRL 3.9 micron (Electron-beam weld by NASA No. 1)

Electron-beam weld is thought to be the most ideal way of mounting a porous pellet onto a plenum, because (1) no brazing material will be introduced to the source which might contaminate the surface, and (2) the possibility of the brazing material penetrating into the porous tungsten, which would reduce the effective cesium emitting area, is eliminated. Rather unexpected results were obtained, however, when the electron-beam welded source was tested. Figure 16 shows the neutral fraction as a function of current density. This source consistently showed very high neutral fraction ($\sim$ 15 per cent at 20 ma/cm^2) even after more than thirty hours

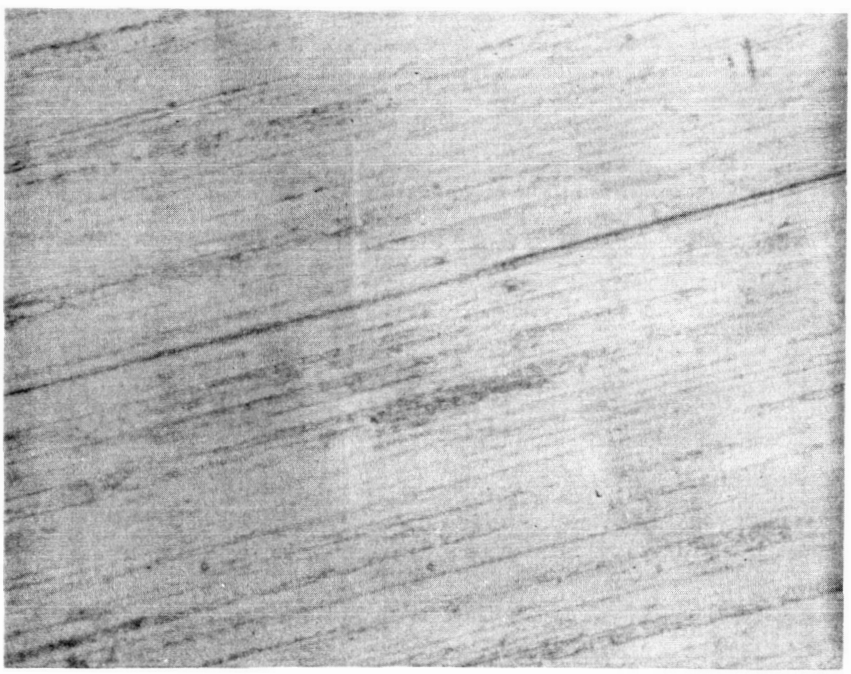

Figure 11. Photomicrograph of HRL 3.9 micron after machining

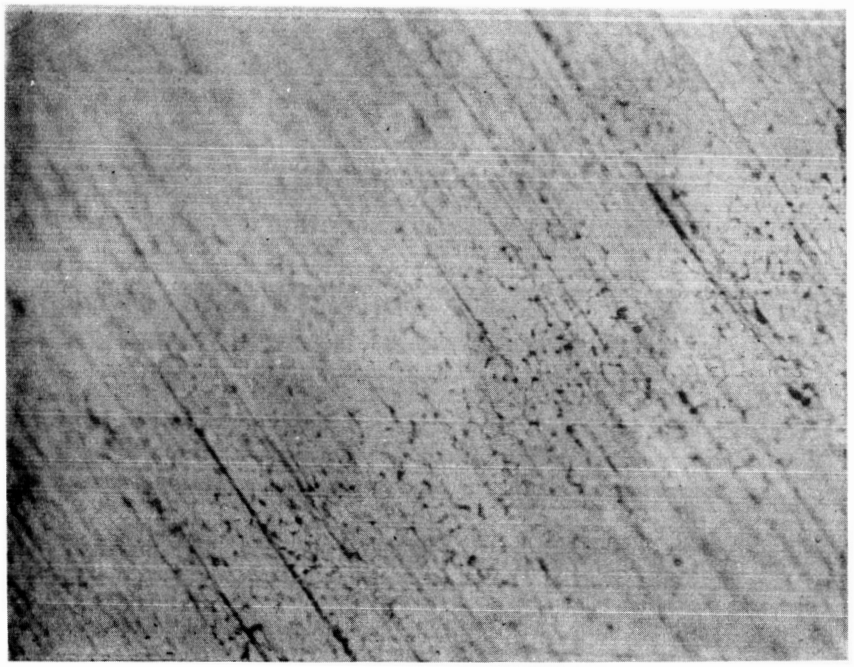

Figure 12. Photomicrograph of HRL 3.9 micron after de-infiltration of copper

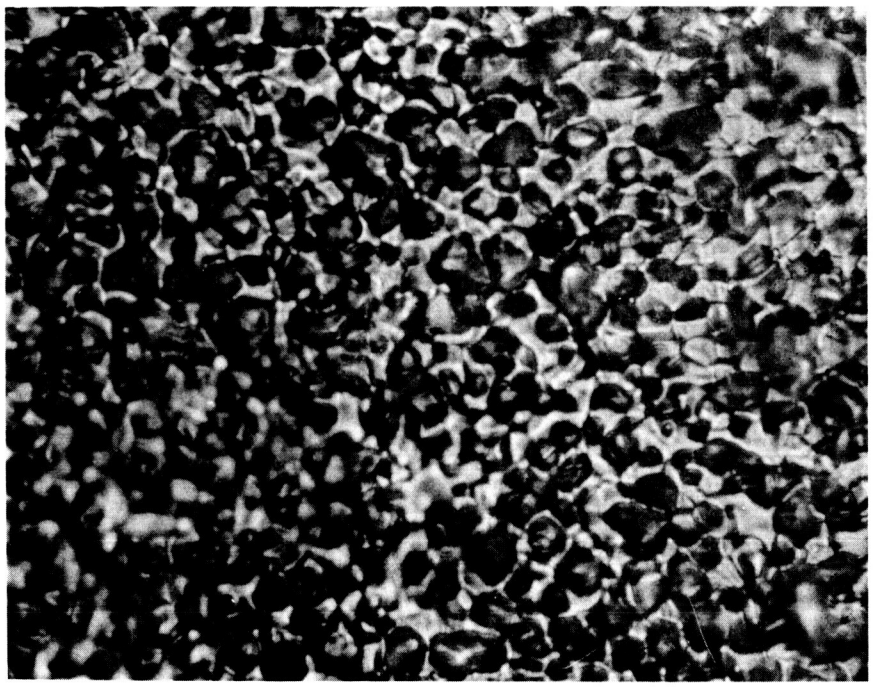

Figure 13. Photomicrograph of HRL 3.9 micron after slight electrolytic etching

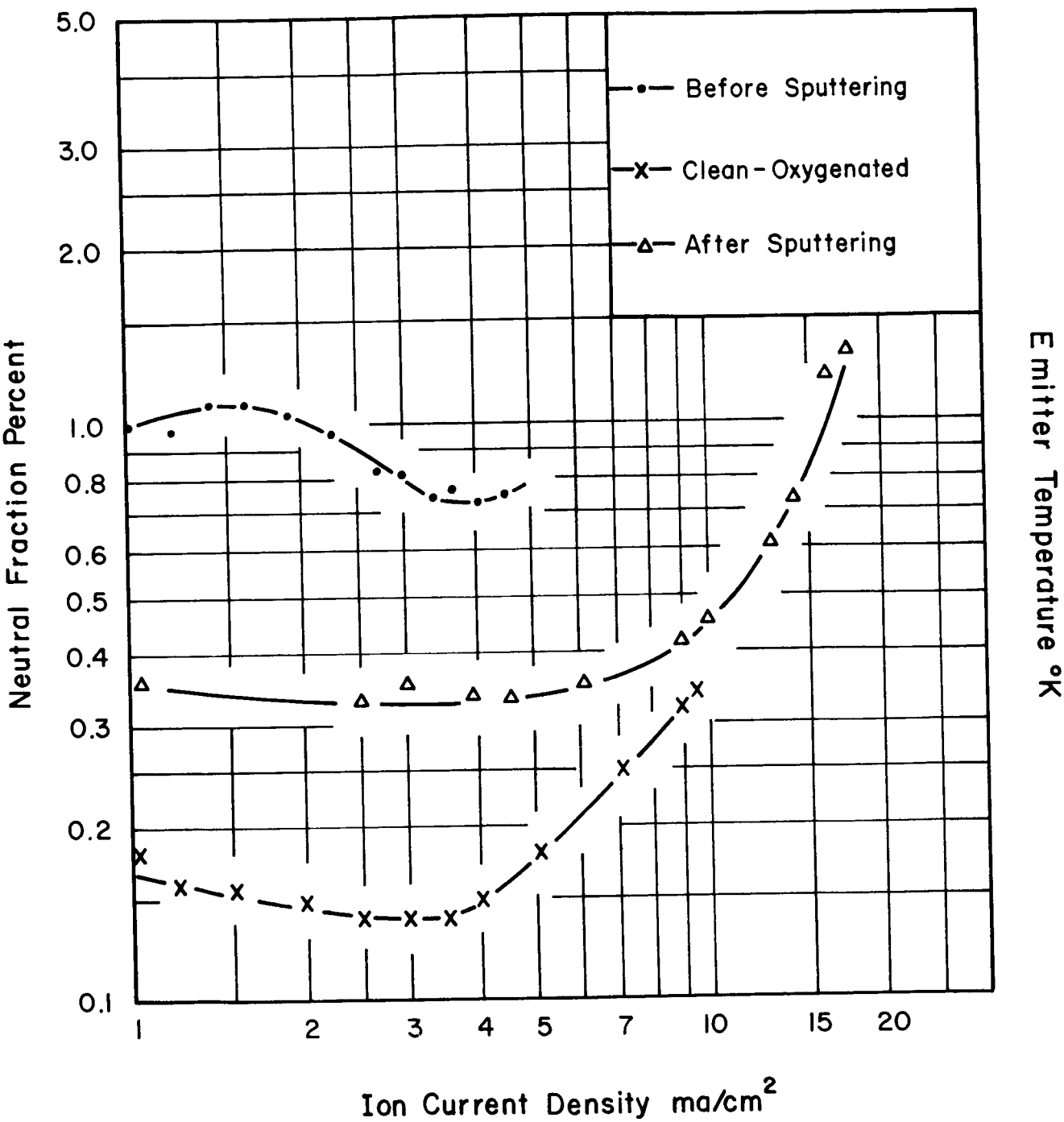

Figure 14. Neutral fraction as a function of current density

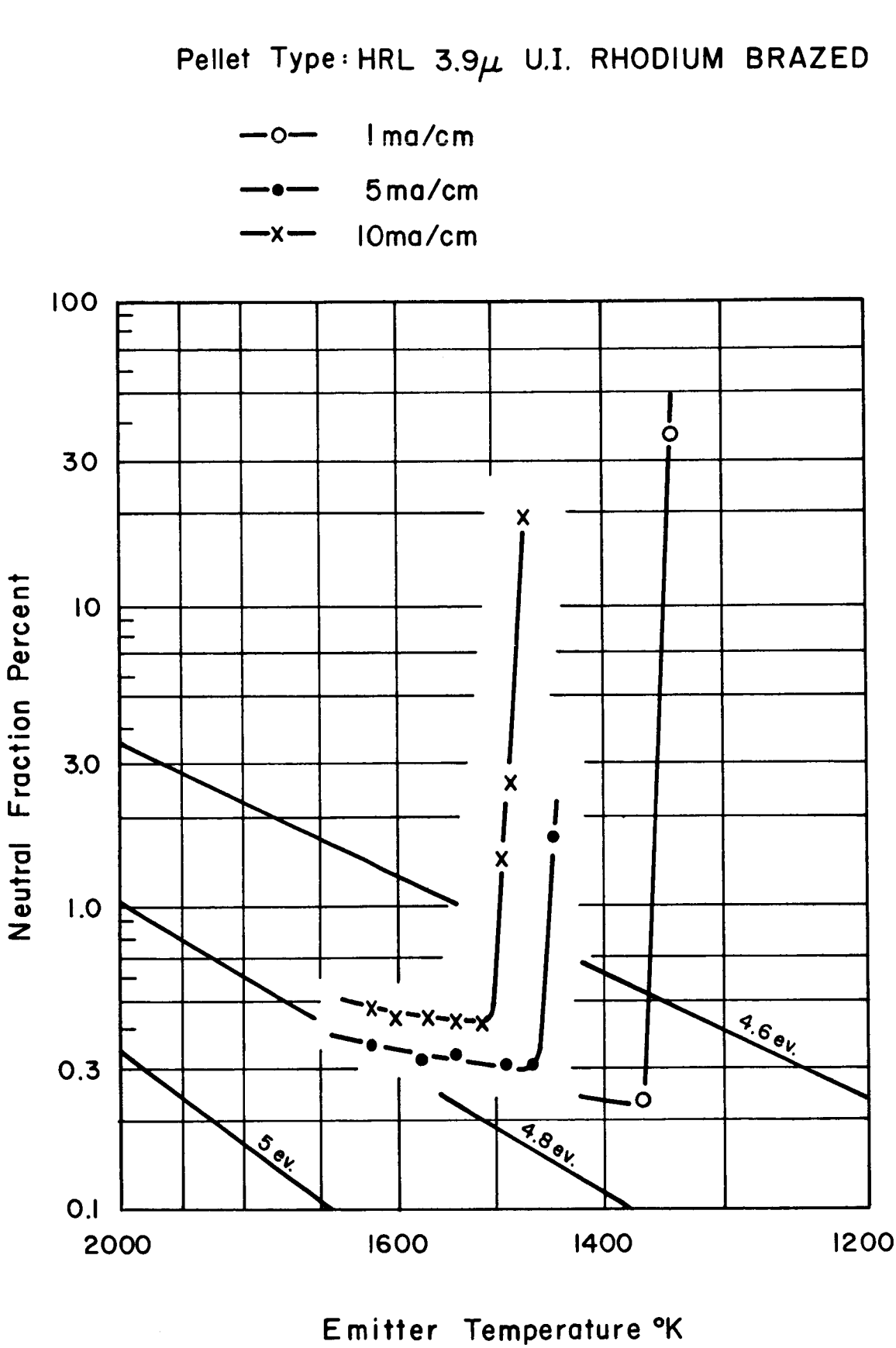

Figure 15. Neutral fraction as a function of emitter temperature

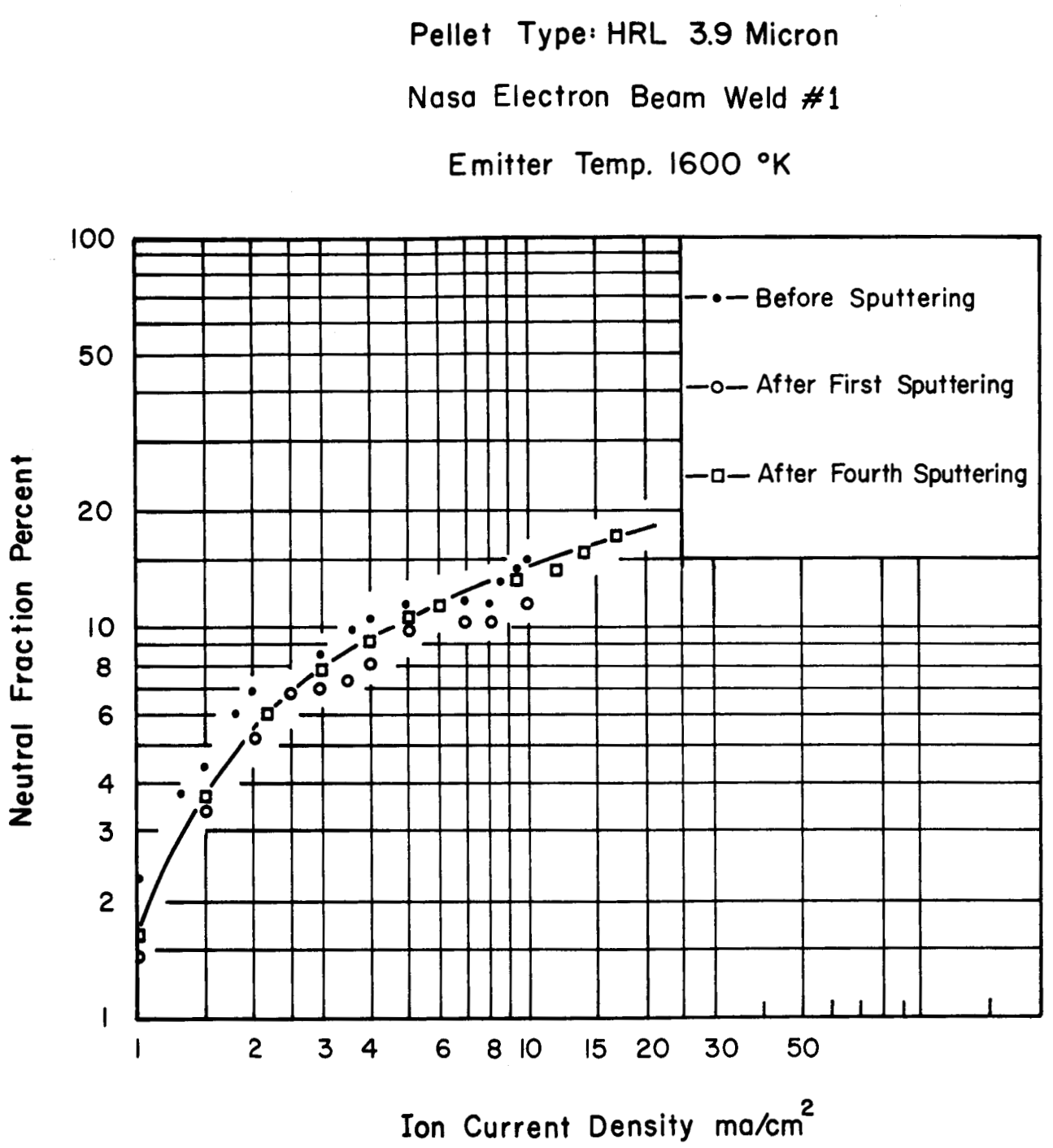

Figure 16. Neutral fraction as a function of cesium ion current density

of operation and four sputter cleanings. To assure that the high neutral readings were not due to our testing system, a tested HRL 3.9 μ U. of I. rhodium brazed source was used. The data from this source showed low neutral readings which coincided exactly with the previous results. This not only proved the contaminants of the HRL 3.9 μ electron beam welded source are on the source (possibly introduced in great depth during the welding) but also showed the consistency of our tests.

The critical temperatures of this source at 1, 5, 10 and 20 ma/cm^2 are shown in Figure 17. The measured transmissivity was 1.15×10^{-4} before the testing and 1.275×10^{-4} after the testing.

Test No. 4 - HRL 3.9 micron (NASA electron-beam welded No. 2)

In an attempt to explain the unexpected high neutral fraction of the previous sample, a second HRL 3.9 micron NASA electron-beam welded source was extensively tested. Special care was taken in the welding process to minimize the possibility of contamination. Figure 18 indicates an improvement in neutral fraction after each sputter cleaning. The decrease in neutral fraction by a factor of ten after the first sputtering indicates the majority of the contaminants are only on the surface of this source.

In Figure 19 the critical temperatures taken after each sputtering shows a decrease over 100 degrees after four sputter cleanings. Figure 20 illustrates the critical temperature vs. current densities for the clean surface.

The results of subjecting a clean surface to about one torr of air for thirty seconds are shown in Figures 21 and 22. The data shown in these figures was taken with the chamber pumped down to an order of 10^{-8} torr. The surface with adsorbed oxygen shows a low neutral fraction and

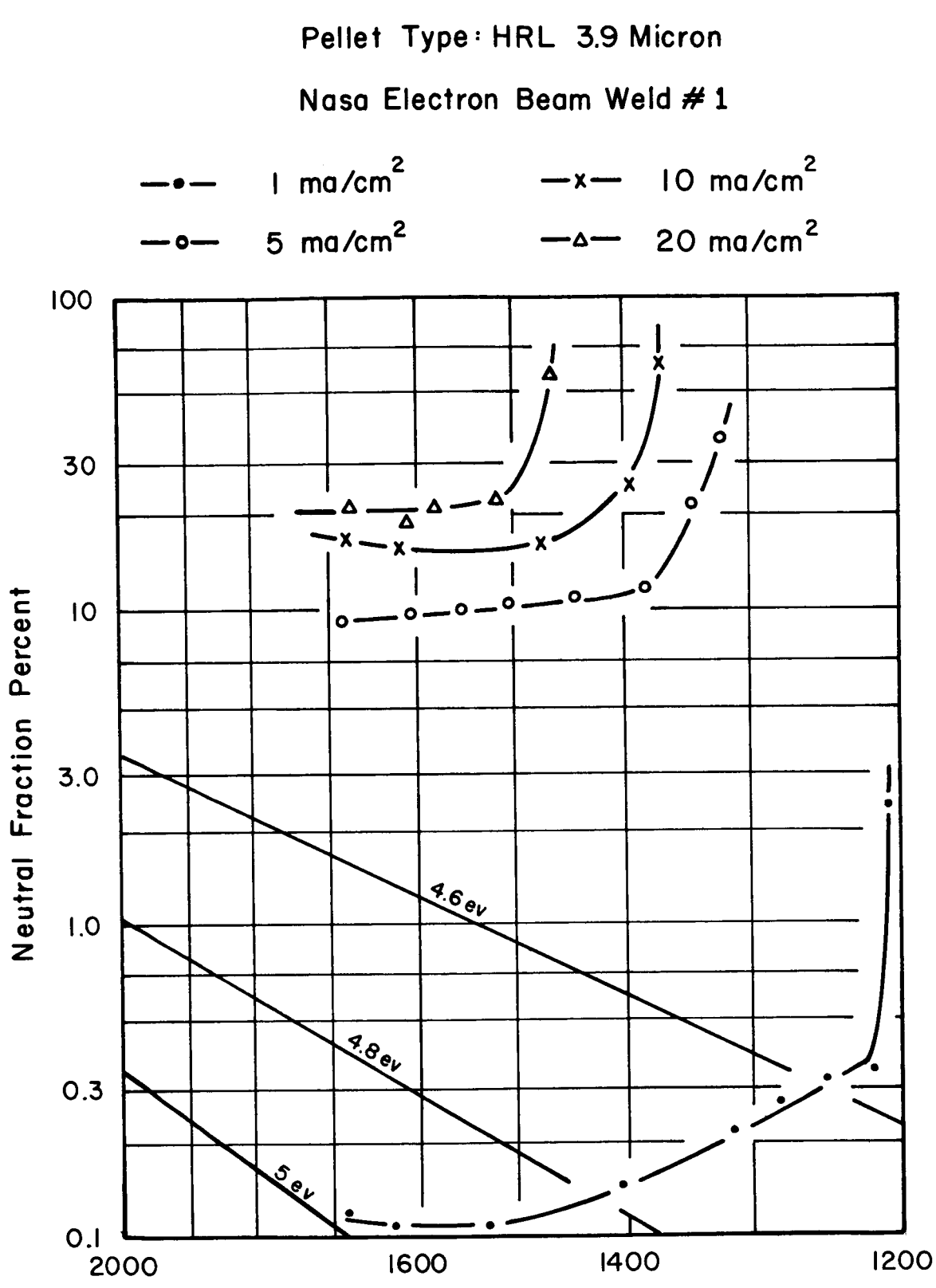

Figure 17. Neutral fraction as a function of emitter temperature

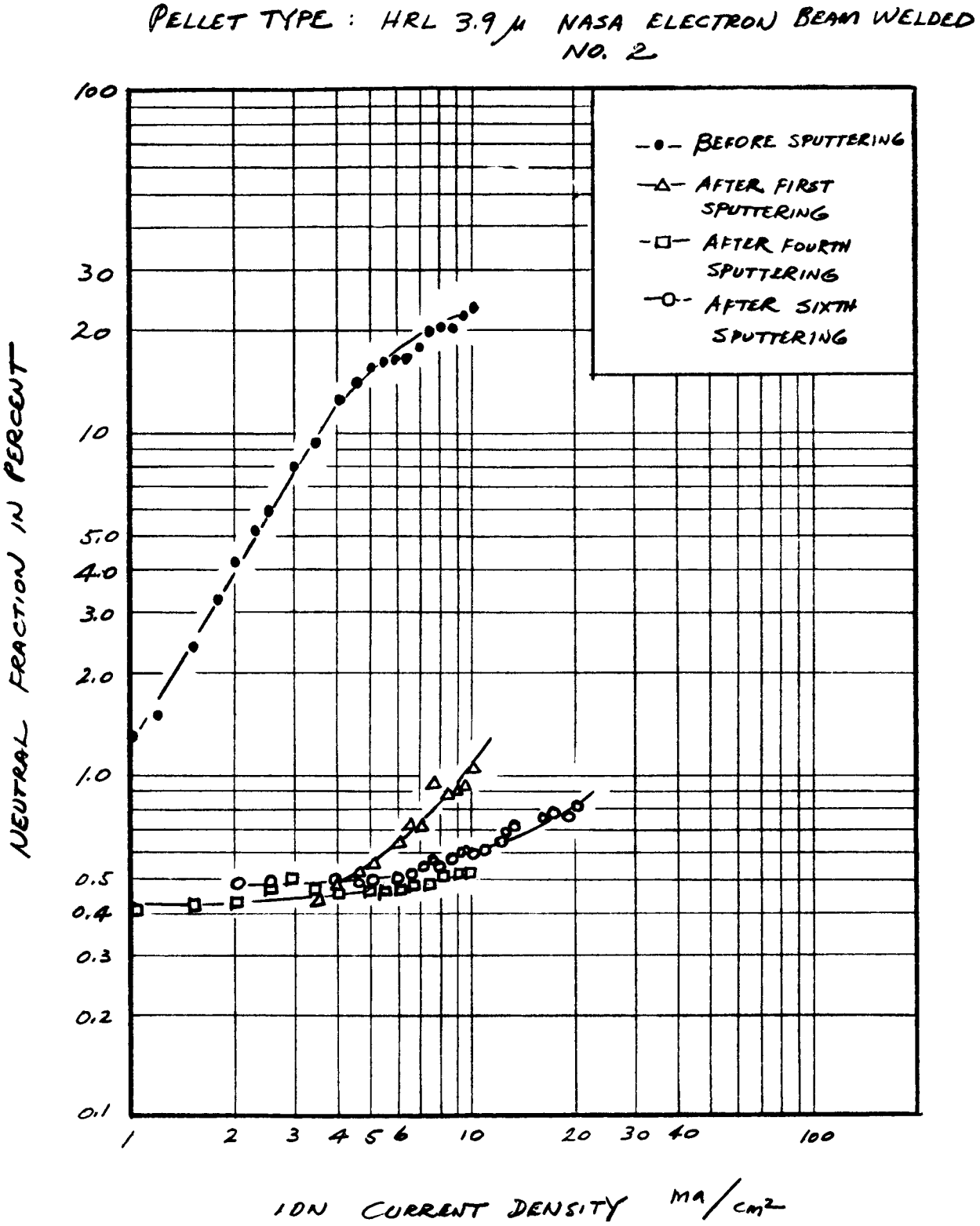

Figure 18. Neutral fraction as a function of cesium ion current density

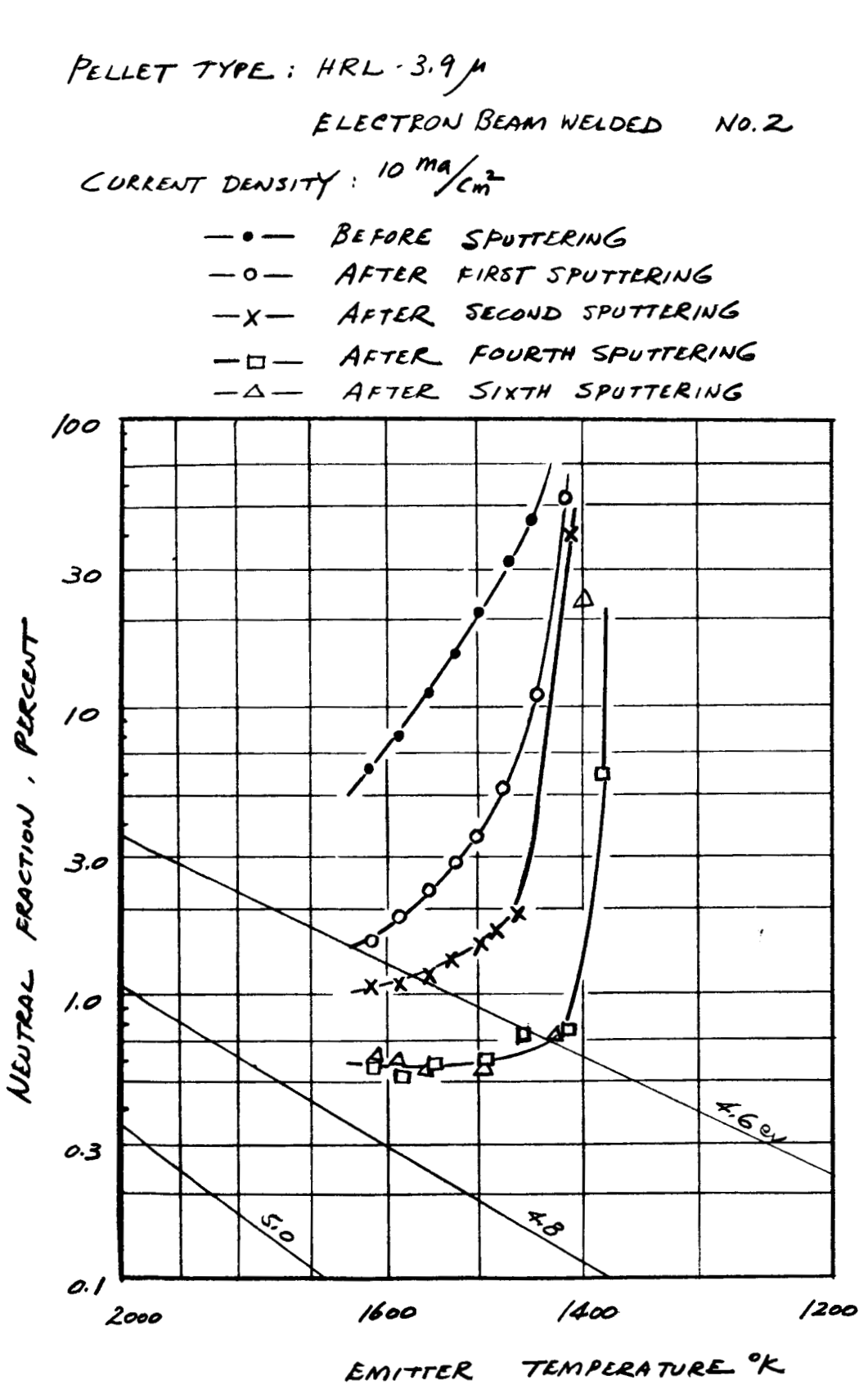

Figure 19. Improvement of critical temperatures after each sputter cleaning by cesium ions

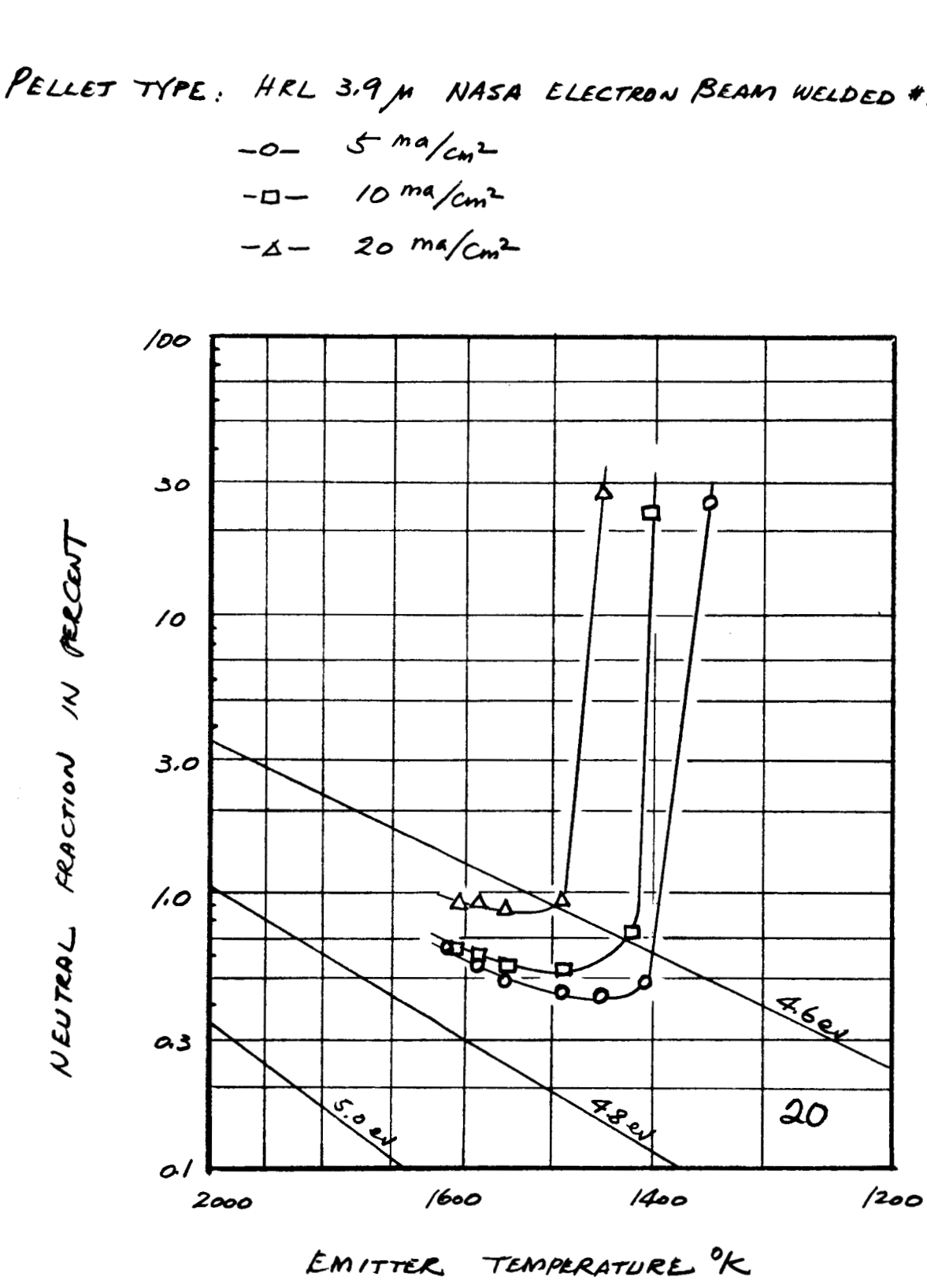

Figure 20. Neutral fraction as a function of emitter temperature

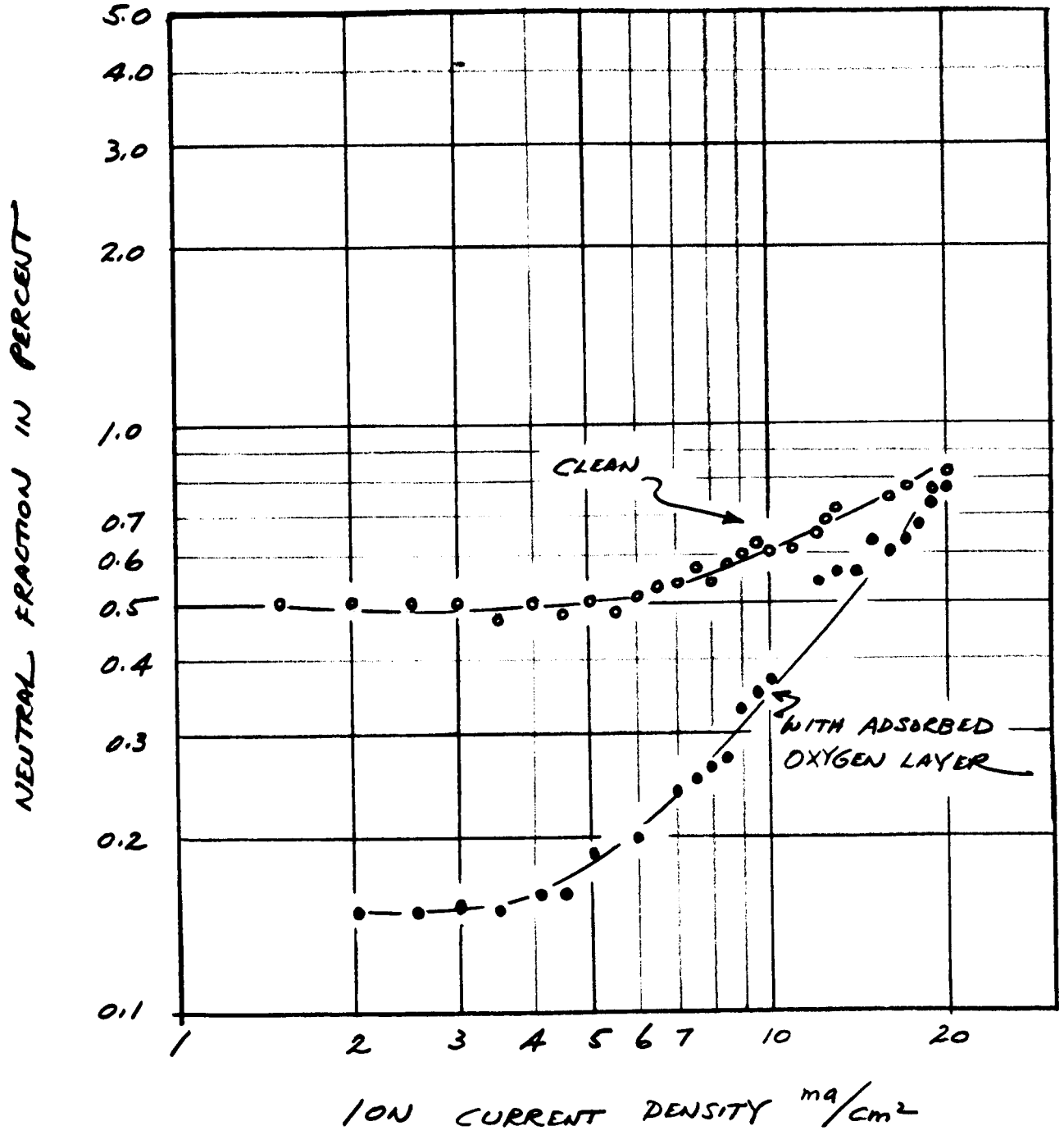

Figure 21. Neutral fraction as a function of cesium ion current for clean and oxygenated surface

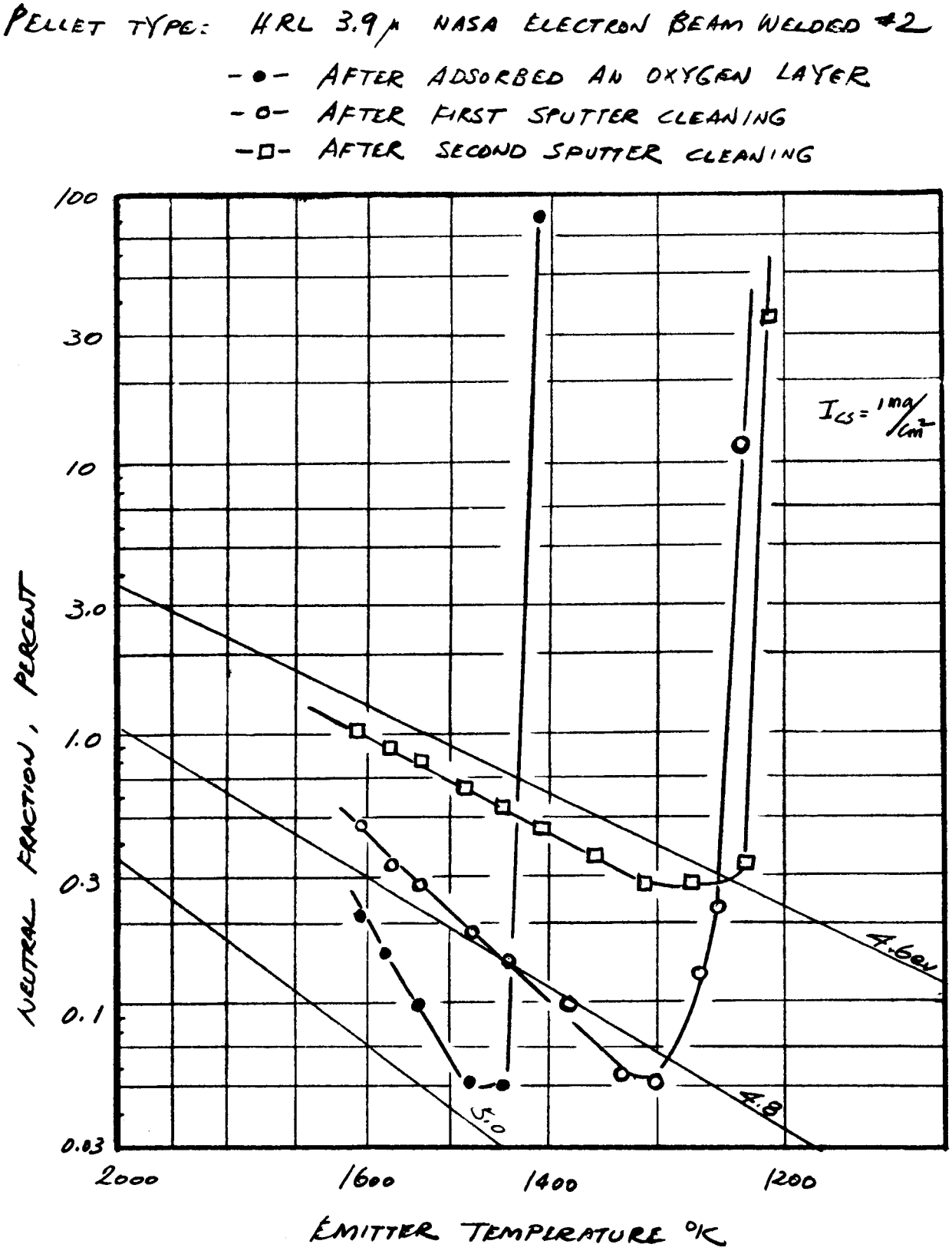

Figure 22. Sputter cleaning of an adsorbed oxygen layer on a clean tungsten surface

a high critical temperature. The decrease in critical temperature after two sputterings indicates that a clean surface can be obtained readily.

The transmissivity of this source was measured to be 1.30×10^{-4} before the testing and 1.31×10^{-4} after the testing.

Test No. 5 - LeRC 4.2 micron (NASA electron-beam welded)

In Figure 23 are shown the results of measurements of per cent neutral fraction as a function of current density from the source. The results show a very high neutral fraction before the first sputtering cleaning of the source. An immediate improvement is noted after the source was sputterred the first time. However, after seven sputterings, the neutral fraction was further reduced only by a factor of about two at low current density (1-5 ma/cm^2) and almost not at all for current densities above 6 ma/cm^2.

Figure 24 shows the neutral fraction as a function of emitter temperature for current densities of 1, 5, 10 and 20 ma/cm^2 after sputtering cleaning. The rapid degradation of performance with increasing current density and the slow increase of neutral emission at critical temperatures are the characteristic of this source.

The measured transmissivity of this source was 1.18×10^{-4} before testing and 1.13×10^{-4} after testing.

Test No. 6 - EOS 1B-N20 (EOS electron-beam welded)

Figures 25 and 26 are photomicrographs of the surface of EOS 1B-N20 with magnifications of 500 and 1000 respectively. This pellet has a very low equivalent solid density (51.55 per cent). It can be seen from the micrographs that the structure is very different from that of compressed spherical powders. The large dark areas of the micrographs should not be

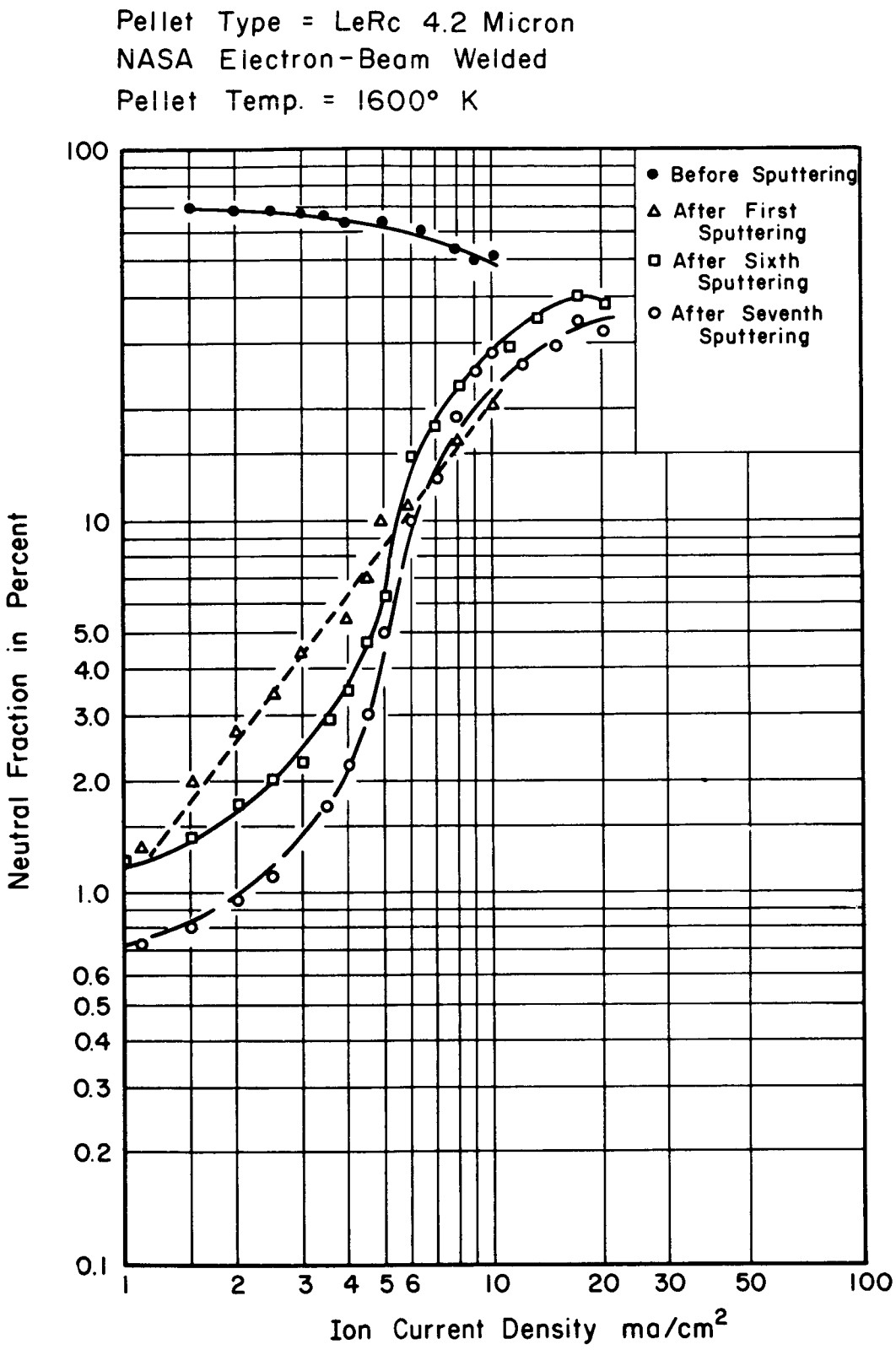

Figure 23. Neutral fraction as a function of cesium ion current density

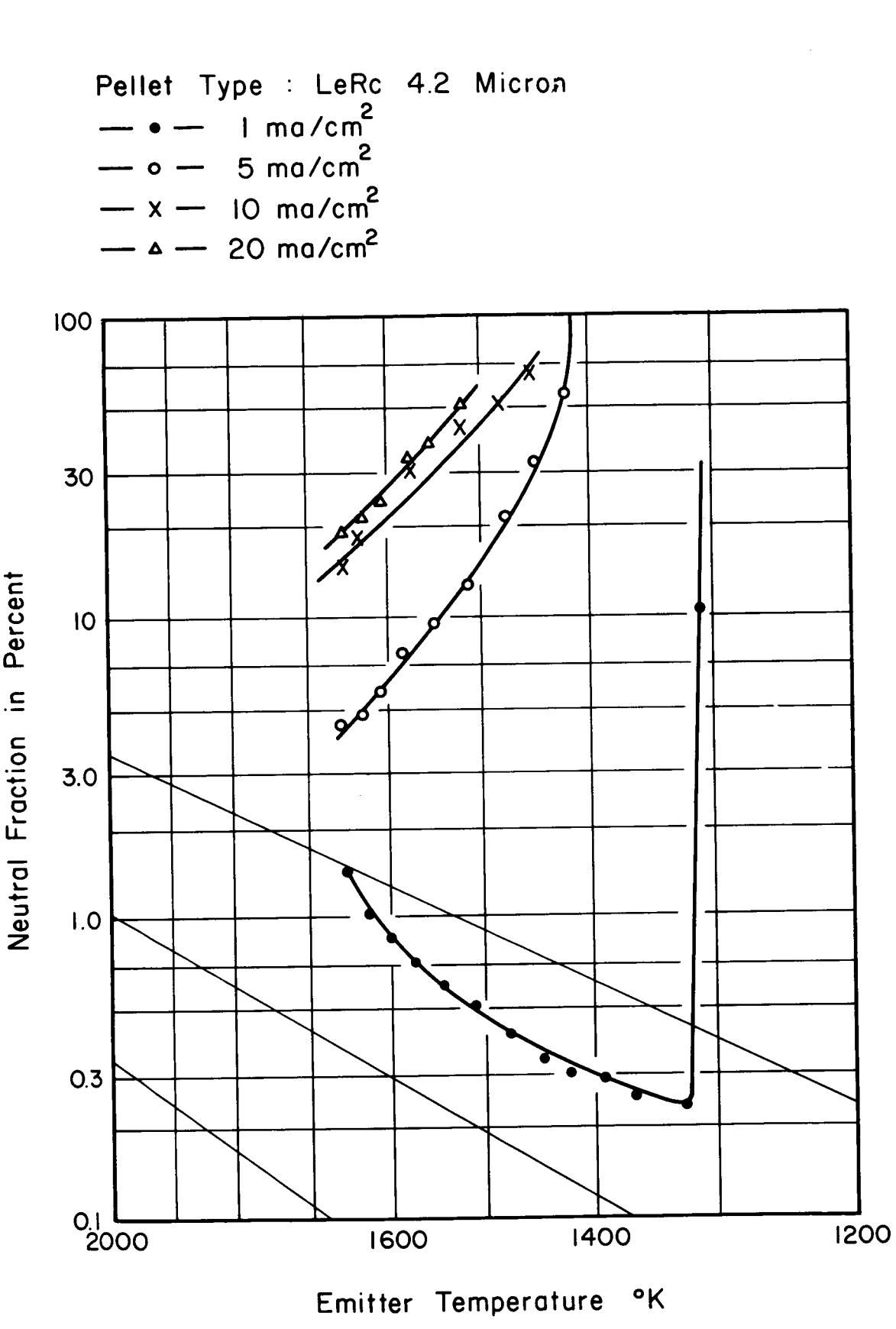

Figure 24. Neutral fraction as a function of emitter temperature

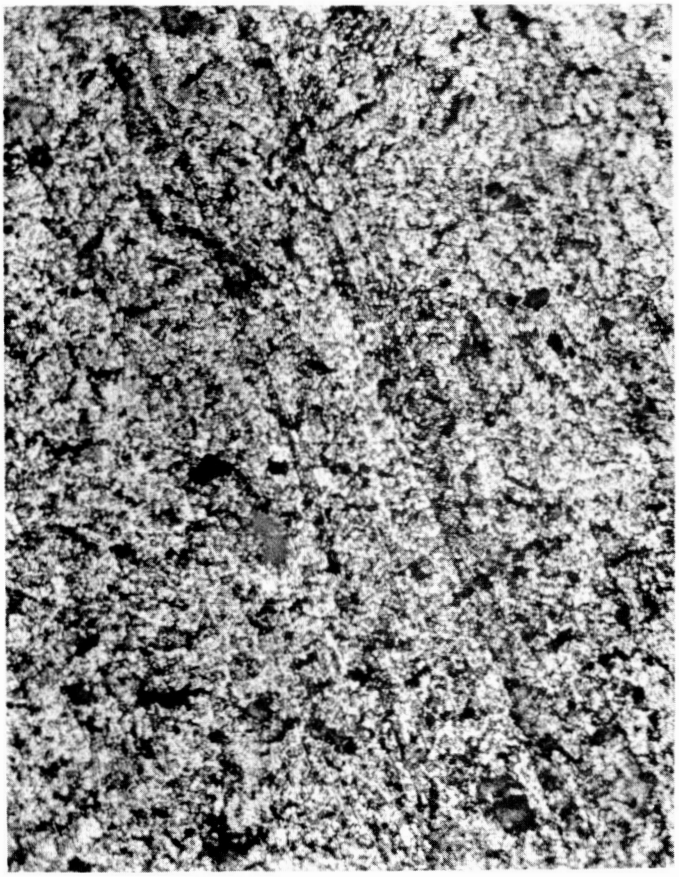

Figure 25. Photomicrograph at 500x of EOS 1B-N20

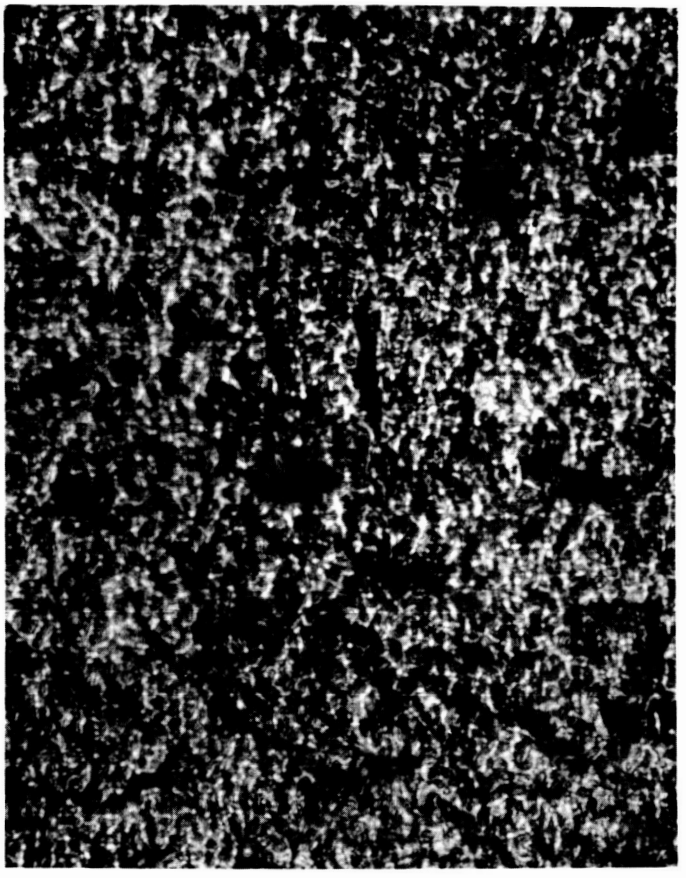

Figure 26. Photomicrograph at 1000x of EOS 1B-N20

interpreted as holes on the surface but rather are actually cavities of the same material from the surface. The method of preparation of this pellet was not supplied.

Figure 27 shows the percent neutral fraction as a function of current density to 10 ma/cm^2. It should be noted that there was little change in the source after the initial cleaning. It is obvious that extreme care was taken in the preparation and mounting of this source to avoid any possible contamination of the surface. The curve in Figure 1 is extended as a dotted portion into the range above 10 ma/cm^2. This represents our estimation of the higher current density behavior of the source. Data was not taken in this range because of the extra area of this particular source. The system used in these tests were designed to handle a source of 0.12 cm^2 area at a current density of up to 20-25 ma/cm^2. To reach the same current densitites with an increase in the source area to 0.168 cm^2 and maintain emission limited characteristics required higher potentials than are possible in the system. Consequently data are reported only to 10 ma/cm^2.

Figure 28 shows the neutral fraction as a function of the source temperature and provides critical temperature data for the source. The curves shown are for the clean source. The source critical temperature when initially mounted (no cleaning) as compared with the critical temperature after one sputtering was about 60° higher. Successive cleanings (sputterings) did not change the critical temperature by more than 15 to 20 degrees.

The transmissivity of this source was measured and found to be 2.26 x 10^{-4} before mounting in the test system. After removal of the source from the test system the transmissivity was 2.85 x 10^{-4}.

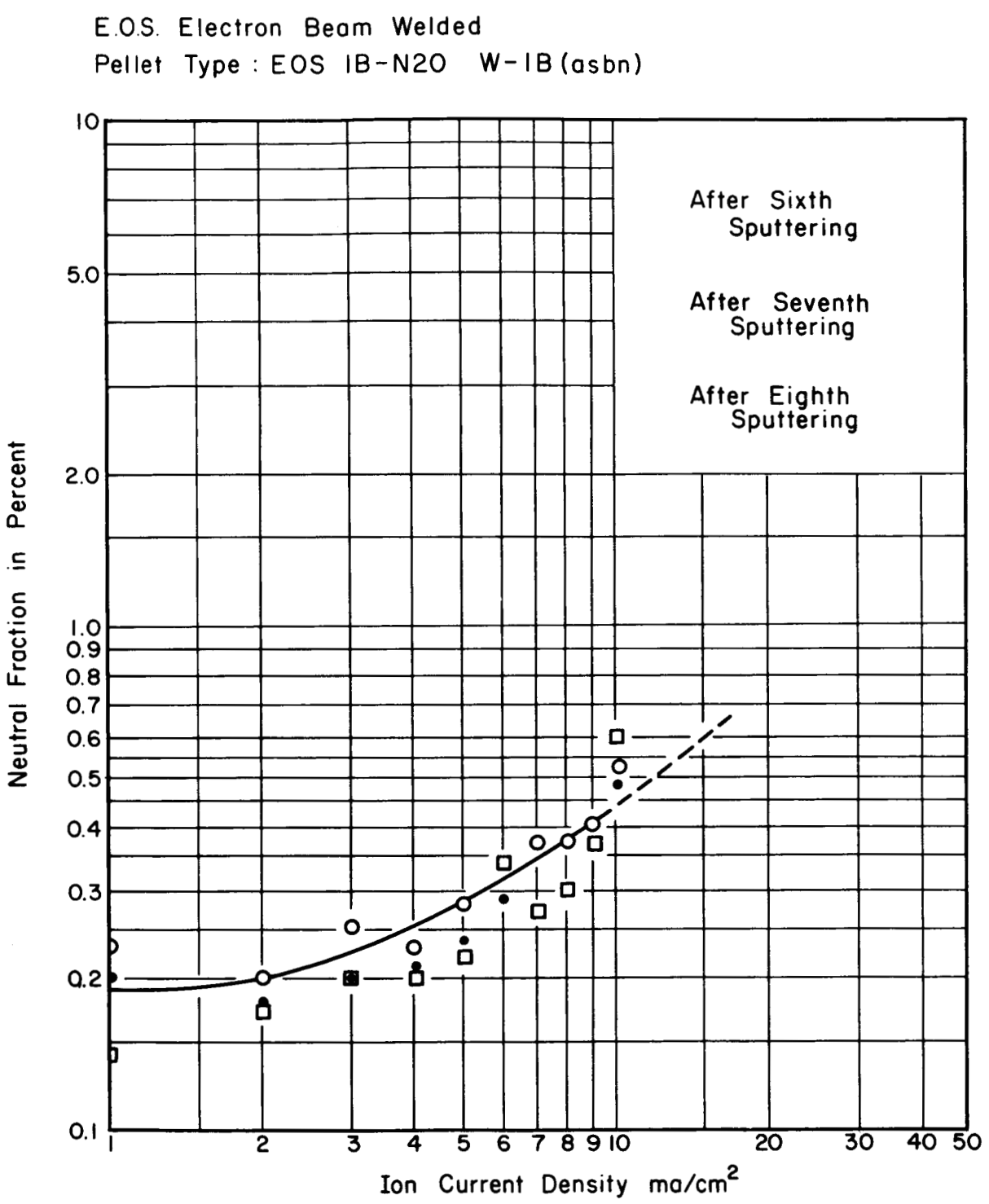

Figure 27. Neutral fraction as a function of cesium ion current density

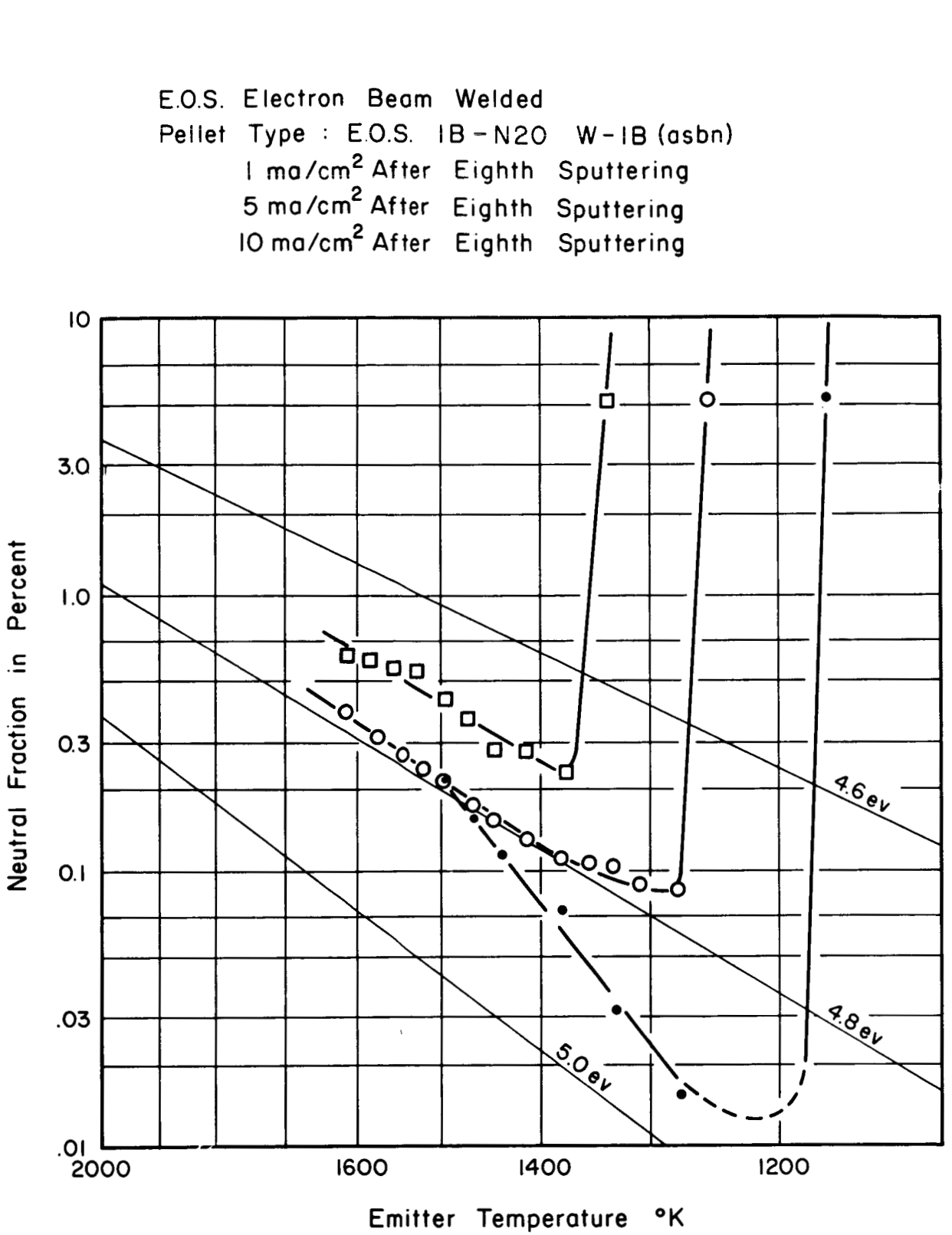

Figure 28. Neutral fraction as a function of emitter temperature

From all indications this source has excellent characteristics and as has been mentioned, was prepared with extreme cleanliness.

Test No. 7 - LeRC 3.5 micron

Figure 29 shows the cesium neutral fraction as a function of ion current density for this source. Before the source was cleaned by sputtering the neutral fraction tended to be relatively high at the higher current densities. After several sputterings to clean the surface, the source appeared to be clean and behaved as it should for a clean surface. The curve designated "after fourth sputtering" is typical. Several cycles of the source were made with ion current densities from 1.0 to 20.0 ma/cm^2. During one of these cycles, a problem in the system developed and the vacuum chamber was opened to correct the fault. Following pump-down, the source was operated throughout the same range of current densities. A typical set of data is shown in Figure 29 and designated "after ninth sputtering." The results shown indicate that the source surface was oxygenated. This assumption is corroborated by the data shown in Figure 30, in which the neutral fraction is displayed as a function of temperature. The critical temperature found on the curve labeled "after fourth sputtering" is much lower than that for the "eighth" and "ninth" sputtering curves thus indicating along with the data in Figure 29 that the source was oxygenated after exposure to the atmosphere as mentioned.

The data shown in Figure 31 was taken after the fourth sputtering and before opening the vacuum system and hence can be considered typical of the source with a clean surface.

The transmissivity of the source was measured both before and after it was tested with cesium. In both cases the transmissivity was found to be 7.5×10^{-5}.

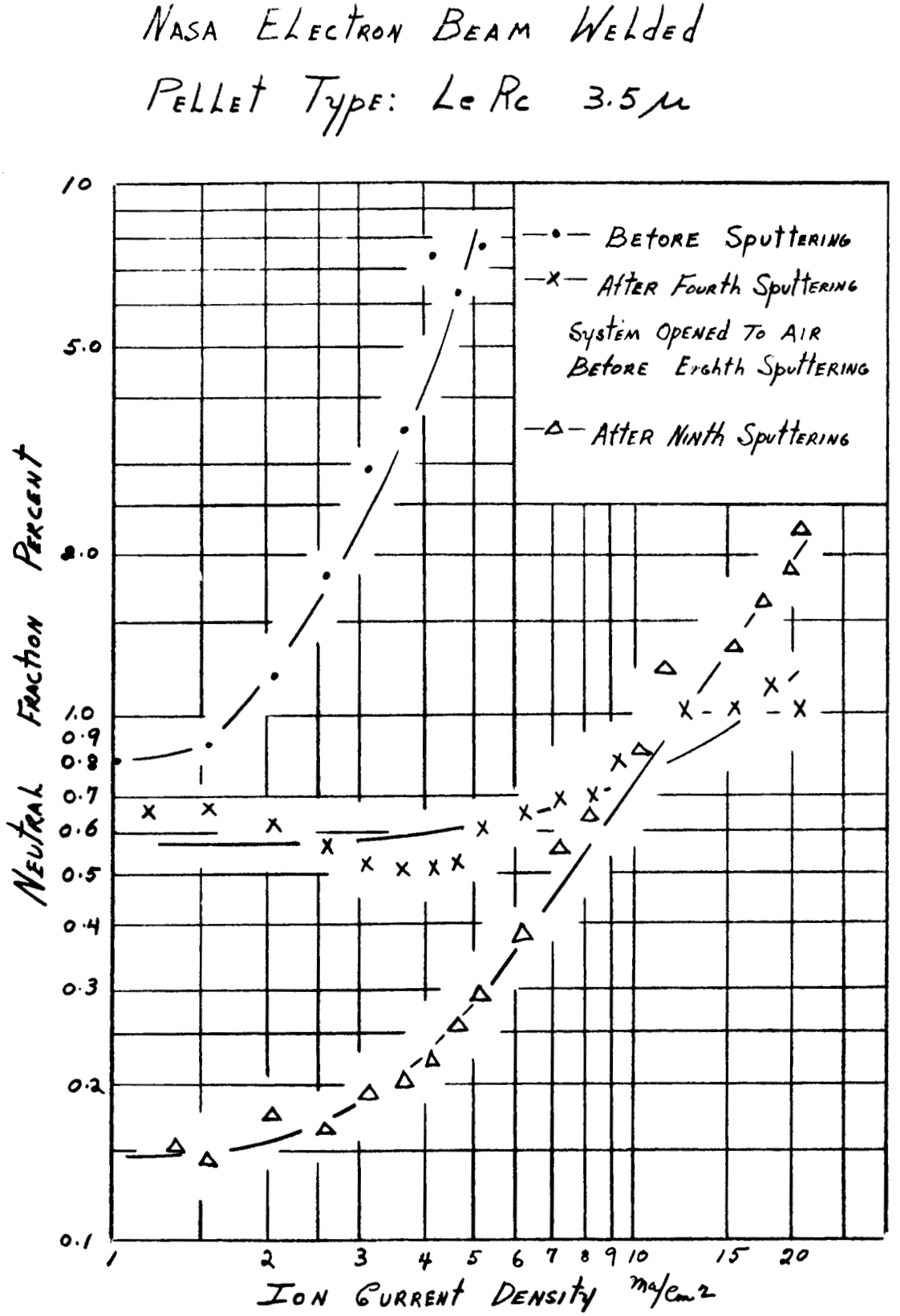

Figure 29. Neutral fraction as a function of current density

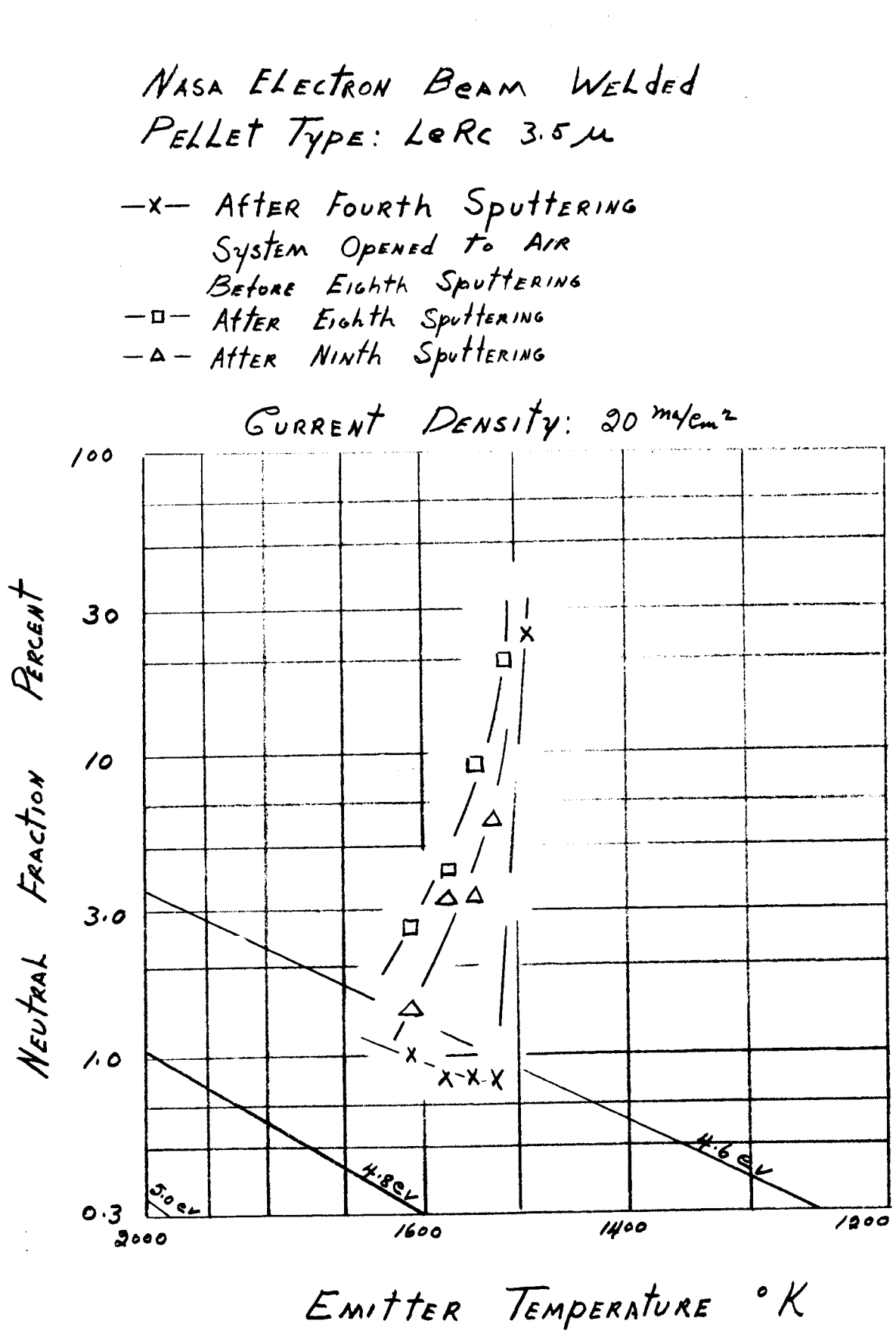

Figure 30. Neutral fraction as a function of emitter temperature

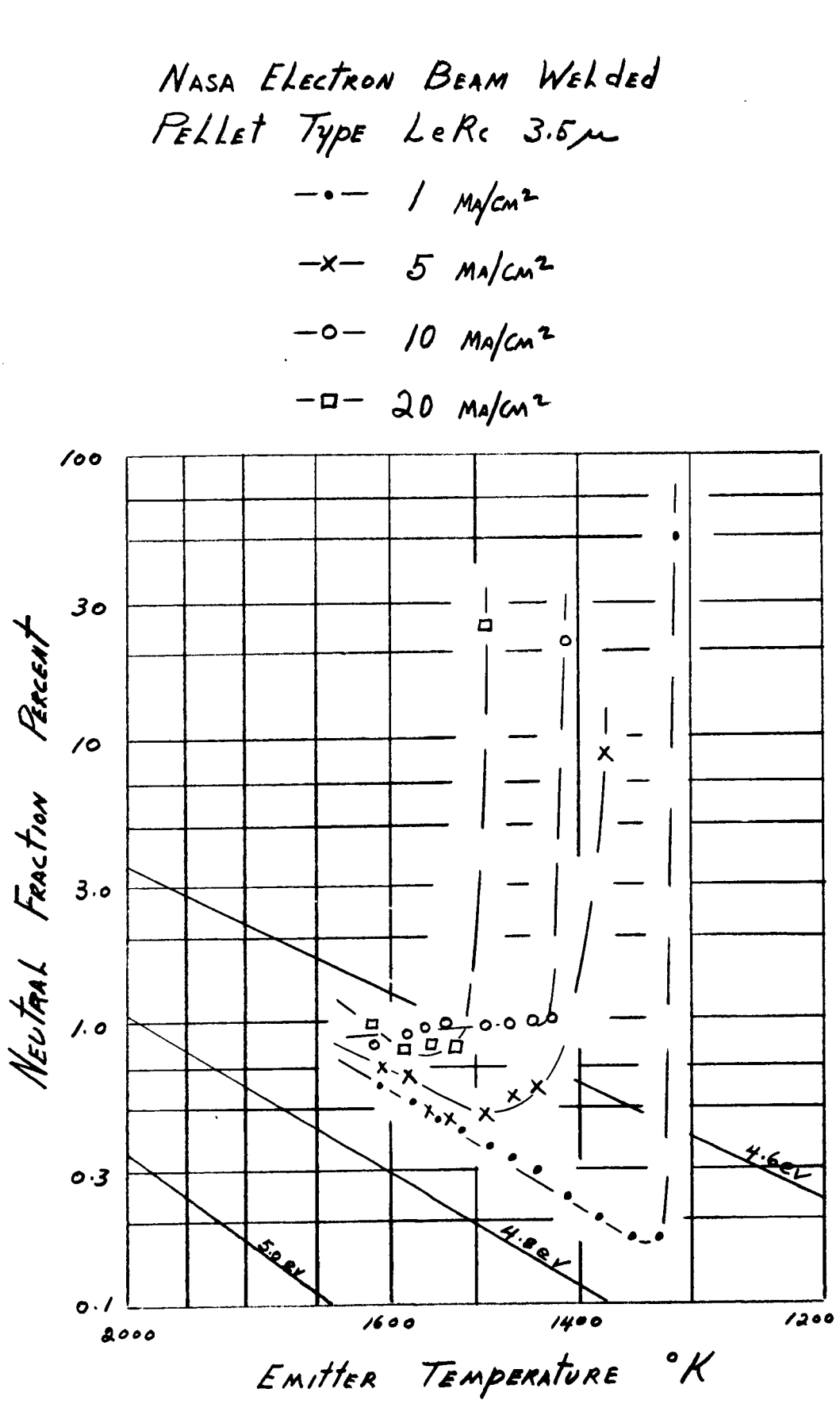

Figure 31. Neutral fraction as a function of emitter temperature

Test No. 8 - EOS ORNL 4.2 micron

When the EOS ORNL 4.2 micron sample was first placed in operation, its neutral fraction was extremely high. The neutral fraction decreased considerably after the first sputtering as shown in Figure 32. The rapid increase of neutral fraction with increasing current density indicates poor pore distribution. The improvement of cesium neutral fraction and critical temperature after repeated sputter cleaning is demonstrated in Figures 32 through 36. The neutral fraction as a function of emitter temperature for a clean surface is shown in Figure 37.

The measured transmissivity was 1.075×10^{-4} before testing and 1.63×10^{-4} after testing.

Test No. 9 - EOS ORNL 3.5 micron

This source is similar to ORNL 4.2 micron in view of the high neutral fraction as it was first placed in operation. The sudden jump in neutral fraction in the first run when the current density increased to 4 ma/cm^2 indicates contaminants were brought out to the surface from the interior of the pores. The improvement of neutral fraction as a function of current density as the source was repeatedly sputter cleaned is shown in Figure 38. Figures 39 through 42 show the change in critical temperatures before and after sputter cleaning for different current densities. The transmissivity was measured to be 1.36×10^{-4} before testing and 1.31×10^{-4} after testing.

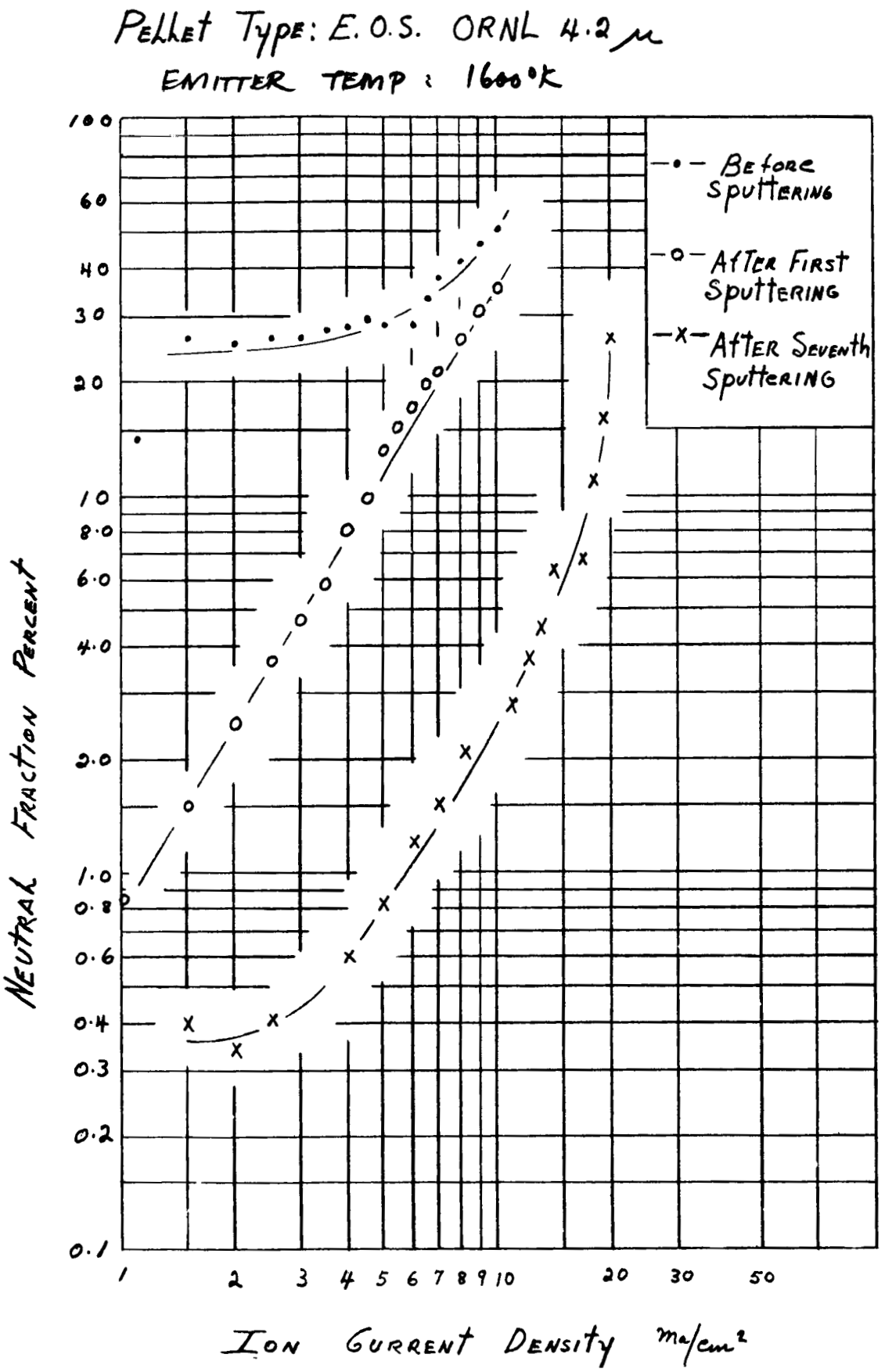

Figure 32. Neutral fraction as a function of current density

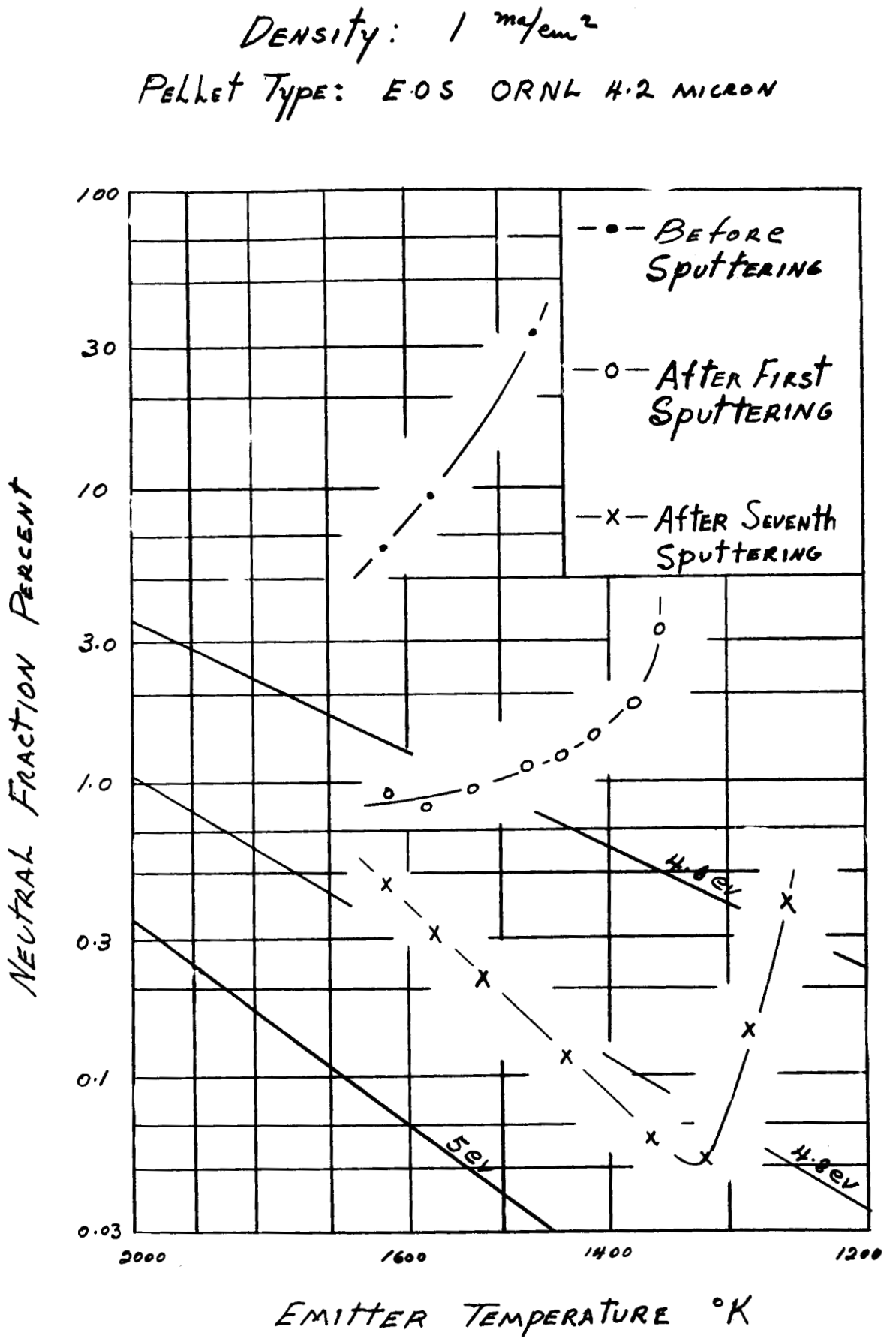

Figure 33. Neutral fraction as a function of emitter temperature

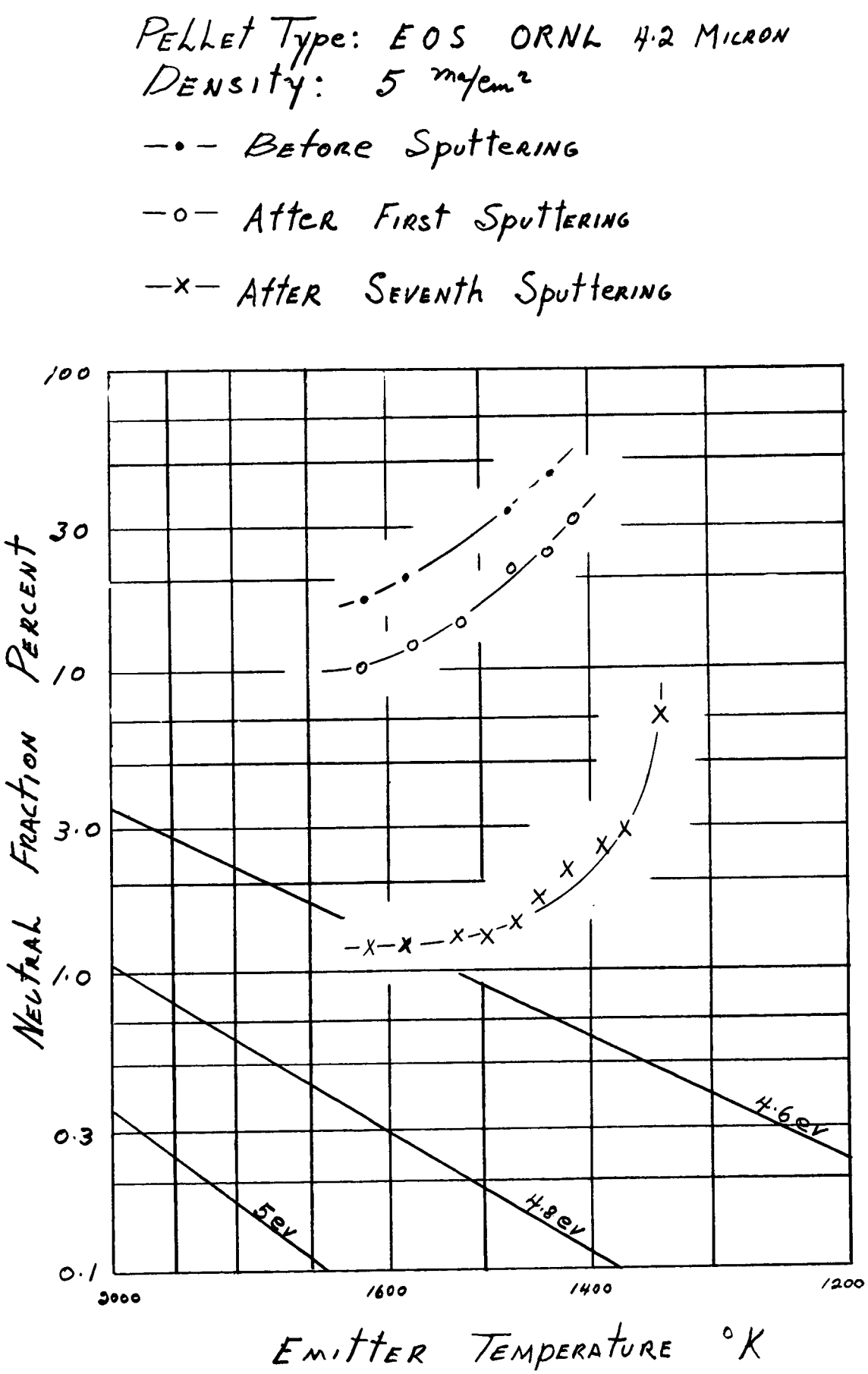

Figure 34. Neutral fraction as a function of emitter temperature

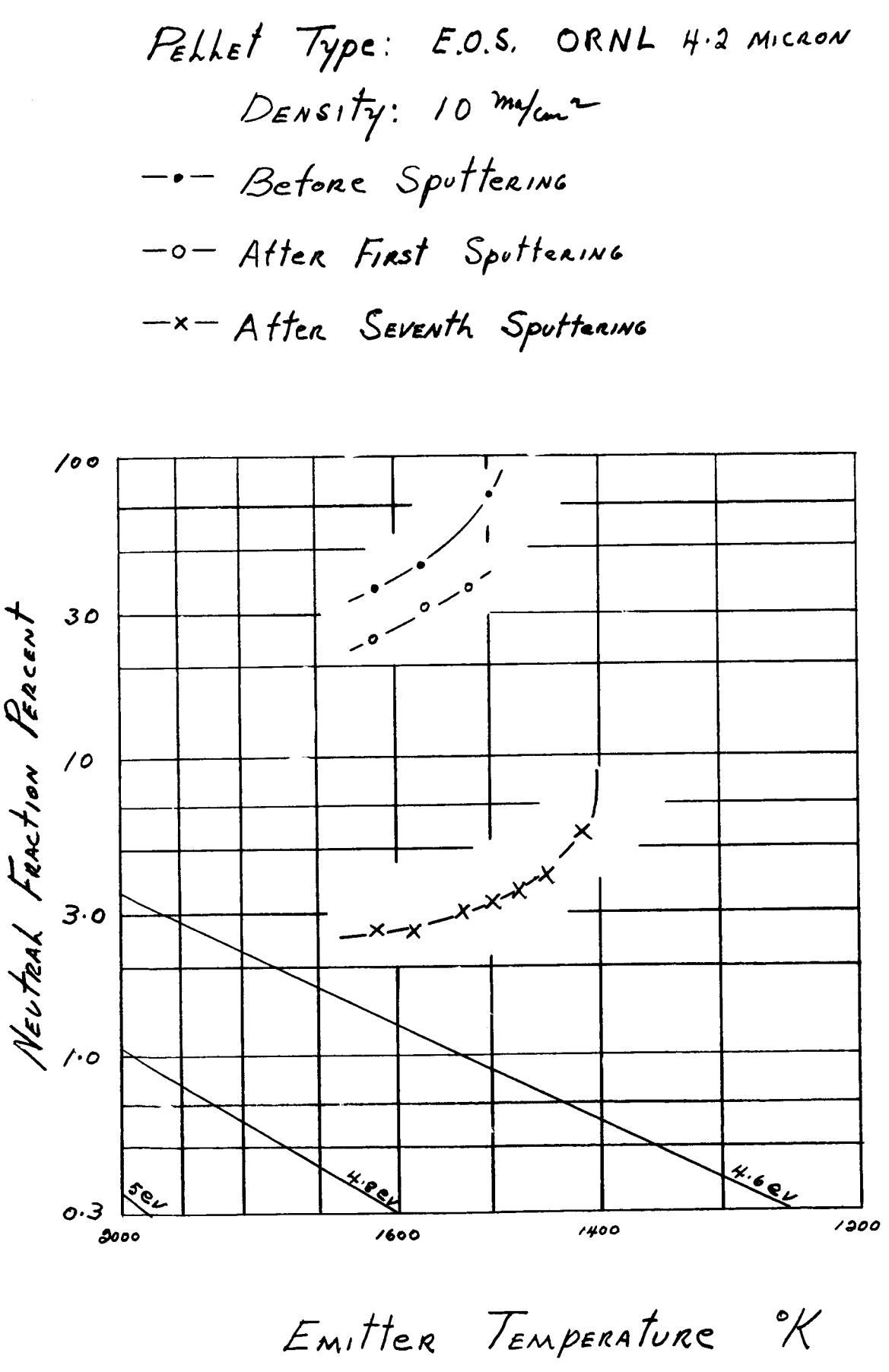

Figure 35. Neutral fraction as a function of emitter temperature

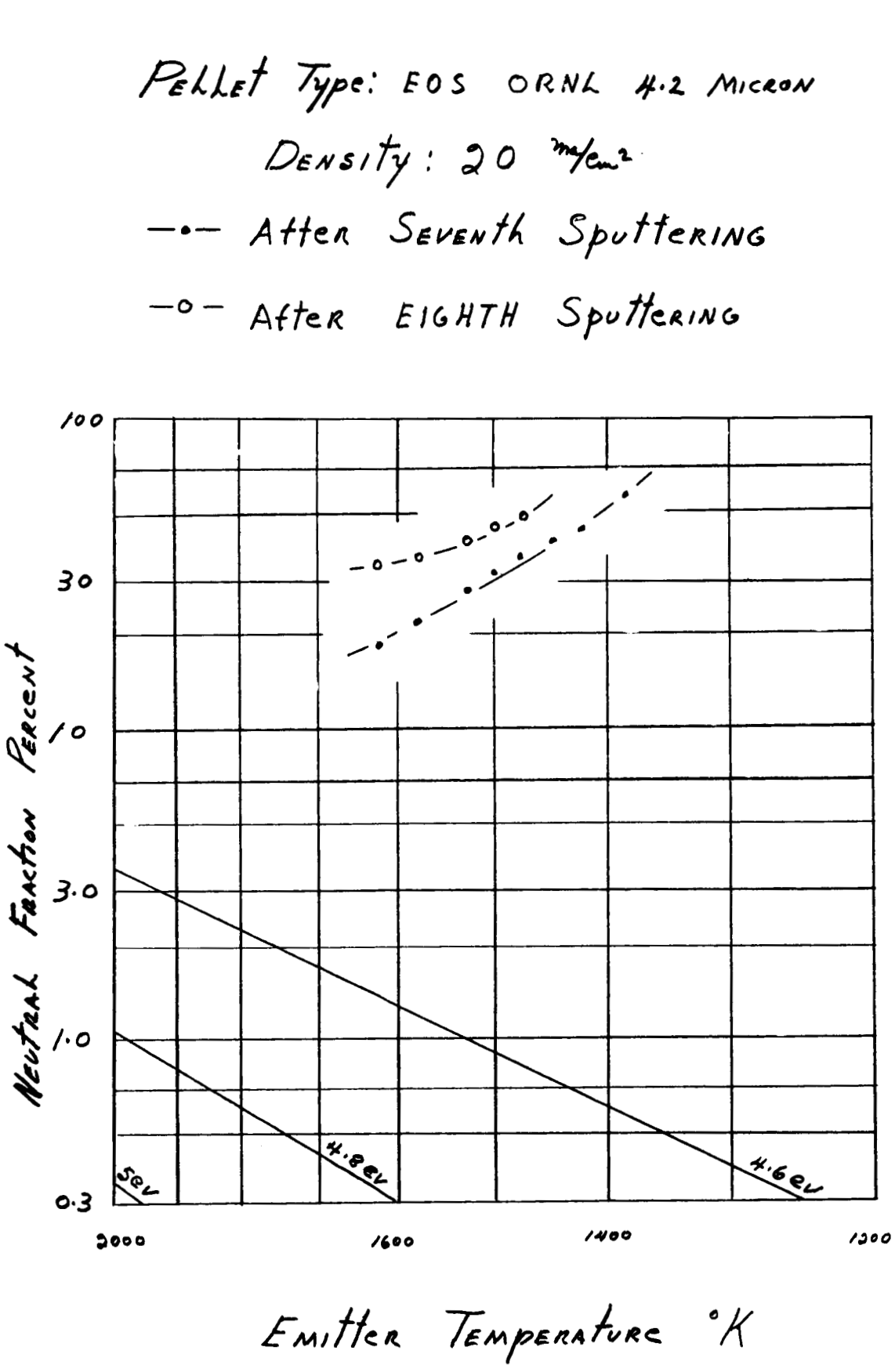

Figure 36. Neutral fraction as a function of emitter temperature

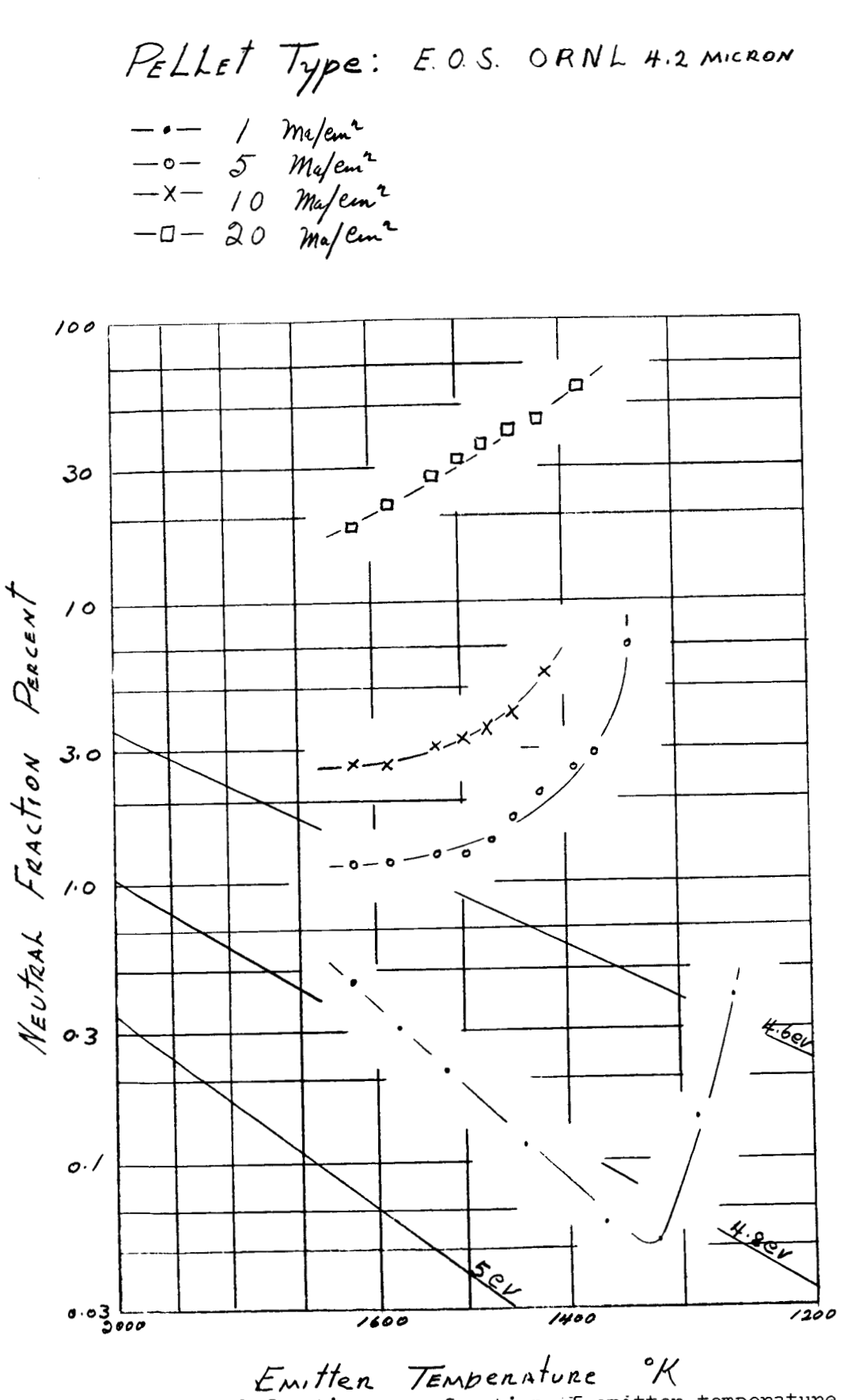

Figure 37. Neutral fraction as a function of emitter temperature

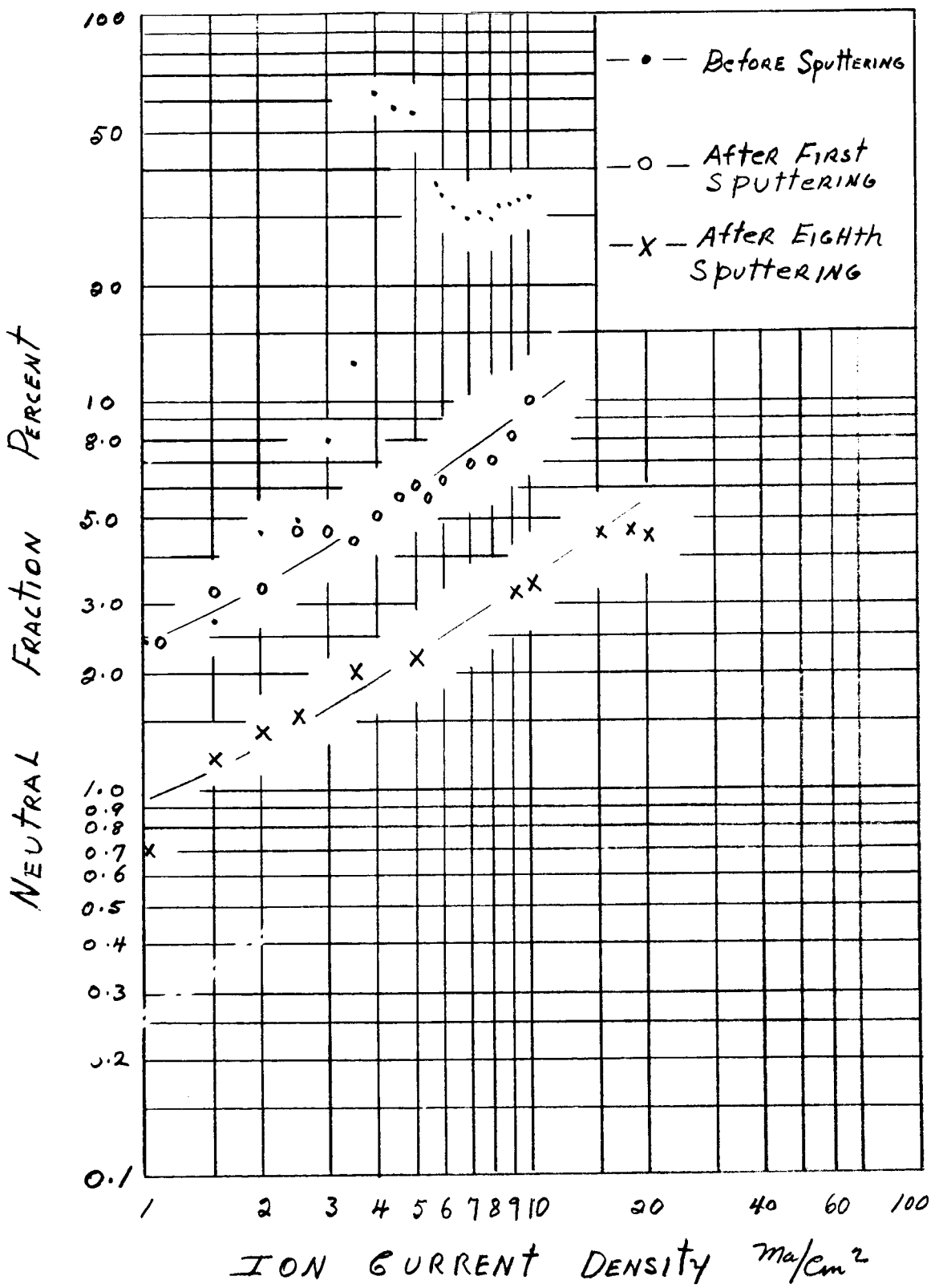

Figure 38. Neutral fraction as a function of current density

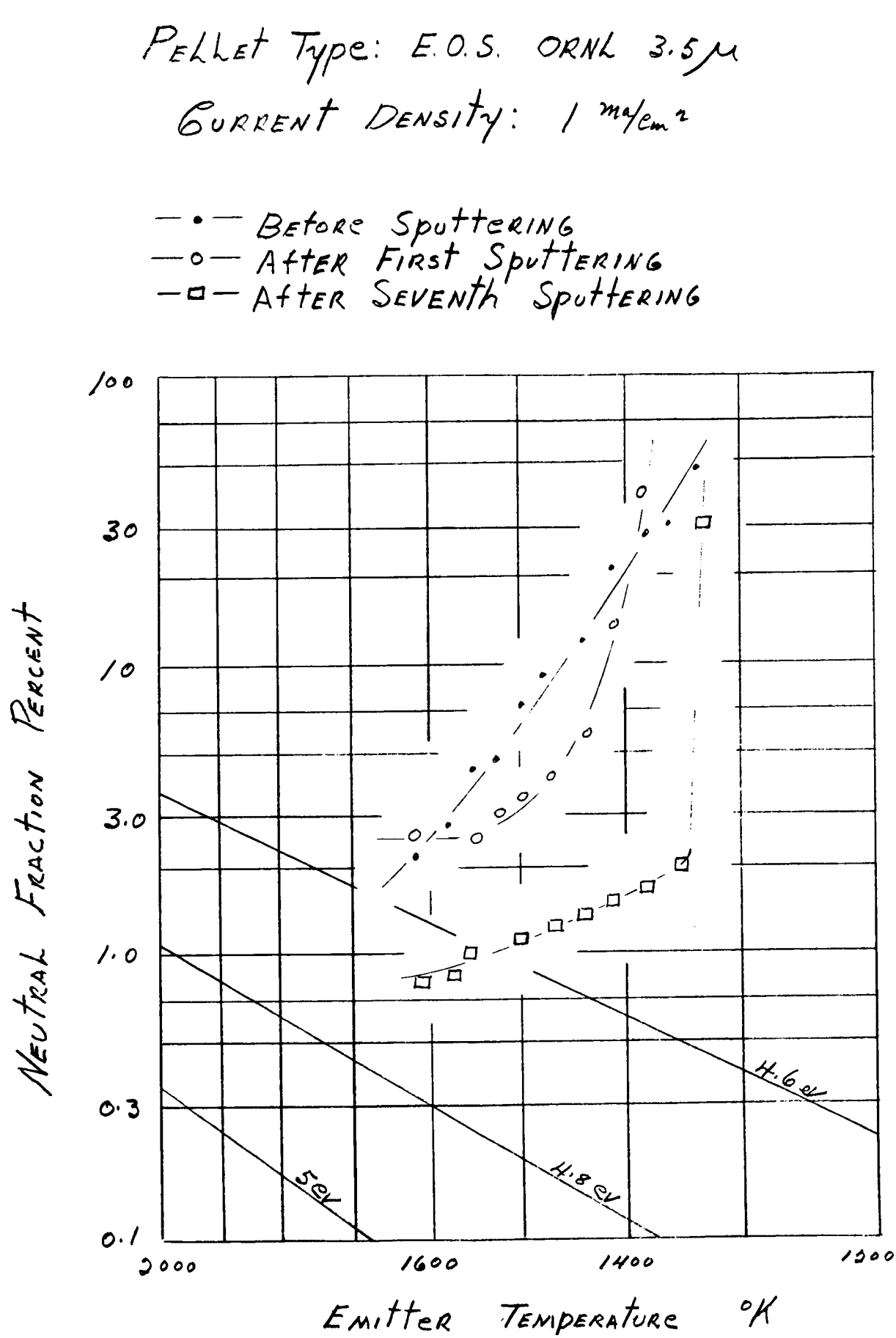

Figure 39. Neutral fraction as a function of emitter temperature

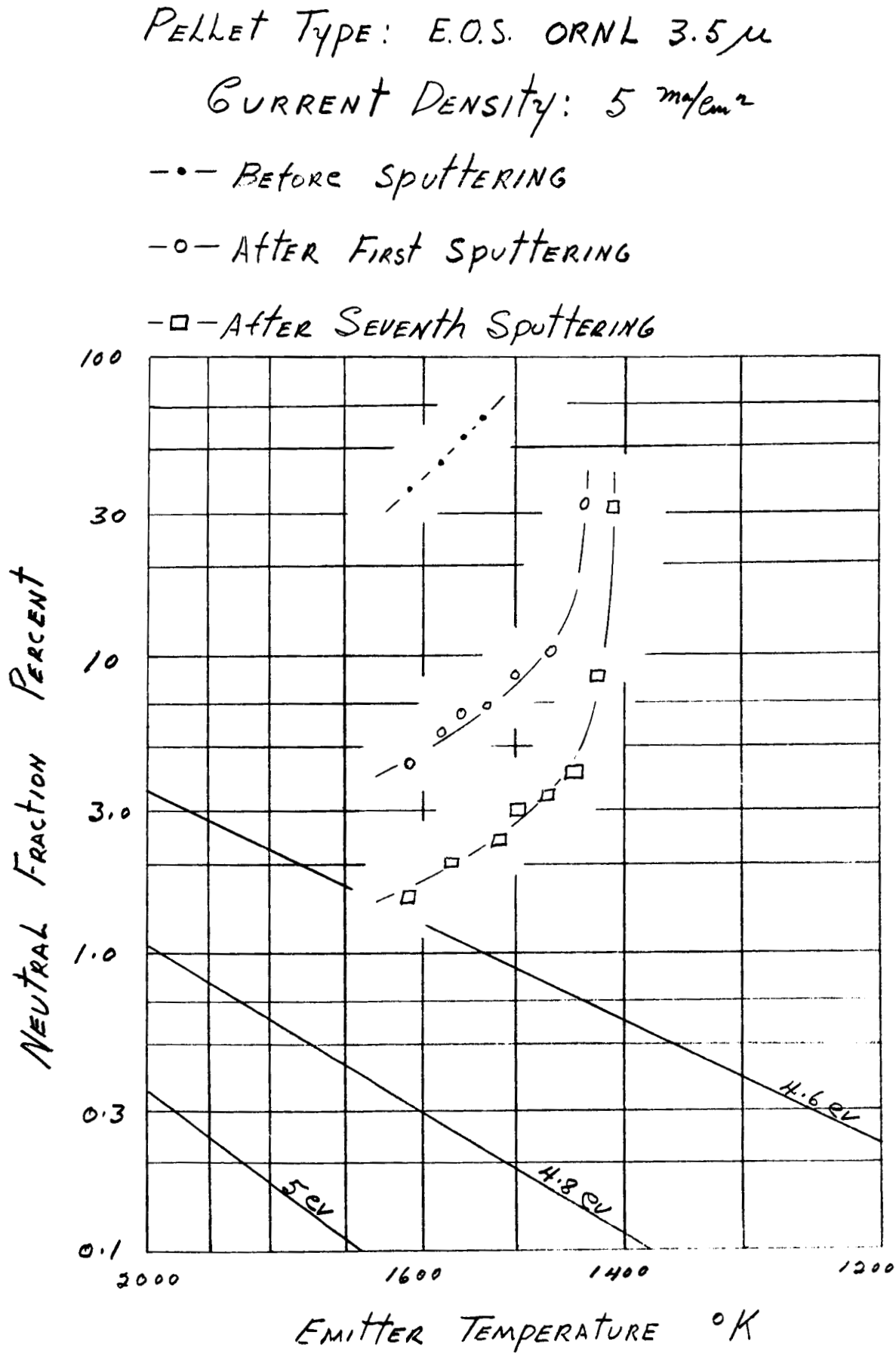

Figure 40. Neutral fraction as a function of emitter temperature

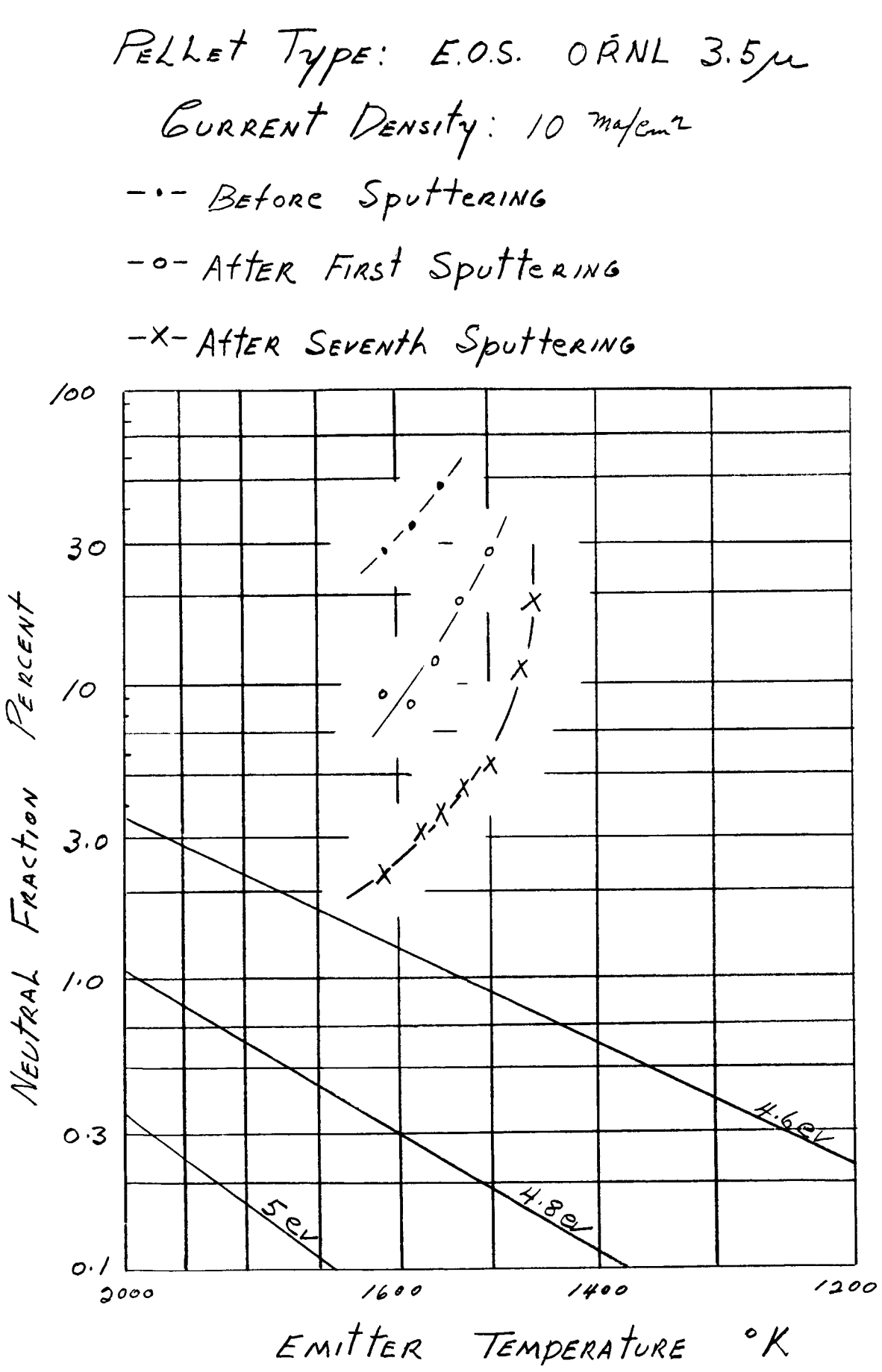

Figure 41. Neutral fraction as a function of emitter temperature

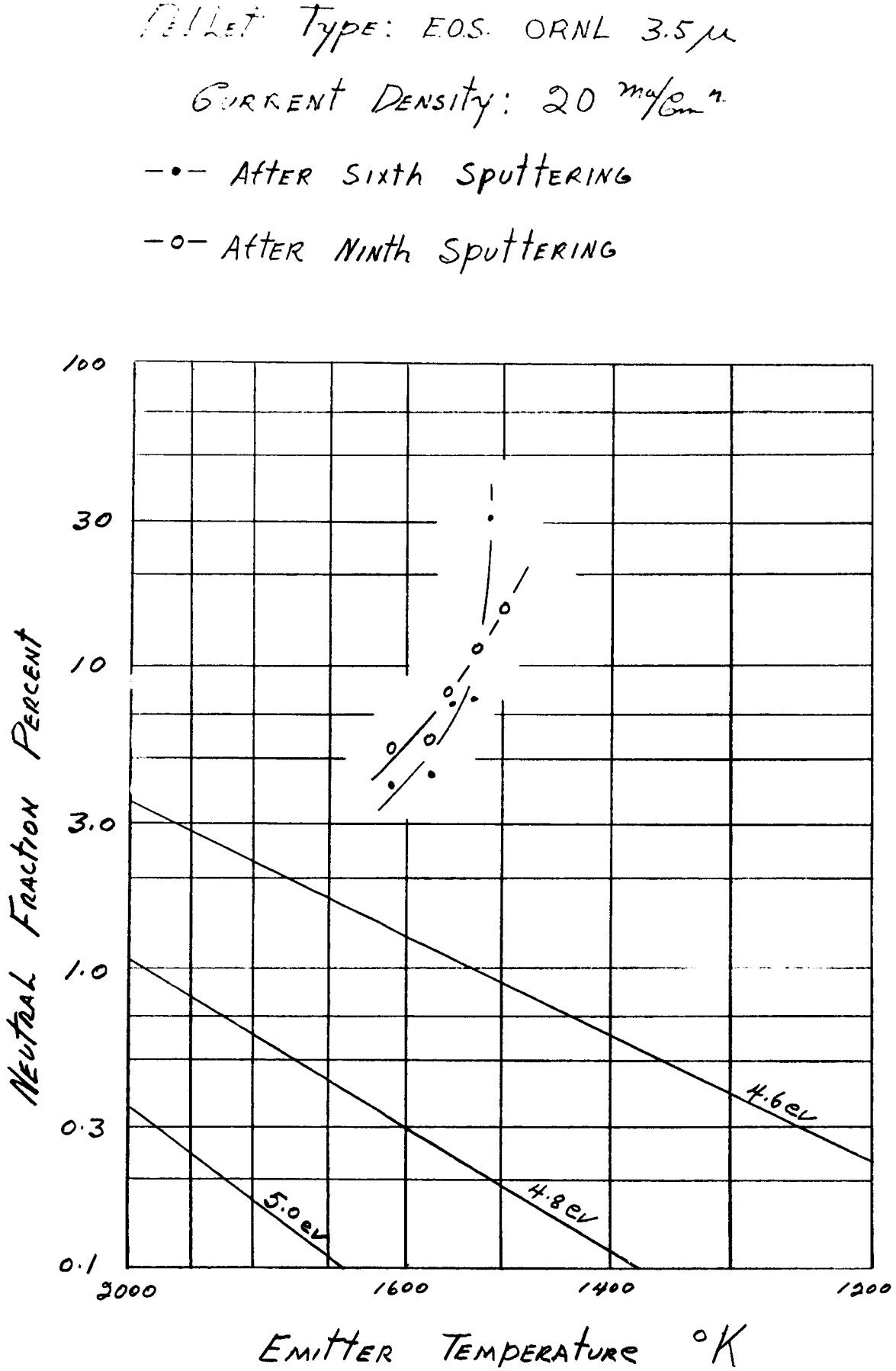

Figure 42. Neutral fraction as a function of emitter temperature

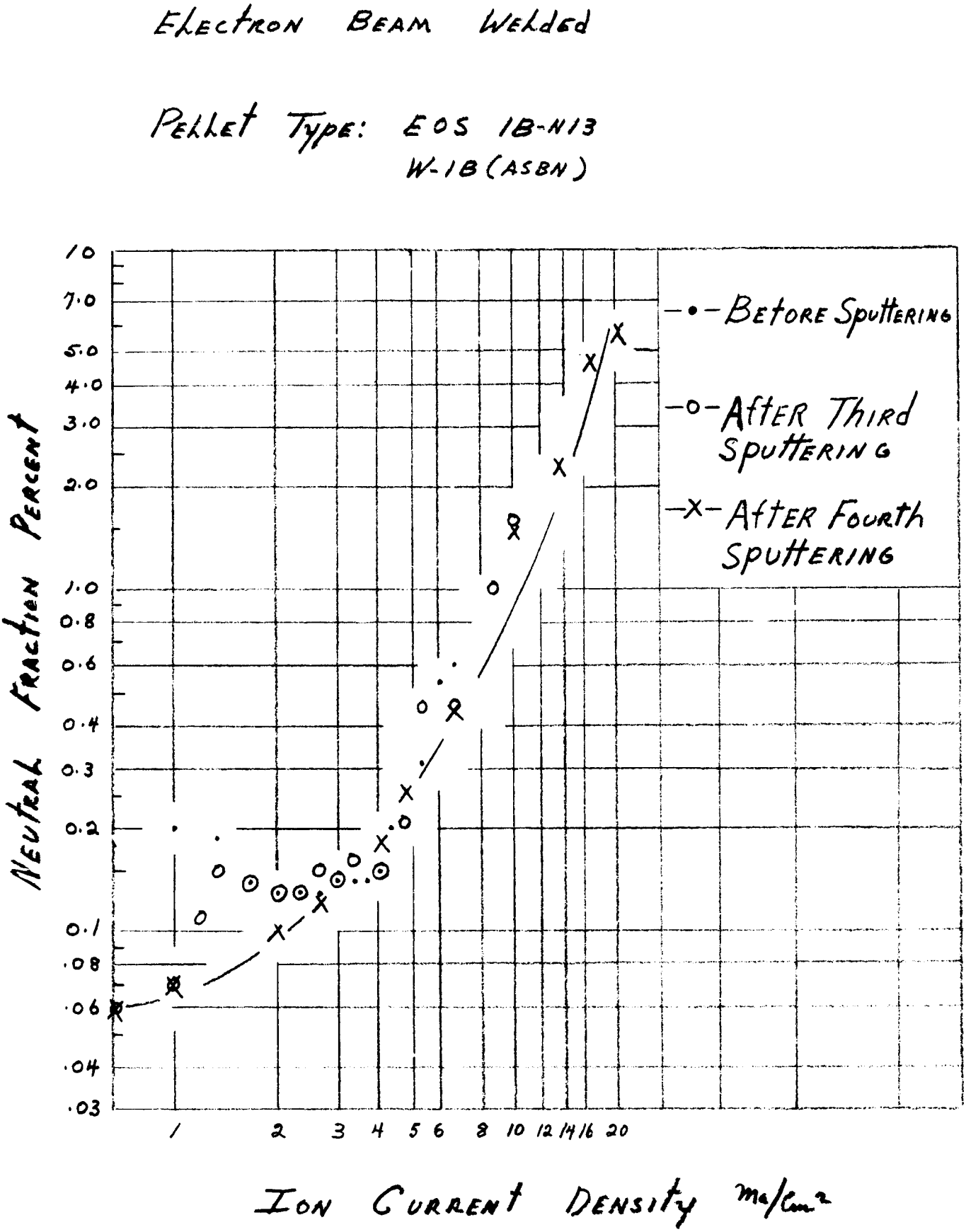

Figure 43. Neutral fraction as a function of current density

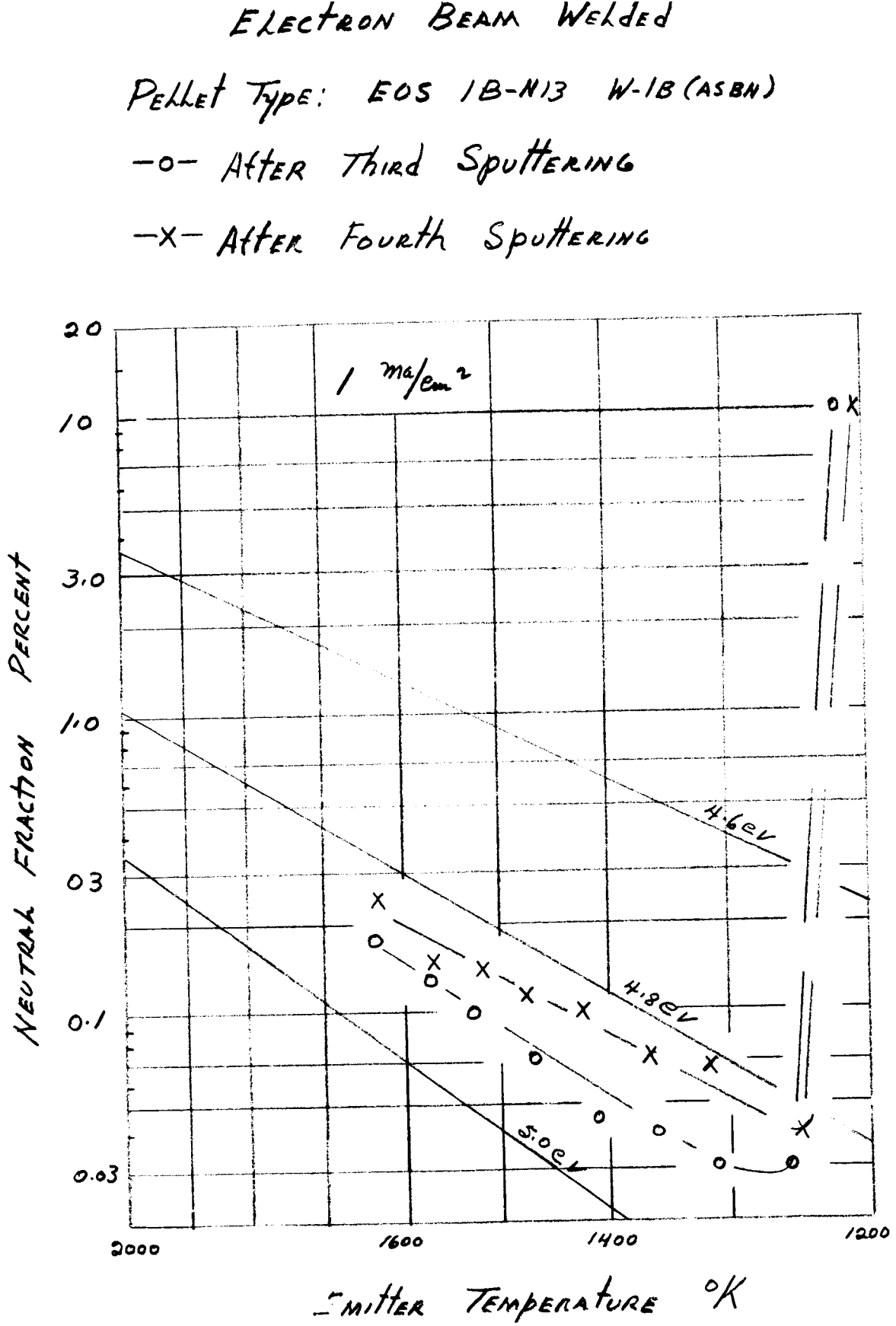

Figure 44. Neutral fraction as a function of emitter temperature

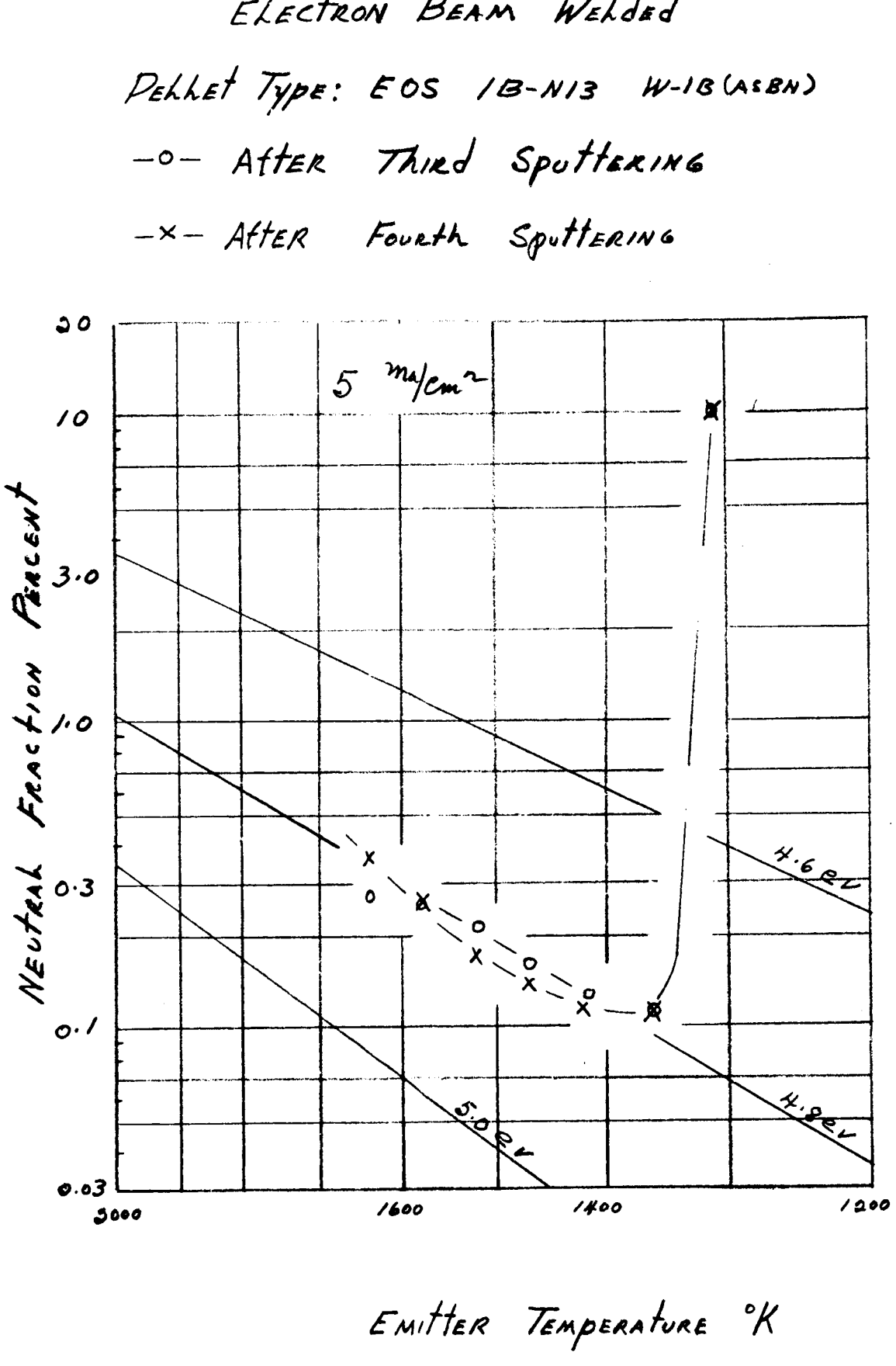

Figure 45. Neutral fraction as a function of emitter temperature

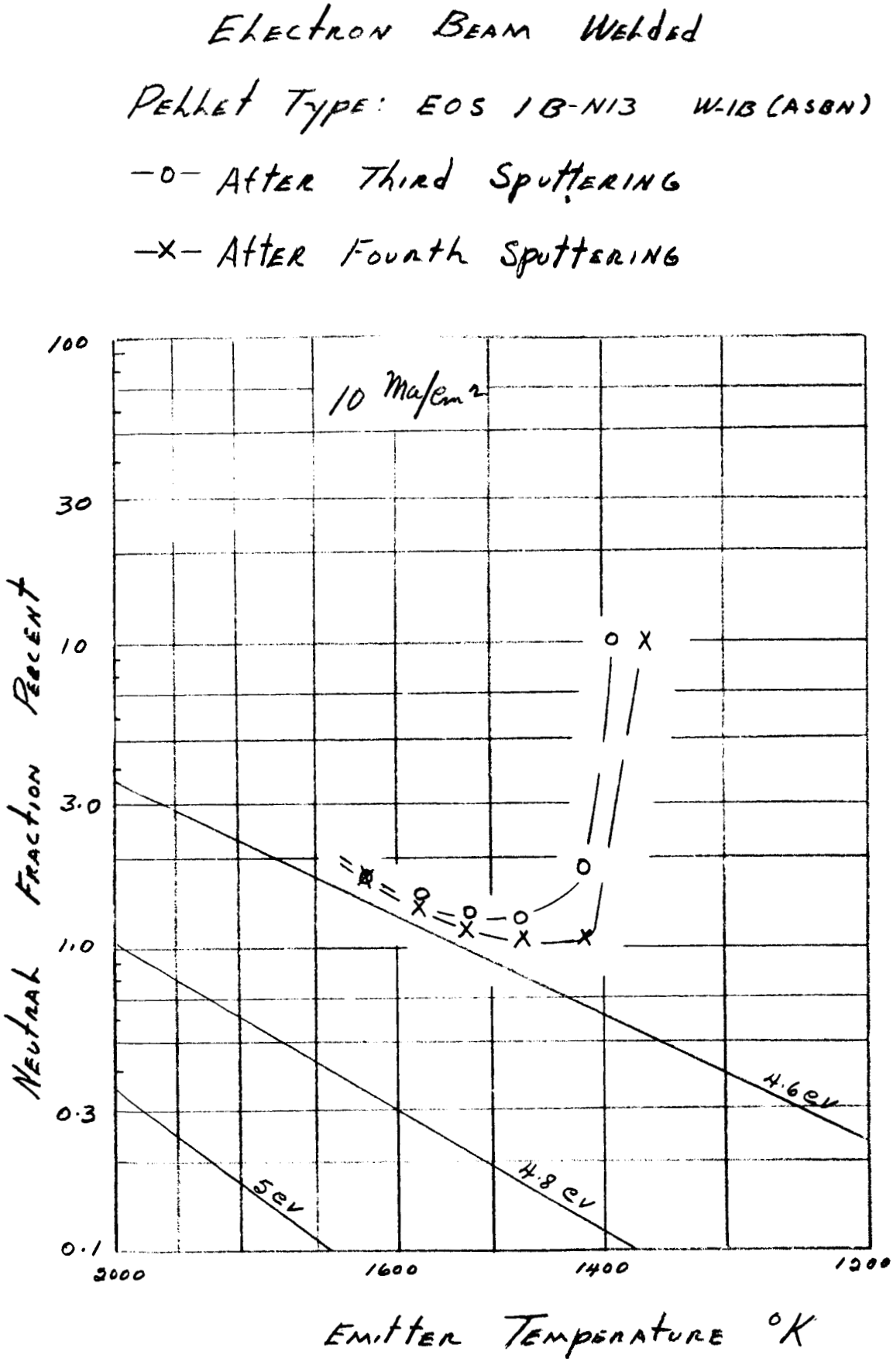

Figure 46. Neutral fraction as a function of emitter temperature

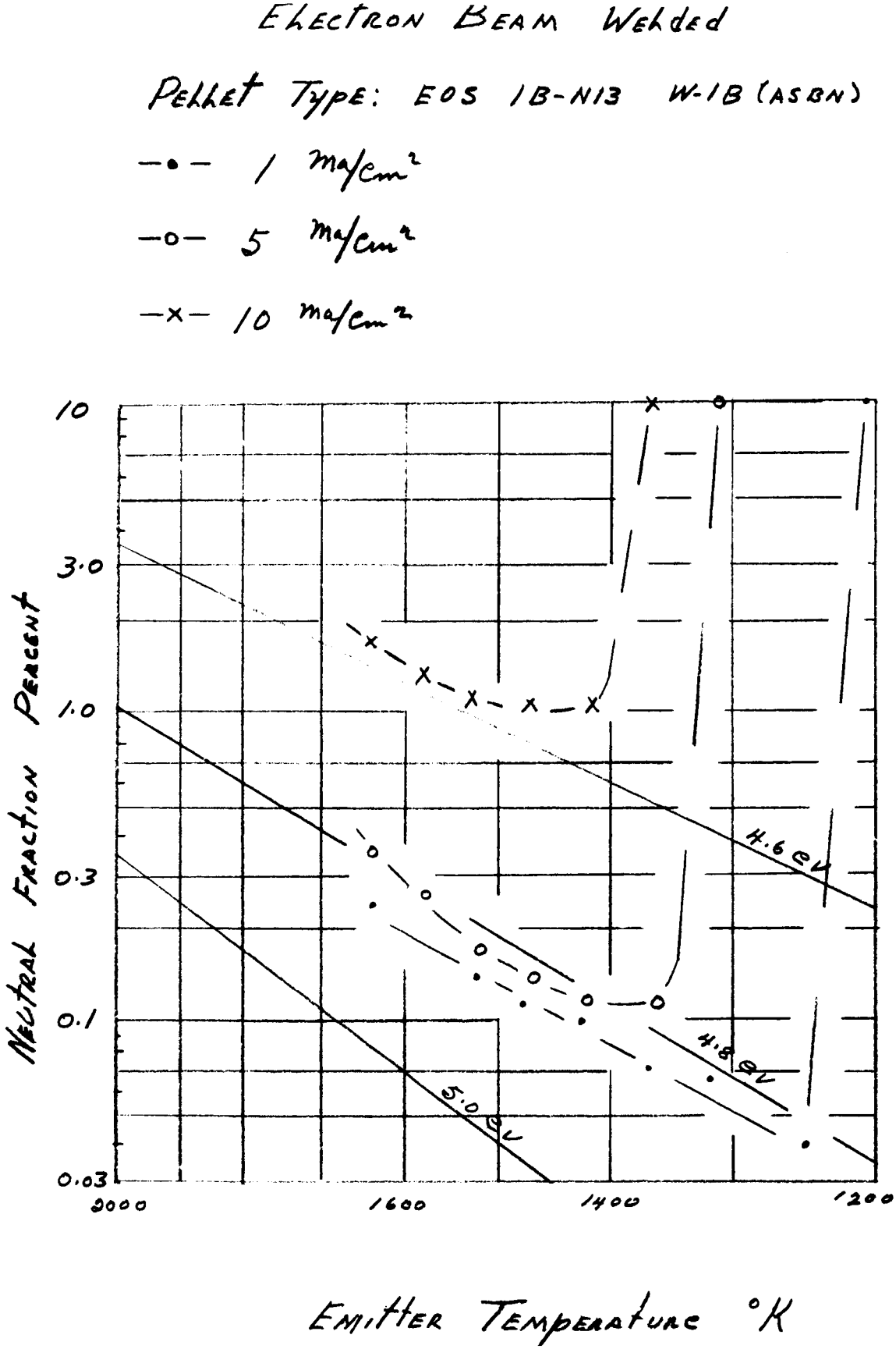

Figure 47. Neutral fraction as a function of emitter temperature

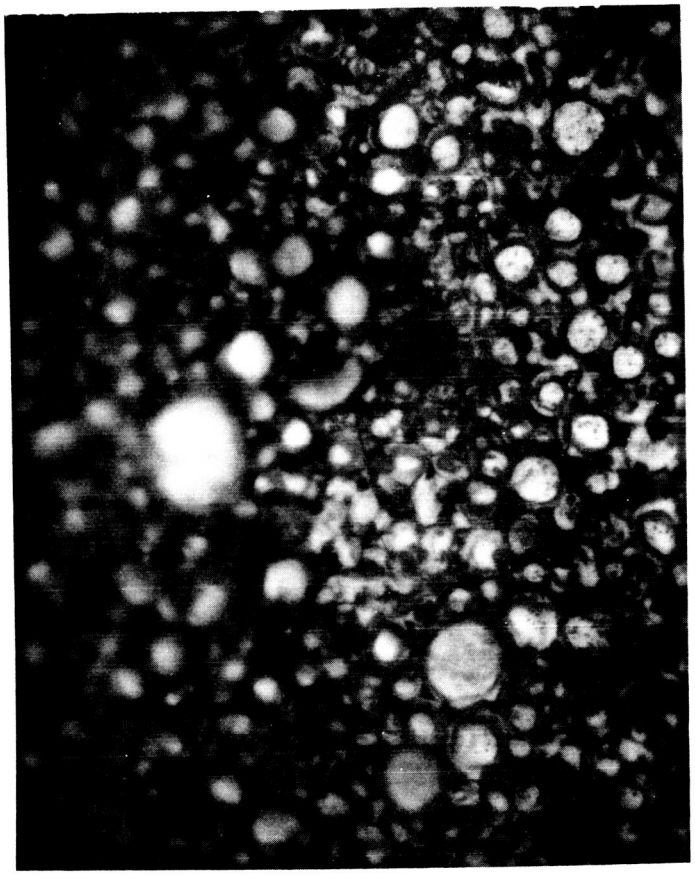

Figure 48. Photomicrograph at 1000x of EOS W-10% ta

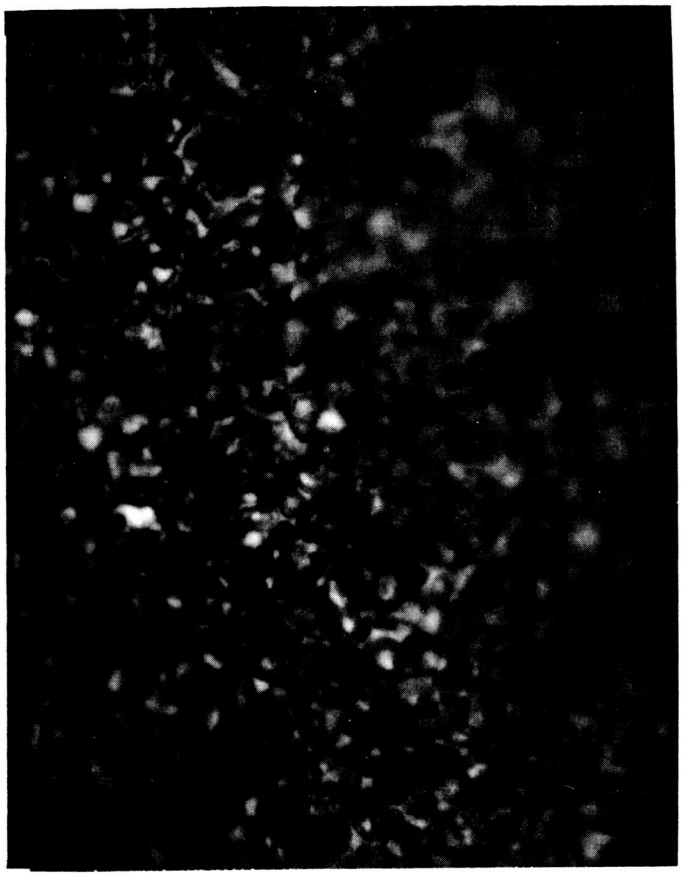

Figure 49. Photomicrograph at 1000x of HRL 3.9 micron

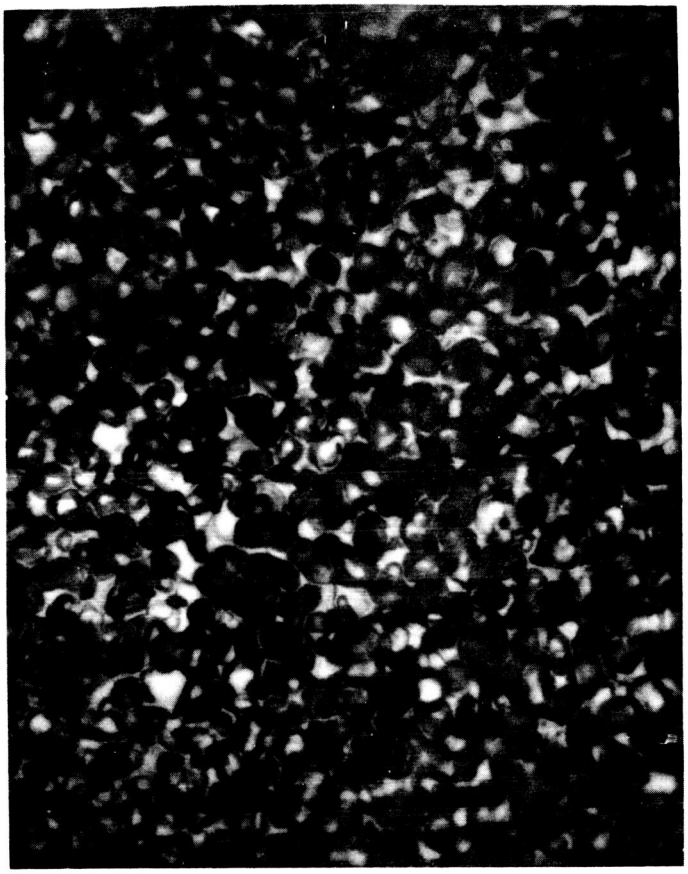

Figure 50. Photomicrograph at 1000x of LeRC 4.2 micron

Figure 51. Photomicrograph at 1000x of LeRC 3.5 micron

Figure 52. Photomicrograph at 1000x of ORNL 4.2 micron

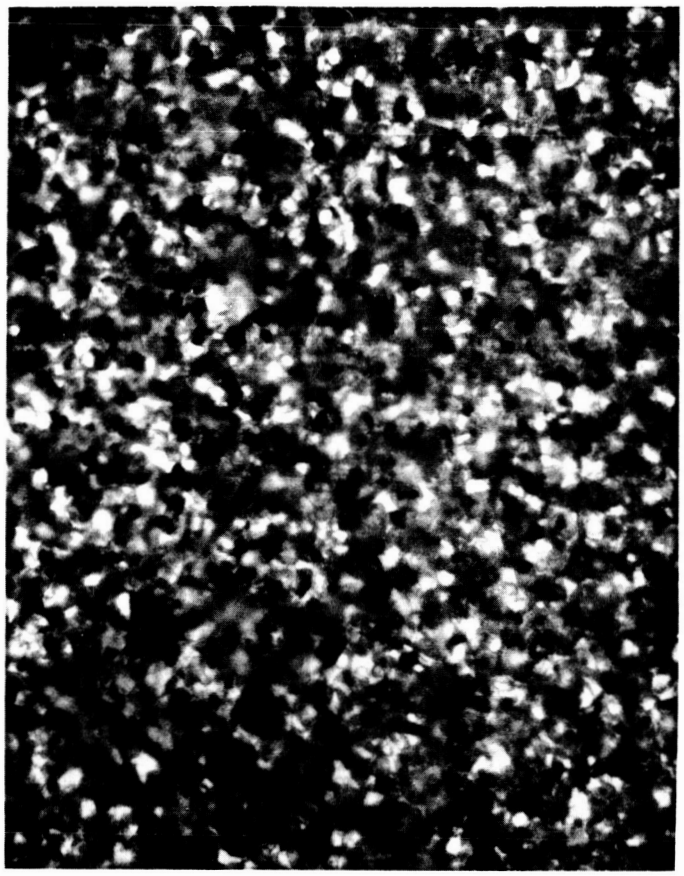

Figure 53. Photomicrograph at 1000x of ORNL 3.5 micron

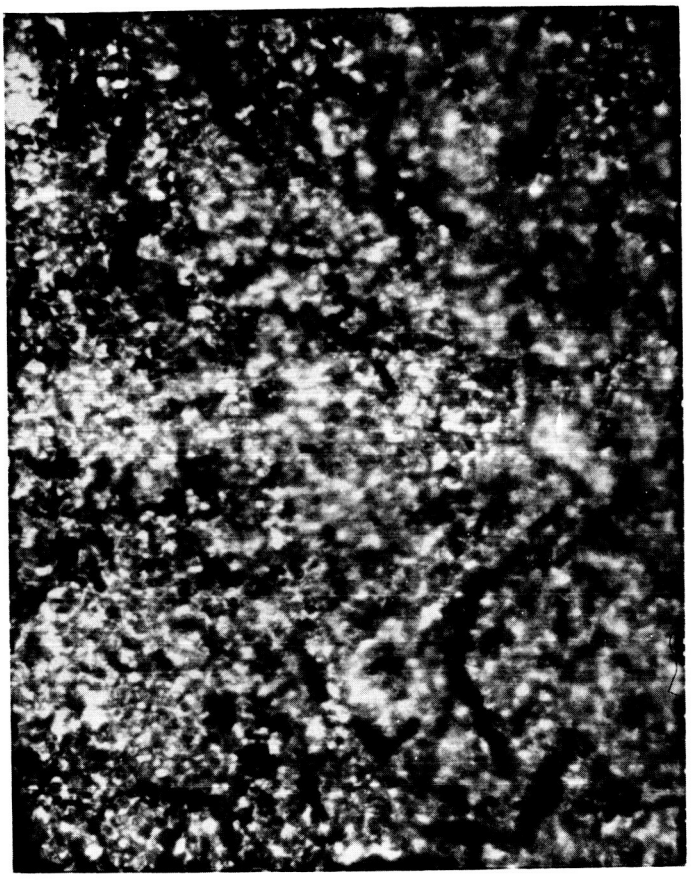

Figure 54. Photomicrograph at 1000x of EOS 1B-N 13

REFERENCES

1. Becker, J. A., E. J. Becker and R. G. Brandes, Journal of Applied Physics, Vol. 32, No. 3, March 1961.

2. Schlier, R. E., Journal of Applied Physics, Vol. 29, No. 8, August 1958.

3. Gasser, R. P. H. and T. F. Patteson, Vacuum, Vol. 14, 1964.

4. Germer, L. H., R. M. Stern and A. U. MacRae, Metal Surface, (Amer. Soc. Metals 1963).

5. Dyubna, B. Ch., O. K. Kultashev, and L. V. Gorshkova, Soviet Physics--Solid State, Vol. 8, No. 4, October 1966.

6. Cho, A. and H. Shelton, "Ion Emitter Studies," TRW Space Technology Laboratories, Final Report (CR-54045) NAS-3-2524, 1964.

   AIAA Aerospace Science Meeting, New York, New York, January 20-22, 1964, Preprint No. 64-11.

   AIAA Journal, Vol. 2, No. 12, December 1964.

7. Cho, A., D. F. Hall, and H. Shelton, "Program of Analytical and Experimental Study of Porous Metal Ionizer," TRW System, Final Report (CR-54325) NAS-3-5254, 1965.

   AIAA 5th Electric Propulsion Conference, March 29, 1966, San Diego, California, Paper No. 66-218.

APPENDIX

IONIZER PELLET EVALUATION REPORT NAS3-8904

Pellet Type EOS W-10% Ta Test No. _____ Date 12 Sept 66

Made By _____ Pores Per CM^2 _____

Average Particle Size _____ Average Pore Size _____

Particle Size Distribution Micron Diameter	Percent
> 7.5	
7.5 - 5.0	
5.0 - 3.3	
3.3 - 2.25	
1.5 - 1.0	
< 1.0	

Pore Size Distribution Micron Diameter	Percent
> 1.6	
1.2 - 1.6	
0.8 - 1.2	
0.4 - 0.8	
< 0.4	

Pellet Diameter (Effective) _____ Average Distance Between Pores _____

Transmission Coefficient 1.5×10^{-5} Thickness _____ Cm, Density _____ %

Pressure _____ Torr $\Delta p/\Delta t$ _____ Torr/sec

Calculated True Density _____ Work Function _____ *, eV

Surface Treatment _____

Sample Information _____

* Saha-L. Eq. - % Neutrals at 1 Ma/cm

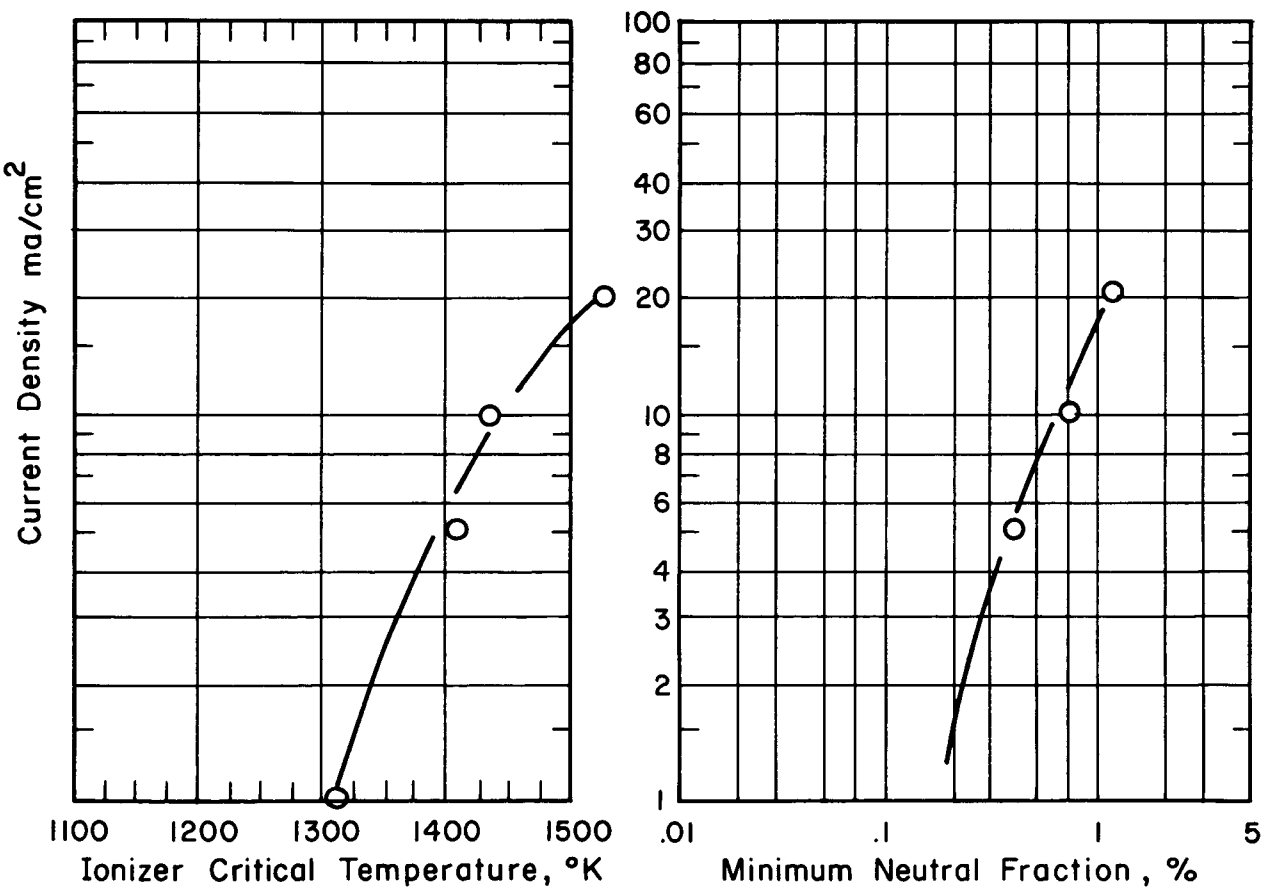

IONIZER PELLET EVALUATION REPORT

Pellet Type HRL 3.9 μ U. of I. No.2 Test No. _____ Date 22 Sept 66

Made By _____ Pores Per CM^2 _____

Average Particle Size _____ Average Pore Size _____

Particle Size Distribution Micron Diameter	Percent	Pore Size Distribution Micron Diameter	Percent
> 7.5		> 1.6	
7.5 - 5.0		1.2 - 1.6	
5.0 - 3.3		0.8 - 1.2	
3.3 - 2.25		0.4 - 0.8	
1.5 - 1.0		< 0.4	
< 1.0			

Pellet Diameter (Effective) _____ Average Distance Between Pores _____

Transmission Coefficient 6.85×10^{-5} Thickness _____ Cm, Density _____ %

Pressure _____ Torr $\Delta p/\Delta t$ _____ Torr/sec

Calculated True Density _____ Work Function _____ *, eV

Surface Treatment _____

Sample Information _____

* Saha-L. Eq. - % Neutrals at 1 Ma/cm

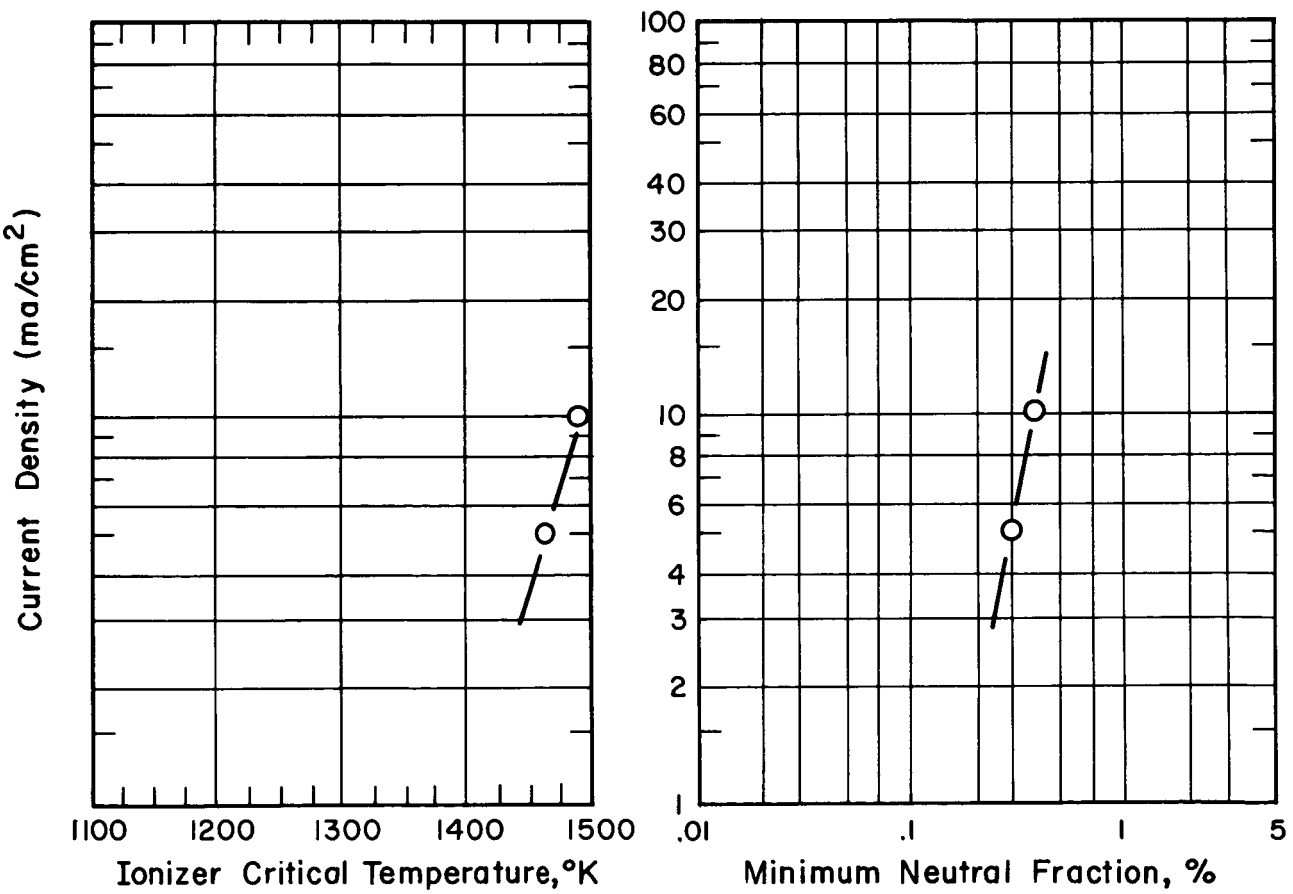

IONIZER PELLET EVALUATION REPORT NAS3-8904

Pellet Type Hughes 3.9 Micron NASA Electron Beam Welded
Made By _____

Test No. _____ Date _____

Pores Per CM^2 _____

Average Particle Size _____

Average Pore Size _____

Particle Size Distribution

Micron Diameter	Percent
> 7.5	
7.5 - 5.0	
5.0 - 3.3	
3.3 - 2.25	
1.5 - 1.0	
< 1.0	

Pore Size Distribution

Micron Diameter	Percent
> 1.6	
1.2 - 1.6	
0.8 - 1.2	
0.4 - 0.8	
< 0.4	

Pellet Diameter (Effective) _____
Transmission Coefficient 1.15×10^{-4}
Pressure _____ Torr
Calculated True Density _____
Surface Treatment _____
Sample Information _____

Average Distance Between Pores _____
Thickness _____ Cm, Density _____ %
$\Delta p/\Delta t$ _____ Torr/sec
Work Function _____ *, eV

* Saha-L. Eq. - % Neutrals at 1 Ma/cm

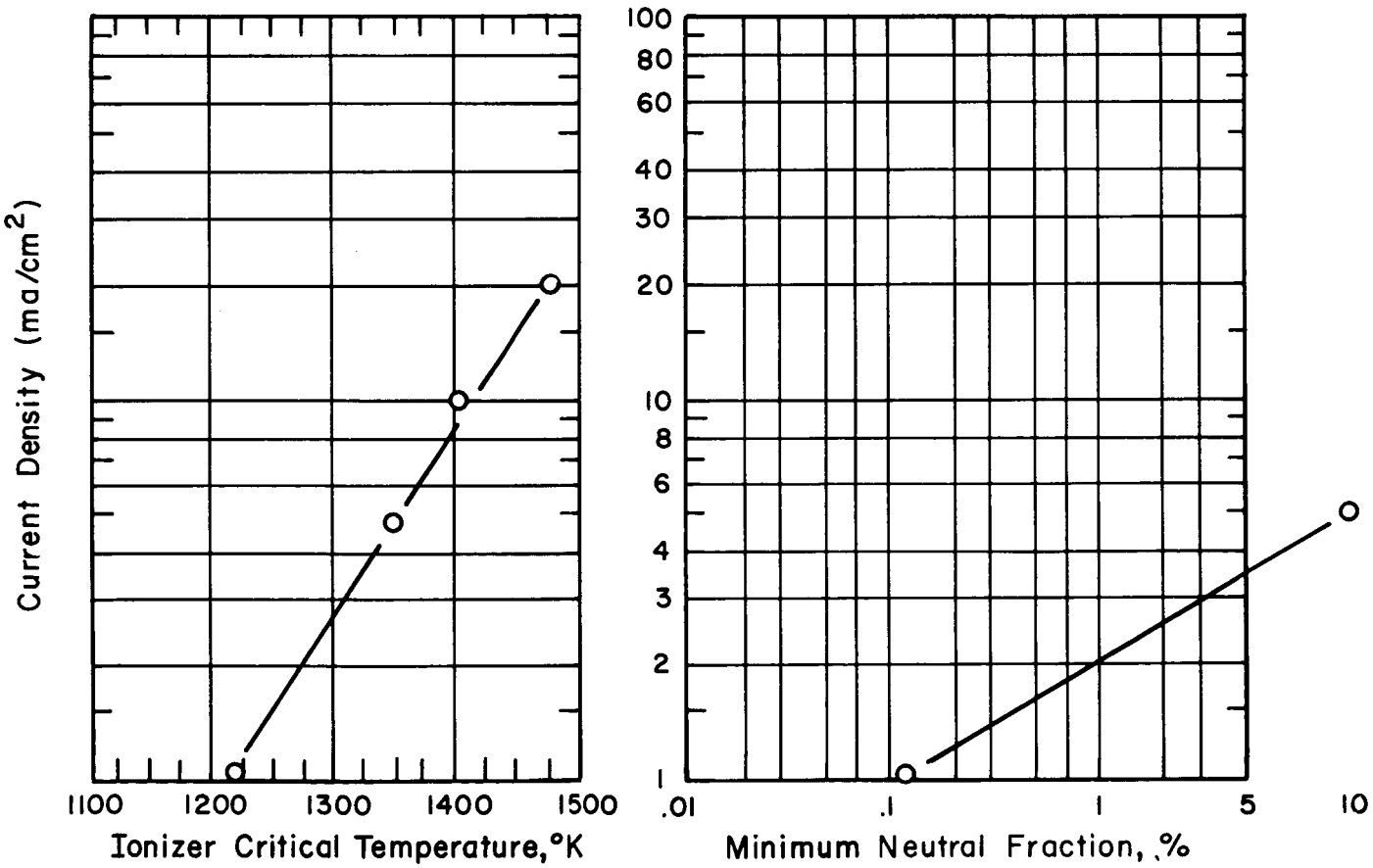

IONIZER PELLET EVALUATION REPORT NAS3-8904

Pellet Type HRL 3.9 micron LRC-4 NASA Electron Beam Welded #2 Test No. _____ Date 27 Oct 66

Made By _____ Pores Per CM^2 _____

Average Particle Size _____ Average Pore Size _____

Particle Size Distribution Micron Diameter	Percent	Pore Size Distribution Micron Diameter	Percent
> 7.5		> 1.6	
7.5 - 5.0		1.2 - 1.6	
5.0 - 3.3		0.8 - 1.2	
3.3 - 2.25		0.4 - 0.8	
1.5 - 1.0		< 0.4	
< 1.0			

Pellet Diameter (Effective) _____ Average Distance Between Pores _____

Transmission Coefficient 1.3×10^{-4} Thickness _____ Cm, Density _____ %

Pressure _____ Torr $\Delta p/\Delta t$ _____ Torr/sec

Calculated True Density _____ Work Function _____ *, eV

Surface Treatment _____

Sample Information _____

* Saha-L. Eq. - % Neutrals at 1 Ma/cm

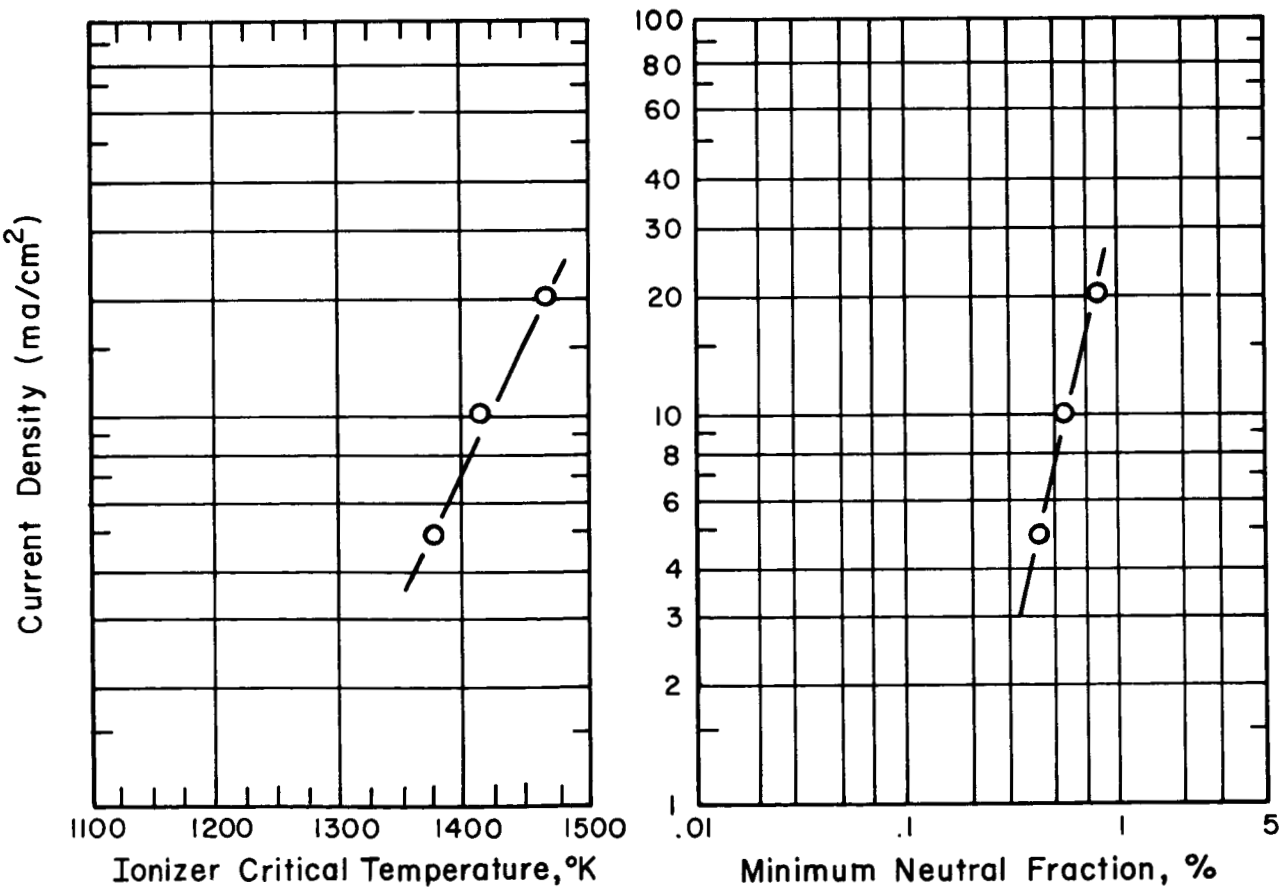

IONIZER PELLET EVALUATION REPORT NAS3-8904

Pellet Type LERC 4.2 Micron Test No. _____ Date 12 Dec 66

Made By _____ Pores Per CM^2 _____

Average Particle Size _____ Average Pore Size _____

Particle Size Distribution

Micron Diameter	Percent
> 7.5	
7.5 - 5.0	
5.0 - 3.3	
3.3 - 2.25	
1.5 - 1.0	
< 1.0	

Pore Size Distribution

Micron Diameter	Percent
> 1.6	
1.2 - 1.6	
0.8 - 1.2	
0.4 - 0.8	
< 0.4	

Pellet Diameter (Effective) _____ Average Distance Between Pores _____

Transmission Coefficient 1.18×10^{-4} Thickness _____ Cm, Density _____ %

Pressure _____ Torr $\Delta p/\Delta t$ _____ Torr/sec

Calculated True Density _____ Work Function _____ *, eV

Surface Treatment _____

Sample Information _____

* Saha-L. Eq. - % Neutrals at 1 Ma/cm

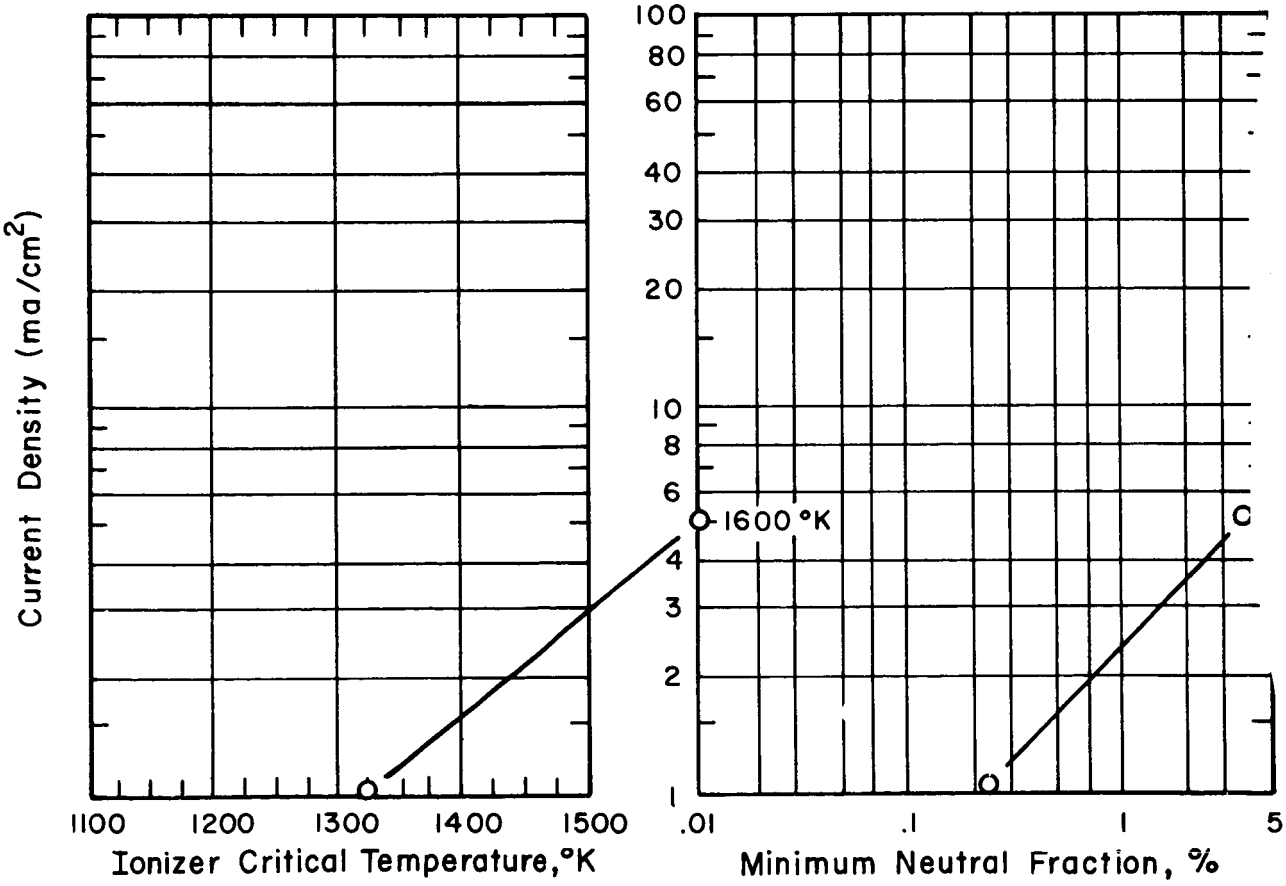

IONIZER PELLET EVALUATION REPORT NAS3-8904

Pellet Type EOS 1B-N20 W-1B(asbn) Test No. _____ Date 20 Jan 67

Made By _____ Pores Per CM^2 _____

Average Particle Size _____ Average Pore Size _____

Particle Size Distribution Micron Diameter	Percent
> 7.5	
7.5 - 5.0	
5.0 - 3.3	
3.3 - 2.25	
1.5 - 1.0	
< 1.0	

Pore Size Distribution Micron Diameter	Percent
> 1.6	
1.2 - 1.6	
0.8 - 1.2	
0.4 - 0.8	
< 0.4	

Pellet Diameter (Effective) _____ Average Distance Between Pores _____
Transmission Coefficient 2.26×10^{-4} Thickness _____ Cm, Density _____ %
Pressure _____ Torr $\Delta p/\Delta t$ _____ Torr/sec
Calculated True Density _____ Work Function _____ *, eV
Surface Treatment _____
Sample Information _____ * Saha-L. Eq. - % Neutrals at 1 Ma/cm

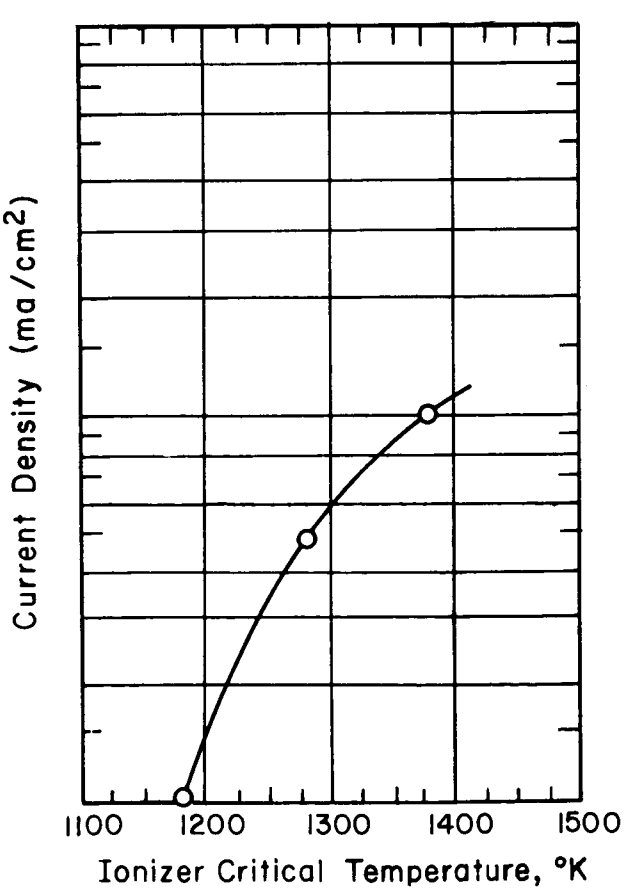

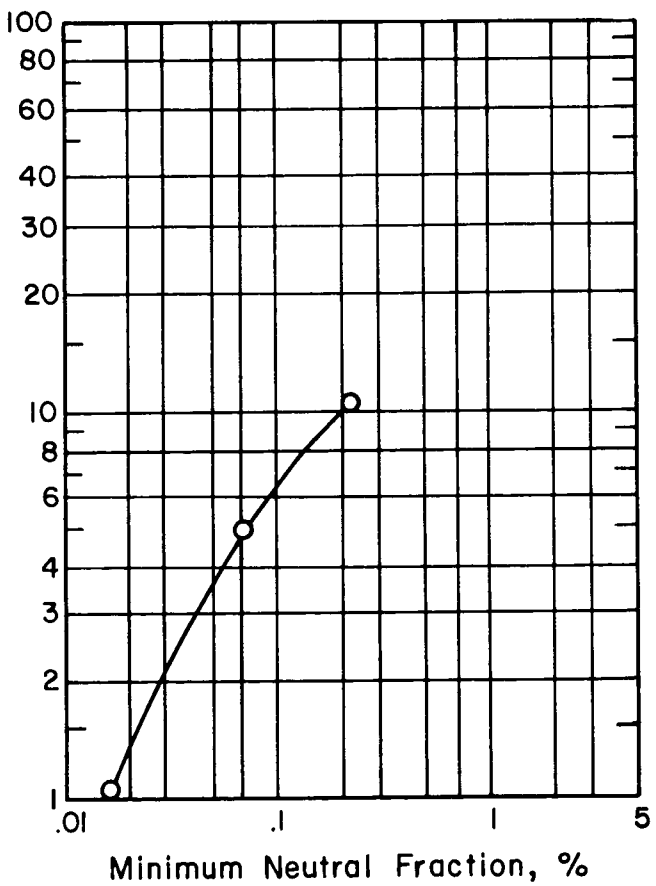

IONIZER PELLET EVALUATION REPORT NAS3-8904

Pellet Type LERC 3.5 Micron Test No. _____ Date 8 Feb 67

Made By _____ Pores Per CM^2 _____

Average Particle Size _____ Average Pore Size _____

Particle Size Distribution Micron Diameter	Percent
> 7.5	
7.5 - 5.0	
5.0 - 3.3	
3.3 - 2.25	
1.5 - 1.0	
< 1.0	

Pore Size Distribution Micron Diameter	Percent
> 1.6	
1.2 - 1.6	
0.8 - 1.2	
0.4 - 0.8	
< 0.4	

Pellet Diameter (Effective) _____ Average Distance Between Pores _____

Transmission Coefficient 7.5 x 10^{-5} Thickness _____ Cm, Density _____ %

Pressure _____ Torr $\Delta p/\Delta t$ _____ Torr/sec

Calculated True Density _____ Work Function _____ *, eV

Surface Treatment _____

Sample Information _____ * Saha-L. Eq. - % Neutrals at 1 Ma/cm

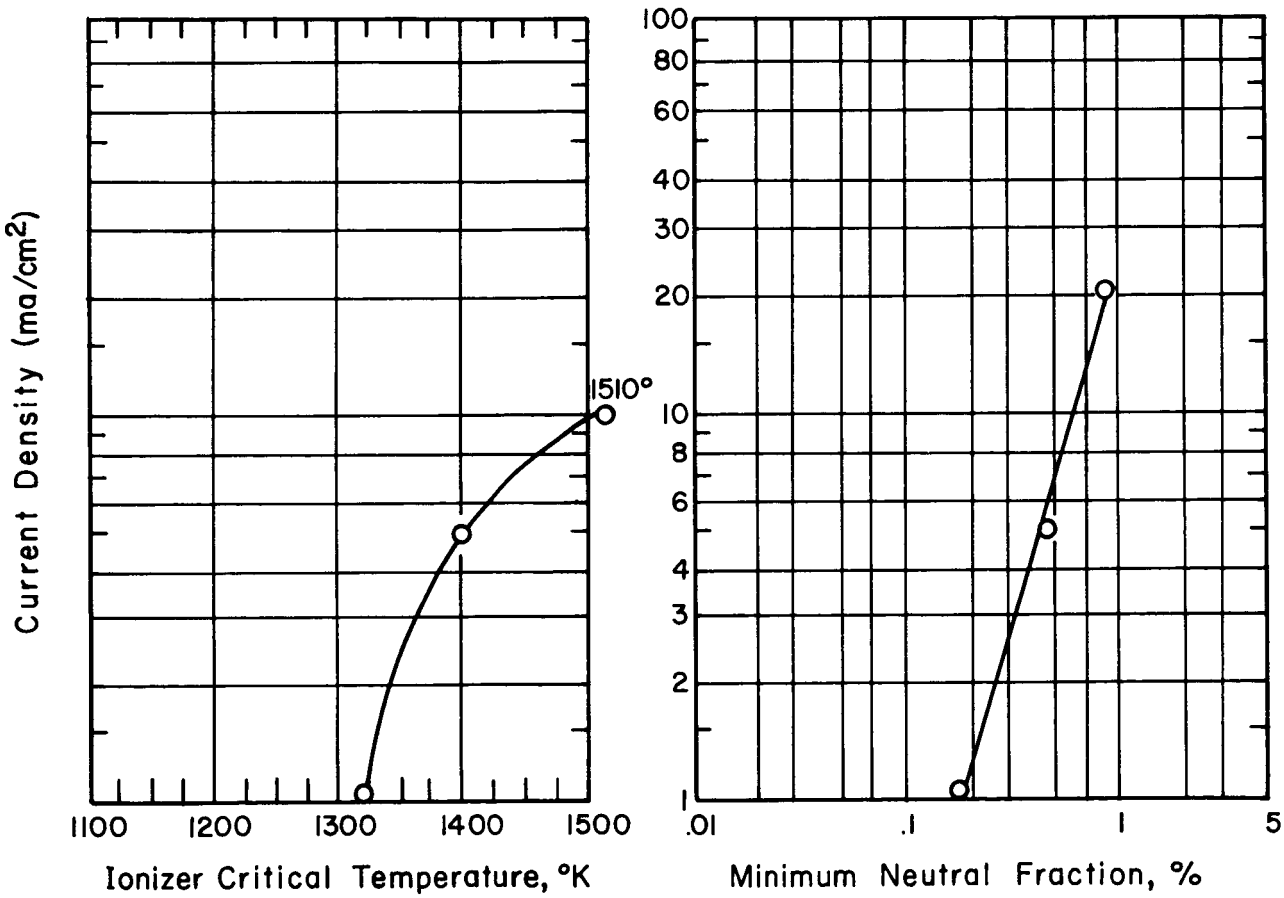

IONIZER PELLET EVALUATION REPORT NAS3-8904

Pellet Type EOS ORNL 4.2 μ Test No. _____ Date 27 Feb 67

Made By _____ Pores Per CM^2 _____

Average Particle Size _____ Average Pore Size _____

Particle Size Distribution Micron Diameter	Percent
> 7.5	
7.5 - 5.0	
5.0 - 3.3	
3.3 - 2.25	
1.5 - 1.0	
< 1.0	

Pore Size Distribution Micron Diameter	Percent
> 1.6	
1.2 - 1.6	
0.8 - 1.2	
0.4 - 0.8	
< 0.4	

Pellet Diameter (Effective) _____ Average Distance Between Pores _____

Transmission Coefficient 1.075×10^{-4} Thickness _____ Cm, Density _____ %

Pressure _____ Torr $\Delta p/\Delta t$ _____ Torr/sec

Calculated True Density _____ Work Function _____ *, eV

Surface Treatment _____

Sample Information _____ * Saha-L. Eq. - % Neutrals at 1 Ma/cm

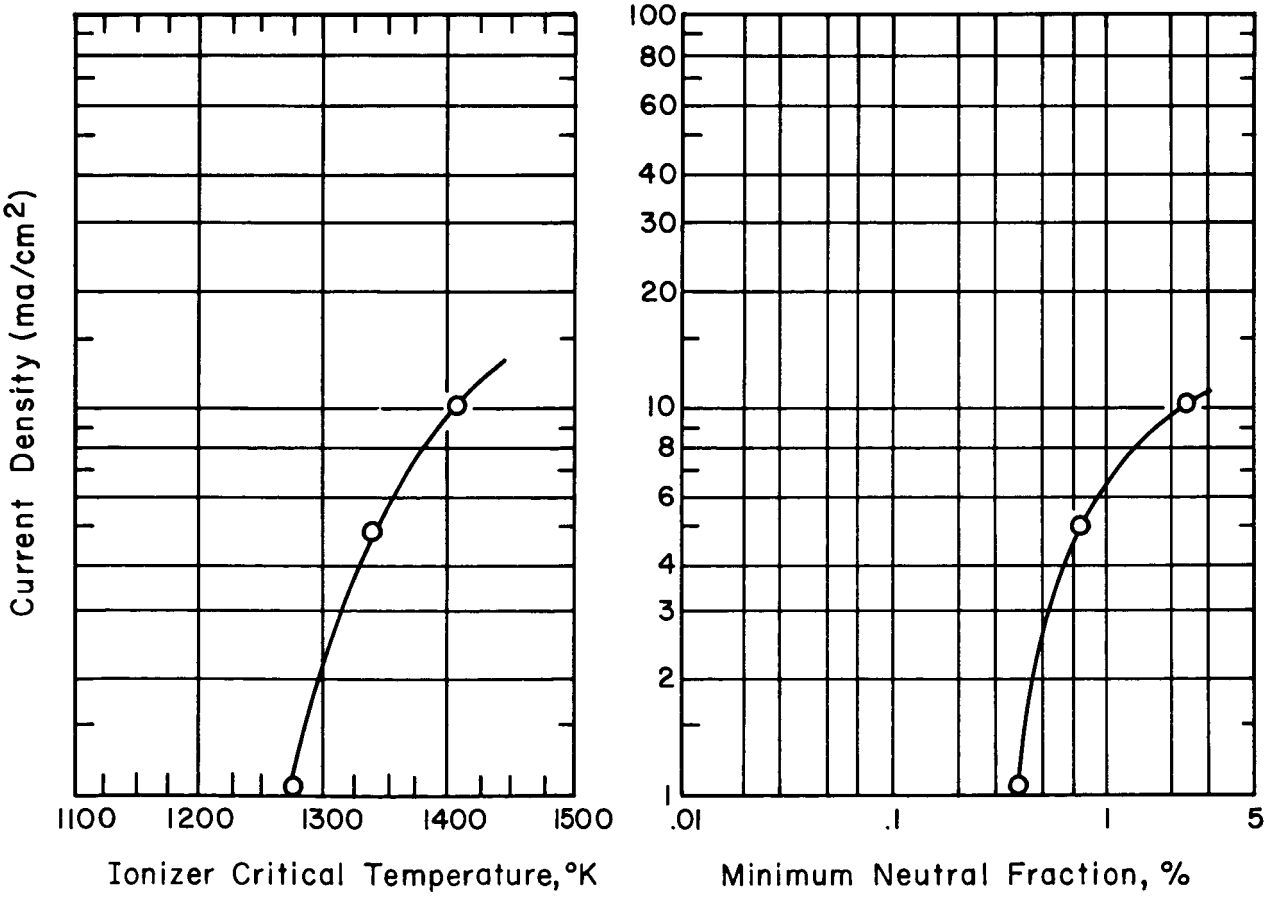

IONIZER PELLET EVALUATION REPORT NAS3-8904

Pellet Type EOS ORNL 3.5 μ Test No. _____ Date 2 Feb 67

Made By _____ Pores Per CM^2 _____

Average Particle Size _____ Average Pore Size _____

Particle Size Distribution

Micron Diameter	Percent
> 7.5	
7.5 - 5.0	
5.0 - 3.3	
3.3 - 2.25	
1.5 - 1.0	
< 1.0	

Pore Size Distribution

Micron Diameter	Percent
> 1.6	
1.2 - 1.6	
0.8 - 1.2	
0.4 - 0.8	
< 0.4	

Pellet Diameter (Effective) _____ Average Distance Between Pores _____

Transmission Coefficient 1.36×10^{-4} Thickness _____ Cm, Density _____ %

Pressure _____ Torr $\Delta p/\Delta t$ _____ Torr/sec

Calculated True Density _____ Work Function _____ *, eV

Surface Treatment _____

Sample Information _____ * Saha-L. Eq. - % Neutrals at 1 Ma/cm

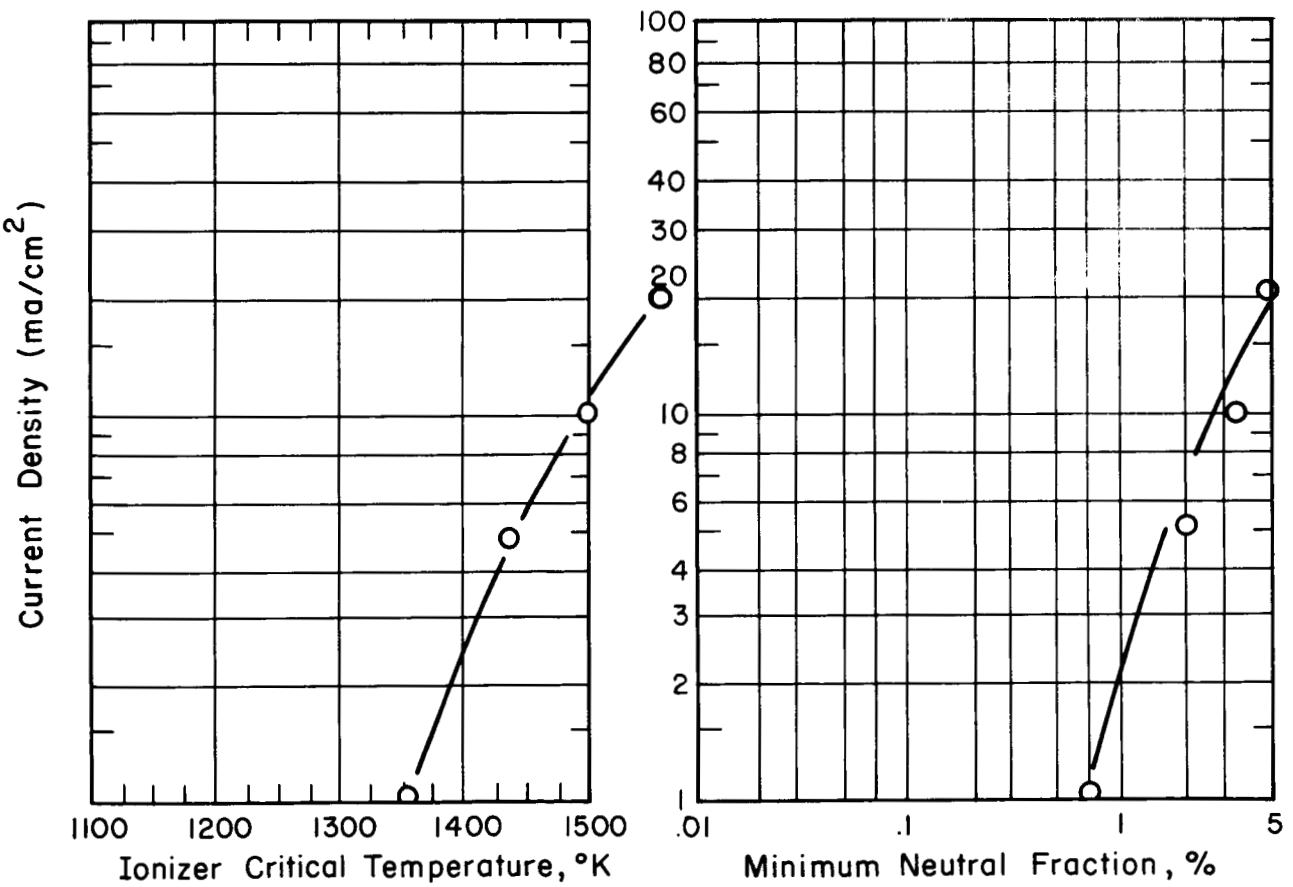

IONIZER PELLET EVALUATION REPORT NAS3-8904

Pellet Type EOS 1B-N13 W-1B (asbn) Test No. _____ Date _____

Made By _____ Pores Per CM^2 _____

Average Particle Size _____ Average Pore Size _____

Particle Size Distribution Micron Diameter	Percent	Pore Size Distribution Micron Diameter	Percent
> 7.5		> 1.6	
7.5 - 5.0		1.2 - 1.6	
5.0 - 3.3		0.8 - 1.2	
3.3 - 2.25		0.4 - 0.8	
1.5 - 1.0		< 0.4	
< 1.0			

Pellet Diameter (Effective) _____
Transmission Coefficient 1.79x10-4
Pressure _____ Torr
Calculated True Density _____
Surface Treatment _____
Sample Information _____

Average Distance Between Pores _____
Thickness _____ Cm, Density _____ %
$\Delta p/\Delta t$ _____ Torr/sec
Work Function _____ *, eV

* Saha-L. Eq. - % Neutrals at 1 Ma/cm